

Markerless 3D Assessment of Severity and Progression of Scoliosis Using Surface
Topography on Isolated Back Scans

by

Andrew William Teal

A thesis submitted in partial fulfillment of the requirements for the degree of

Master of Science

in

Structural Engineering

Civil and Environmental Engineering
University of Alberta

© Andrew William Teal, 2019

Abstract

The objectives of the thesis were to:

1. Determine if open source software can be use in markerless asymmetry analysis of surface topography.
2. Determine if isolated back scans can be used in markerless asymmetry analysis of surface topography.

Markerless asymmetry analysis of surface topography utilizes 3D scan points collected from patients with scoliosis. This analysis can help reduce the number of x-rays required in the course of treatment for scoliosis patients, thus reducing cancer risks associated with repeated x-ray exposure during treatment. Previous studies used full torso scans and analysed these scans using proprietary software.

Full torso scans from 67 patients were analyzed utilizing the markerless asymmetry analysis techniques previously reported by Komeili et al. The scans were analyzed with the open source software and the results were compared to the results from previous studies.

For the second part of the study, the points in the full torso scan associated with the back only were isolated and the analysis was repeated. Results from the isolated back analysis were compared with the results of the full torso analysis for asymmetry values associated with identified patches of scoliotic deformity.

The use of the open source software provided analysis results that were within 2.2 mm of the results from previous studies with a 95% confidence interval for both the max deviation and root

mean square results. 3.4 mm was the threshold of acceptable agreement, based on previous studies of asymmetry of healthy patients.

The analysis of the isolated back using the same method provided results with a 95% confidence interval of 16.1 mm on max deviation and 3.1 mm on root mean square.

3.4 mm was the threshold of acceptable agreement, based on previous studies of asymmetry of healthy patients. The open source software approach provided accurate results when compared with the previous studies that utilized proprietary software, demonstrating that the open source software provides a viable alternative to the higher priced proprietary option.

The analysis of the isolated back scans showed that the decision trees and indices developed by Komeili et al. cannot be applied to analysis results obtained from the isolated back scans in the same way they are applied to the full torso back scans. The use of the isolated back scans would require further research into the application of other methods of analyzing surface topography.

Contents

Abstract ii

Table of Figures vi

Table of Tables viii

List of Abbreviations/Acronyms..... ix

List of Appendices x

Chapter 1 - Literature Review..... 1

 What is Scoliosis..... 1

 Classifications of Scoliosis 4

 Specifics of Adolescent Idiopathic Scoliosis 7

 Impacts on patients 7

 Treatment options 8

 Curve progression 9

 Methods for diagnosing and monitoring..... 9

 Surface Topography 10

 Open Source Software Approach..... 16

 Thesis objectives..... 18

 Problem statement 18

 Objectives..... 18

 Outline 19

Chapter 2 – An Open Source Software Approach to Markerless 3D Assessment of Adolescent Idiopathic Scoliosis Using Asymmetry 20

 Description of Full Torso Asymmetry Analysis..... 20

 Data used..... 24

 Results..... 26

 Comparison of maximum deviation..... 26

 Discussion..... 32

Chapter 3 – Applying the Method of Markerless 3D Assessment of Adolescent Idiopathic Scoliosis to Isolated Back Scans 36

 Isolated Back Analysis 36

 Data used..... 41

 Results..... 42

 Isolated Back Analysis Discussion 47

Chapter 4 – Conclusion..... 56

 Future Work 57

References..... 59

Table of Figures

Figure 1-1 Illustrations of the Coronal, Sagittal, and Axial Planes (4)..... 1

Figure 1-2 Illustration of the Skeletal Anatomy of the Back (4) 2

Figure 1-3 Illustration of the Measurement of the Cobb Angle (2) 3

Figure 1-4 Example of Moire Fringe Topograph (33)11

Figure 1-5 Example Deviation Color Map 13

Figure 1-6 - Color Map Legend and Limits..... 13

Figure 1-7 Color Patch Classification Table (13) 14

Figure 2-1 Example Deviation Color Map 21

Figure 2-2 Example Of Excluded Data - Insufficient RMS for 9.33mm Threshold 26

Figure 2-3 Full Torso Analysis – Scatter Plot of CloudCompare Max Deviation vs Geomagic
Max Deviation 27

Figure 2-4 Scatter Plot of the Measured Differences Between CloudCompare Max Deviation and
Geomagic Max Deviation..... 28

Figure 2-5 Scatter Plot of CloudCompare RMS vs Geomagic RMS..... 30

Figure 2-6 Scatter Plot of the measured differences between CloudCompare RMS and Geomagic
RMS 31

Figure 2-7 Geomagic (31) and CloudCompare Output Comparison..... 35

Figure 3-1 Isolated Back Points and Offset Coronal Plane 38

Figure 3-2 Isolated Back Mesh (Color Indicates Point Cloud Density) 38

Figure 3-3 Visualization of Mirroring Mesh About Sagittal Plane..... 39

Figure 3-4 Registration of Mirrored Copy of Back Mesh 39

Figure 3-5 Distance Between Measured and Mirrored Meshes applied to Original as Deviation
 Color Map 40

Figure 3-6 Final Colorized Isolated Back Mesh 40

Figure 3-7 View of Colored Back Mesh, Looking Up From The Bottom Of The Mesh. Illustrates
 Color Mapping on Actual Contours 41

Figure 3-8 Scatter Plot of Measure Values of Maximum Deviation Between Full Torso Analysis
 and Isolated Back Analysis 43

Figure 3-9 Scatter Plot of the Measured Differences Between Full Torso Max Deviation and
 Isolated Back Max Deviation..... 44

Figure 3-10 Scatter Plot of Measure Values of Root Mean Square Between Full Torso Analysis
 and Isolated Back Analysis 45

Figure 3-11 Scatter Plot of the Measured Differences Between Root Mean Square Results of Full
 Torso Analysis and the Isolated Back Analysis 46

Figure 3-12 Visual Comparison of Full Torso Analysis and Isolated Back Analysis 47

Figure 3-13 Illustration of Differences Between Maximum Deviation and RMS During
 Registration 50

Figure 3-14 Illustration of Max Deviation and RMS Calculations Per Patch 51

Table of Tables

Table 1-1 Classifications of Idiopathic Scoliosis..... 4

Table 1-2 Classification Categories for the King Classification System for Scoliosis (19)..... 5

Table 1-3 Lenke Classification Structure (22) 6

Table 2-1- Description of Participants 24

Table 2-2 Full Torso Maximum Deviation Comparison Results 29

Table 2-3 Full Torso RMS Comparison Results 31

Table 2-4 Full Torso Analysis Results Comparison..... 32

Table 3-1- Description of Participants 41

Table 3-2 Isolated Back Max Deviation Comparison Results 44

Table 3-3 Isolated Back RMS Comparison Results..... 46

Table 3-4 Comparison for Patch Max Deviation Determined Via the Full Torso Analysis and the Isolated Back Analysis 49

Table 3-5 Comparison for Patch RMS Values Determined Via the Full Torso Analysis and the Isolated Back Analysis 49

List of Abbreviations/Acronyms

Abbreviation/Acronym	Meaning
AIS	Adolescent Idiopathic Scoliosis
CSVL	Central sacral vertical line
DCM	Deviation color map
GPL	General Public License
GNU	Phonetically pronounced – guh-new. A recursive acronym based on computer code. The letters do not each stand for a word, but a program operator. GNU is a free operating system used in the development of open source software.
HRQL	Health related quality of life
PMC	Plane of maximum curvature
RMS	Root mean square
SD	Standard deviation

List of Appendices

Appendix A –Surface Topography Asymmetry Analysis Procedure Using CloudCompare

Appendix B – Procedure for Isolation of Back Only Points Using CloudCompare

Chapter 1 - Literature Review

What is Scoliosis

Scoliosis is defined as one or more substantial abnormal curves in the vertebral column (1) (2). Normally the back has curvature in the sagittal plane and is straight vertically in the coronal plane, but scoliosis patients experience 3-dimensional curvature and twisting of the spine that results in abnormal curvature in both the coronal and sagittal planes (3).

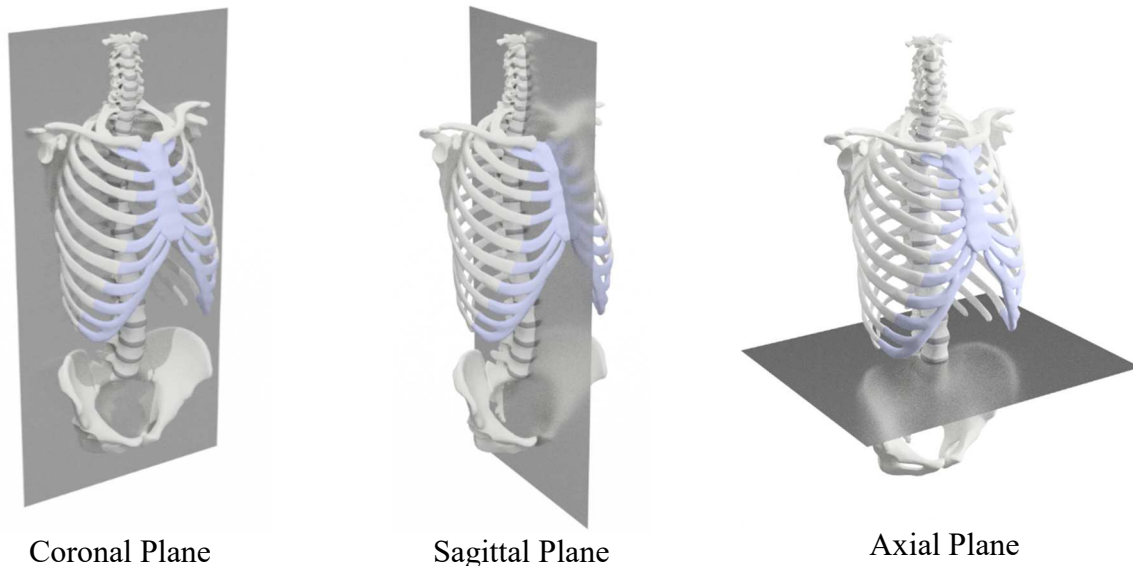


Figure 1-1 Illustrations of the Coronal, Sagittal, and Axial Planes (4)

Although the exact causes of scoliosis are not known (5), the abnormal curvature can be influenced by a number of factors, including rotation of the vertebrae in the axial plane (6), imbalances in muscular development (7), structural abnormalities of the skeleton (6), or neuromuscular or musculoskeletal disorders (8). The abnormal curves can be present in the lower or upper portion of the back (lumbar or thoracic) or can bridge the two. It is important to keep in mind the 3D nature of the curves, although the 2D lateral curvature in the coronal plane is used to officially diagnose Scoliosis (5).

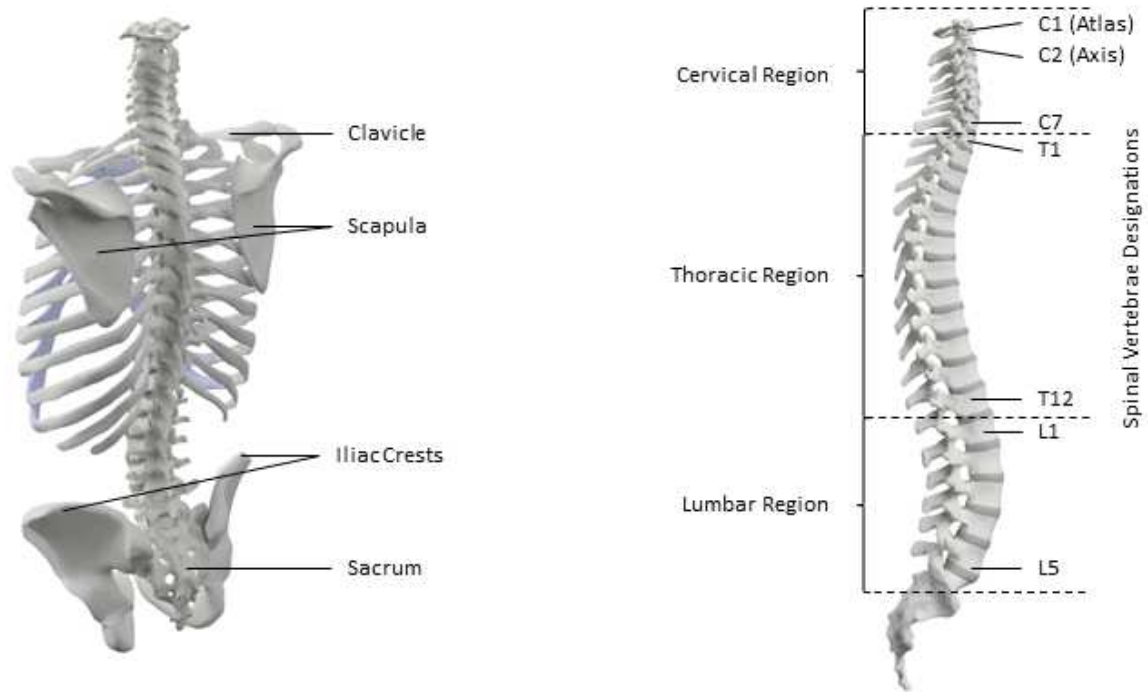


Figure 1-2 Illustration of the Skeletal Anatomy of the Back (4)

The Cobb angle is the most common measurement of the severity and extent of Scoliosis, often referred to as the “gold standard” for diagnosis of scoliosis (9) (10) (11) . The Cobb angle is measured in the coronal plane from two-dimensional X-rays by measuring the angle formed between a line drawn parallel to the top of the most tilted vertebrae above the spinal curve and a second line drawn parallel to the bottom of the most tilted vertebrae below the spinal curve (12). The curves are identified by identifying the apex of the curve and the significant vertebrae at the top and bottom of the curve (6). Kim et al. identify the apex of the curve as the vertebrae or disk with the greatest rotation or farthest deviation from the center of the vertebral column. Any vertebrae with maximal tilt towards the apex of the curve are considered part of the curve and are used in the measurement of the Cobb angle (6). This technique allows a measurement to be taken

of the lateral curvature in the 2-dimensional coronal plane only and does not account for the 3-dimensional curvature and twisting of the spine experienced in scoliosis (13).

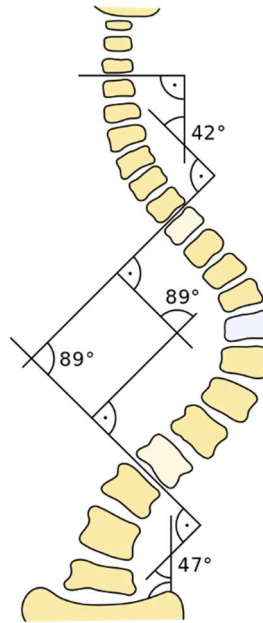


Figure 1-3 Illustration of the Measurement of the Cobb Angle (2)

If one or more of the curves, measured in the lateral plane using the Cobb method, is greater than 10 degrees, it is diagnosed as Scoliosis (14). If the degree of curvature is less than 10 degrees, it is known as spinal asymmetry (15). The measurement of the Cobb angle has also been found to have significant inter-observer and intra-observer variation. When using traditional radiograph techniques, variability of up to 4.9 degrees has been found in intra-observer observations, and 7.2 degrees in inter-observer readings (16). Digitally acquired radiographs have proven to help reduce the variability of Cobb angle measurements, with both intra and inter observer variability falling to 1.3 degrees when digitally acquired radiographs are used (16) (17).

One or more lateral curves may be present in the spine of the patient (14). These curves, regardless of the spinal region in which they occur, are categorized as structural or non-structural (6). Major curves are also called primary curves and are the largest of the abnormal curves and

the first to develop (6). Non-structural curves, or secondary curves, are smaller and are considered to develop after the development of the primary curve as a form of compensation by the body (6)

Although terms “structural” and “primary” curve are often used interchangeably, it is more accurate to label a curve structural if the residual coronal curve is 25 degrees or more as identified in an ipsilateral side bending radiographic view (6) (18).

Classifications of Scoliosis

The features of scoliosis which must be identified and understood include identifying the vertebrae that form the curve (which indicates the extent of spinal involvement), the curve type (structural or non-structural), right or left, the degree of angulation, and the degree of vertebral rotation (6).

Idiopathic scoliosis is classified according to the age of the patient (6) and the categories are related to levels of skeletal maturity, as shown in Table 1-1.

Table 1-1 Classifications of Idiopathic Scoliosis

Classification	Description
Infantile Scoliosis	Occurs in patients 0 – 3 years old
Juvenile Scoliosis	Occurs in patients 4 – 10 years old
Adolescent Idiopathic Scoliosis	Occurs in patients 11 – 18 years old
	After Skeletal Maturity
Adult Idiopathic Scoliosis	
Degenerative Scoliosis	

For cases of secondary scoliosis, where the appearance of symptoms of scoliosis are due to other factors, the categories are further broken down based on congenital, developmental, neuromuscular, or tumor associated causes of the scoliotic deformity (6). Of all the classifications of the scoliosis, Adolescent Idiopathic Scoliosis (AIS) is the most prevalent form with 80% of cases of pediatric scoliosis being classified as Adolescent Idiopathic Scoliosis (8).

Two main classification systems exist to specify the extent and severity of scoliosis (6). The King classification takes into account 5 different curve types (19), describing curves as shown in Table 1-2. This system was developed in 1983 to enable treatment of scoliosis using Harrington rod instrumentation (20), which was a stainless steel rod inserted into the patients body along the spinal column to treat abnormal spinal curvature (21).

Table 1-2 Classification Categories for the King Classification System for Scoliosis (19)

Curve Classification	Classification Criteria
Type 1	An S-shaped curve with the thoracic and lumbar curves meeting tangentially at the mid line and the lumbar curve larger than the thoracic curve
Type 2	Similar to the Type 1 curve, but with a larger thoracic curve than lumbar curve
Type 3	A curve in the thoracic region in which the lumbar curve does not cross the midline
Type 4	A long thoracic curve in which the L5 vertebrae is centered on the midline over the sacrum
Type 5	Double thoracic curve

As newer segmental instrumentation based techniques became more common, the King classification system was found to not provide sufficient guidelines for determining levels of vertebral fusion (20). The need for more specific classification lead to the development of the Lenke system in 2001 (18). The Lenke classification includes 6 classifications as shown in Table 1-3 (18). The curve classifications are based on 3 criteria:

1. Identification of the Major Curve
 - a. Based on which of the three regions of the spine the curve occurs in. There are 6 categories of designation for the spinal curve type
2. Assign a lumbar spine modifier to account for the distance of the center of the lumbar spine to the midline

- Assign a sagittal thoracic modifier which addresses the amount of lateral curvature to the thoracic region.

Table 1-3 Lenke Classification Structure (22)

CURVE TYPE				
Type	Proximal Thoracic	Main Thoracic	Thoracolumbar/Lumbar	Description
1	Non-Structural	Structural (Major)*	Non-Structural	Main Thoracic (MT)
2	Structural	Structural (Major)*	Non-Structural	Double Thoracic (DT)
3	Non-Structural	Structural (Major)*	Structural	Double Major (DM)
4	Structural	Structural (Major)*	Structural (Major)*	Triple Major (TM) ⁵
5	Non-Structural	Non-Structural	Structural (Major)*	Thoracolumbar/Lumbar (TL/L)
6	Non-Structural	Structural	Structural (Major)*	Thoracolumbar/Lumbar-Main Thoracic (TL/L-MT)

STRUCTURAL CRITERIA
(Minor Curves)

- Proximal Thoracic - Side Bending Cobb $\geq 25^\circ$
- T2-T5 Kyphosis $\geq +20^\circ$
- Main Thoracic - Side Bending Cobb $\geq 25^\circ$
- T10-L2 Kyphosis $\geq +20^\circ$
- Thoracolumbar/Lumbar - Side Bending Cobb $\geq 25^\circ$
- T10-L2 Kyphosis $\geq +20^\circ$

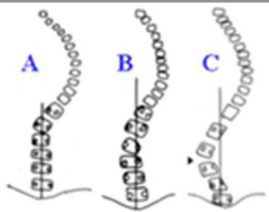
*Major = Largest Cobb measurement, always structural
Minor = All other curves with structural criteria applied
⁵Type 4 - MT or TL/L can be major curve

LOCATION OF APEX
(SRS Definition)

CURVE	APEX
Thoracic	T2-T11/12 Disc
Thoracolumbar	T12-L1
Thoracolumbar/Lumbar	L1/2 Disc-L4

Modifiers

Lumbar Spine Modifier	CSVL to Lumbar Apex
A	CSVL between pedicles
B	CSVL touches apical body(ies)
C	CSVL completely medial



Thoracic Sagittal Profile T5-T12	
- (Hypo)	$< 10^\circ$
N (Normal)	$10^\circ - 40^\circ$
+ (Hyper)	$> 40^\circ$

Curve Type (1-6) + Lumbar Spine Modifier (A, B, C) + Thoracic Sagittal Modifier (-, N, +)
Classification (e.g. 1B+): _____

The Lenke classification system is more widely used because it includes lumbar, thoracolumbar and thoracic curves, describes curves in the sagittal plane (which the King system does not) and has been found to have higher interobserver and intraobserver agreement than the King system (6).

Specifics of Adolescent Idiopathic Scoliosis

Adolescent Idiopathic Scoliosis is the most common form of scoliosis, accounting for 80% of all pediatric scoliosis cases, and has no known causes (2). AIS affects 2 to 3% of the overall population (23). Progression of scoliosis is a key concern, but adolescent idiopathic scoliosis tends to progress less than juvenile and infantile scoliosis (6). Only 5% of AIS patients experience curve progression beyond a Cobb angle of 30% (6). It is generally recommended that patients with AIS are monitored every 4 to 12 months, depending on their age and the progression of the curves. (6).

AIS primarily affects girls and is defined by a lateral spinal curvature before spinal maturity. The ratio of AIS patients is 4:1 girls to boys (6), and the most common lateral curvature is dextroscoliosis. Smaller curves tend to occur to a similar extent in both boys and girls (10) but more severe curves and progressing curves are more likely in girls, where a spinal curve with a Cobb angle exceeding 30 degrees is 10 times more likely in girls than boys (9).

Skeletal maturity is a major factor in the progression of scoliosis, making AIS particularly difficult because this stage involves significant skeletal growth at a relatively quick rate. Given that four times more girls than boys form the patient population, and breast tissue is far more susceptible to radiation doses than other tissues (24), current research into reducing x ray exposure is particularly important.

Impacts on patients

Numerous studies have been conducted to determine the impact of scoliosis on the quality of life of the afflicted patients. Multiple studies found that the condition can cause psychological distress, as well as physical distress in the form of back pain due to uneven loading of the spine (2) (10) (23). AIS patients report lower self-image and worse overall health

related quality of life (HRQL) scores (25). Scoliosis can also impair social interactions due to psychological distress and loss of confidence (8).

Patients who have a Cobb angle of 80 degrees or higher have higher rates of back pain and mortality associated with cardio pulmonary complications (6), although cardio pulmonary complications tend not to develop until much later in life (9). The progression of scoliosis after skeletal maturity depends on the severity of curvature (6). If the cob angle is less than 30 degrees after cessation of skeletal growth the curve tends not to progress (9). Curves with a Cobb angle of greater than 30 degrees at skeletal maturity tend to progress at a rate of 1 degree per year (6) (9).

Treatment options

All options for the treatment if scoliosis are focused on correcting the abnormal curvature of the spine. This correction can be accomplished through the use of a brace, physiotherapy, through surgical options, or a combination of these (2) (10). Prevention of curvature by correcting the condition as early as possible during skeletal maturation is key in effective and long-lasting treatment (10).

Braces can be effectively used to treat scoliosis for patients who have not yet reached skeletal maturity and have curves with a Cobb angle between 25 – 40 degrees (10). Braces may be rigid or soft, may be worn full time, part time or only at night, and may be worn until skeletal maturity or for select periods (10) (25).

Surgery is the more invasive option. Current standards suggest that spinal deformities that exceed 45 degrees are an indication for surgical correction (8). Surgery involves the insertion of metal rods in the patients adjacent to the spinal column. The metal rods are connected to the spinal column using screws and hooks which are used to force the spine into a

corrected position (2) (25). The vertebrae can also be fused together using bone grafts to fuse vertebrae together to maintain the corrected posture (26).

Curve progression

Studies have shown that AIS curve progression occurs in 10 to 15% of patients, while 22 to 27% experience spontaneous improvement (8). Note that spinal deformity may progress within a very short period of time (23). A spinal curve is deemed to have progressed if the measurement of the Cobb angle increases by 5 degrees between successive observations (27).

The size of the curve is an independent predictor of curve progression (23). In AIS patients periods of rapid growth may result in significant curve progression in as little as 4 months (6).

Methods for diagnosing and monitoring

X-rays for measuring the Cobb angle have been the go-to standard for diagnosing and monitoring scoliosis (11). AIS requires repeated radiographs until skeletal maturity, creating risks for the health of patients due to the effects of repeated exposure to low dose radiation (6).

Research conducted on female scoliosis patients receiving repeated doses of low-level radiation because of the x-rays during treatment indicates that the risk of breast cancer increases later in life (24). Recommendations have been made to reduce exposures whenever possible without sacrificing information required to effectively treat patients (28) (11).

The measurement of the Cobb angle from a single posterior x-ray does not take the vertebral rotation into account, and only provides a measure of the lateral deflection from the central sacral vertical line (CSVL), a straight vertical line drawn in the coronal plane through the S1 endplate (6). Other systems of classification have been proposed, such as that by Stokes et al. that takes into account the plane of maximum curvature (29). The plane of maximum curvature

(PMC) is defined as the plane passing through the centers of the vertebrae of the two vertebrae at each end of the curve and the vertebrae at the curves apex (30). This plan of maximum curvature measures the curvature angle in a similar manner to the Cobb angle, but uses the plane of maximum curvature as the datum for measuring the angles. While this method improves on the traditional Cobb angle measurement, it still reduces the measurement of the scoliotic deformity to a strictly 2D measurement. Various methods have been developed to analyze and quantify the 3D nature of the spinal deformity, including measurements of surface topography.

Surface Topography

Measuring the surface topography of patients with scoliosis has been explored since the 1960's (11), but recent advances in 3D scanning technology have made methods of analysis based on surface measurement more reliable (31) (13) (27) (32).

Initial efforts to capture and analyze the 3D surface topography of patients focused on the back exclusively and used a variety of tools to quantify characteristics of the surface topography that corresponded to scoliotic deformity. The Moiré fringe topography method (33) used visual light patterns to determine surface topography based on 2D images of fringes by analyzing the patterns resulting from projection onto the back of the patient. An example of the Moiré method is shown in Figure 1-4.

The Moiré method made use of existing photostereometric techniques and technology, providing an opportunity to record and store visual records of scoliotic deformity for record keeping and analysis of progression. The technique was limited in its use because of its tendency to have a high rate of false positives (33).

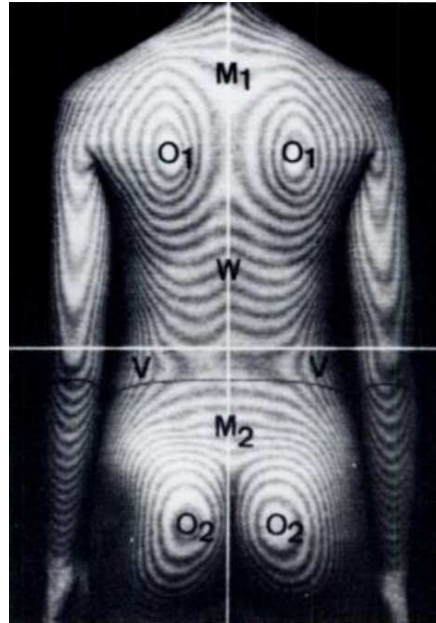


Figure 1-4 Example of Moire Fringe Topograph (33)

More modern techniques of examining the patients back include the use of 3D scanners which use reflected laser measurements to create 3D point clouds. The laser light used to take the measurements is non-invasive and does not subject the patient to radiation. The point clouds produced by this technique have thousands of points that can be measured and manipulated in a computer program to better understand and quantify measurements of the objects from which the measurements were taken (13).

Early attempts to utilize this technique depended on markers placed on various anatomical landmarks to provide a consistent frame of reference, but this proved problematic. It was difficult to consistently identify and mark the anatomical points such as the point of the inferior angle of the scapula and the iliac crests (34). If the markers are not consistently placed in each examination the results of the analysis will not give an accurate picture of the progression of the spinal curves. In order to avoid this drawback, markerless measurement techniques have been developed, such as using anatomical symmetry to provide a measure of deformity (13). This removes the need for markers and enables a rapid measurement of the severity of deformity.

Two approaches to symmetry analysis were examined by Hill et al. for their reliability and effectiveness – rotoinversion and reflection (35). In the reflection technique the plane about which the torso is mirrored is determined by determining a best fit plane that is based on the sagittal plane of the torso. By comparing the position of the sagittal plane to all points within the point cloud, and iteratively adjusting the position of the plane until a best fit position is found, the best possible plane of symmetry is determined. Utilizing rotoinversion involves mirroring the point cloud about the sagittal plane, then using best fit algorithms to adjust the position of the reflected torso until it is as close to coinciding with the original torso model as possible. Both techniques have demonstrated similar results for objects with bilateral symmetry, and Hill et al. demonstrated that either approach can be used to examine asymmetry in torso models for scoliosis patients (35).

Ho et al. built on this work in asymmetry analysis to determine the correlation between surface asymmetry and radiographic measurements of the Cobb angle (13). In this analysis technique, the reflection method from Hill et al. was used to analyze asymmetry in healthy patients who were not diagnosed with symptoms of scoliosis. Visualizations of deviations from symmetry were created by comparing the original surface topography mesh with the mirrored copy of the same mesh. This creates thousands of measurements of deviation, which can be represented by coloring each facet of the mesh with a color corresponding to the deviation. The resulting deviation color map (DCM) provides a visual indicator of the quantified difference between the two meshes, as seen in Figure 1-5. The colors illustrate deviation values assigned to each face of the mesh based on the deviation assigned to each vertex on the face. The color legend in Figure 1-5 has been set to the same intervals and colors as those used by Komeili et al. (31) (13) (27) and Ghaneii et al. (32) and is shown in Figure 1-6.

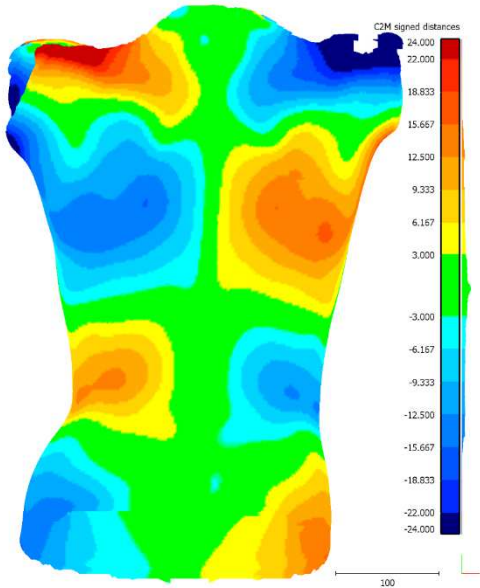


Figure 1-5 Example Deviation Color Map

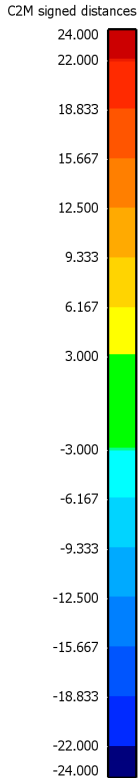
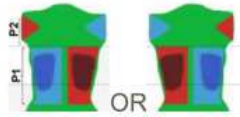
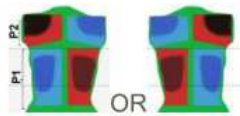
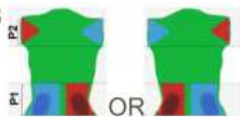

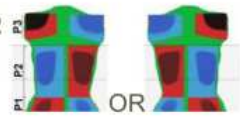



Figure 1-6 - Color Map Legend and Limits

The DCM provides clear indications of the locations of localized deviation patches (31). Komeili et al. applied this technique to patients suffering from Adolescent Idiopathic Scoliosis (31). External deformities in the surface of the patients back were visible as patches on the DCM. The patches were used to understand the number, direction, and severity of the scoliotic curves (31).

Komeili et al. have proposed a rubric for classifying patients with a group identifier based on the location of the deviation patch or patches. Figure 1-7 from “Surface Topography Asymmetry Maps Categorizing External Deformity in Scoliosis” illustrates these groupings.

Group	Subgroup	Description of individual color patches
Group A (2 asymmetry patches)	A1	 <p>First Patch: located in sections 1st and 2 with the center of deformation close to the boundary between sections 1 and 2 representing thoracic/thoracolumbar curves. Second Patch: located in section 3 and characterizes shoulder asymmetry.</p>
	A2	 <p>First Patch: same as subgroup 1. Second Patch: located in section 3 with the center of the patch located close to the scapula.</p>
	A3	 <p>First Patch: located strictly in section 1 representing lumbar curves. Second Patch: located strictly in section 3 and characterizes shoulder asymmetry.</p>
Group B (3 asymmetry patches)	B1	 <p>First Patch: located strictly in section 1 representing lumbar curves. Second Patch: located in sections 1 and 2 with the center of deformation located close to the boundary between sections 1 and 2 representing thoracic and thoracolumbar curves. Third Patch: located in section 3 and characterizes shoulder asymmetry.</p>
	B2	 <p>First and Second Patches: same as subgroup 4. Third Patch: located in section 3 with the center of the patch located close to the scapula.</p>
Group C (4 asymmetry patches)	C1	 <p>First, Second, and Third Patches: located in and between sections 1 and 2. Fourth Patch: located strictly in section 3 and characterizes shoulder asymmetry.</p>

* Sections 1, 2, and 3 represent the *Figure 1-7 Color Patch Classification Table (13)*

Subsequent research by Komeili et al. isolated these patches by selectively filtering for deviations within a given range, then each individual patch can be analyzed for the maximum deviation within the patch and the root mean square of all deviation measurements (13). The measurements of maximum deviation and root mean square of all deviation measurements within a patch can be used to categorize the deformity in decision trees (27). Several limitations were identified with these decision trees related to the sensitivity and specificity of the classification resulting from the use of the trees. In some cases mild curves were mistakenly classified as moderate due to the high sensitivity (95%) and low specificity (35%) of the decision tree classification method. Further research by Ghaneei et al. applied a custom neighborhood classifier algorithm to the classifications based on isolated patches to improve the specificity of the use of the decision trees (32). This research helped to improve the accuracy of the assessment of the curve severity by 17% and progression of scoliotic deformity in subsequent examinations by 58% (32). Ghaneei et al. applied a k-nearest neighbor algorithm to the measured maximum deviation and root mean square values for all patients in the test group (32). A test group of data is used to establish reliable guidelines for assessing the classification of a data point, essentially teaching the algorithm based on a reliable set of classifications. Once the algorithm is prepared through the examination of the test data, new data points can be analyzed and their classification determined based on the decision boundaries determined from the test data. The use of this technique by Ghaneei et al. as helped improve the sensitivity of the use of the decision trees, with a small decrease in specificity (32). Ghaneei et al. also proposed the patch isolation threshold of 9.33mm used in this study (32), as opposed to the 3mm threshold used in previous studies (13) (31) (27). The previously used 3mm threshold was found to sometimes result in two

different patches merging or having indistinct boundaries, or wrapping around the torso to the anterior section (32). The 9.33mm threshold helped to mitigate these issues, allowing most patches to be clearly delineated.

Use of the 3D scanning for markerless 3D assessment of surface topography has provided promising results for determining the severity of scoliotic deformities and their progression. Often the data acquisition for these methods involves a 3D scan of the entire torso of the patient, which can be detrimental to the patient experience. Given that the majority of patients dealing with Adolescent Idiopathic Scoliosis are female and that the progression of scoliotic curves must be monitored frequently throughout adolescence, it is understandable that the process of examination can be uncomfortable for these patients. In order to improve patient comfort during the collection of the 3D data, research has been conducted to determine if a scan of the back alone can provide sufficient data for diagnosis and monitoring of curve progression. Current research into the use of surface topography techniques using landmark based parameters indicate that the isolated back scans do not provide reliable results for monitoring curve progression (36). The method of markerless 3D assessment using asymmetry used by Komeili et al. has not been tested with back only data previously.

Open Source Software Approach

Assessment of 3D surface topographies require several pieces of specialized hardware and software in order to perform the full analysis. The 3D point cloud must be collected utilizing multiple 3D scanners, and specialized software must be used to process, analyze and quantify the results.

The cost of 3D scanners has been steadily declining since their introduction, in part due to their popularity in architecture, engineering and construction applications. As the affordability

of the scanners continues to improve, the cost of hardware will be less and less of an impediment to the clinical application of 3D surface topography assessment.

The software required for extensive 3D point cloud analysis can be very expensive, and often is limited in the scope of its application. It is not uncommon for 3D point cloud analysis programs that can perform the functions necessary for surface topography assessment to cost anywhere from \$5000 to \$20,000 CDN. This high cost can be a challenge for researchers and clinicians in getting funding or budget approval to obtain the necessary software. One possible solution to this problem is to utilize open source software created by community programmers under the GNU General Public License (GNU GPL) license scheme. Software with this license type is free for personal or commercial use, with the only requirement being that any modification to the software or derivative software be made freely available. The full terms and conditions of the GNU GPL can be found at <https://www.gnu.org/licenses/gpl-3.0.en.html>.

If suitable open source software can be employed for 3D point cloud analysis and surface topography assessment this impediment to clinical application could be completely removed. Additionally, the software would be perfect for new researchers to develop software tools that can be freely shared amongst researchers and clinicians, enabling the gradual development of suites of tools that leverage the data available in 3D point clouds. One aim of this paper is to explore the use of a specific open source program called CloudCompare (version 2.9.1) to determine its suitability for use in markerless 3D assessment of surface topographies for treating Adolescent Idiopathic Scoliosis.

Thesis objectives**Problem statement**

The need for repeated radiographs during diagnosis and treatment of adolescent idiopathic scoliosis increases risks of cancer for patients (24) (11). Markerless 3D assessment of asymmetry using deviation color maps has proven to be an effective means of monitoring the progression of scoliotic deformity and reducing the number of x-rays required during treatment (31) (13).

Previous applications of surface topography utilized high cost proprietary software called Geomagic and focused on analysis of the entire torso (27).

Objectives

The objective of this thesis is to determine if open source software can be used as cost effective alternative to proprietary software. The hope is that if the barrier to entry associated with the cost of the analysis tools is lowered, more researchers will be able to make use of this method and patients will more frequently see the benefits of markerless 3D assessment using points clouds.

The second objective of this thesis is to determine if the analysis method used on the full torso scans can be used on isolated back scans. Reducing the area of the torso needing to be scanned to the back alone would improve the patient experience by not requiring them to have their upper torso fully exposed. In addition, many existing techniques for diagnosing and monitoring scoliosis also rely on back only measurements, such as photostereography and multiple measurement indices that rely on anatomical landmarks on the back only (37). Analysis of the isolated back using surface topography could potentially provide better comparisons to existing information databases based on back only data and popular index measurements used in clinical settings.

Outline

In order to determine if open source software can replace the more expensive proprietary software, the original analysis will be replicated with the open source software and the results will be compared.

Once the use of the open source software is demonstrated as viable, this investigation will use the open source software to isolate back only points from the full torso scans used previously and perform the asymmetry analysis on the back only points. Once results are determined using these isolated points, the outcomes of the back only analysis and the full torso analysis will be compared to determine if the back only analysis is a viable alternative.

For both steps in the analysis – the comparison of results between different software programs on the full torso scans, and the comparison of results for the full torso analysis versus the isolated back analysis – the alternative method will be considered acceptable if the 95% confidence interval is within 3.4 mm of the results from the previous study. This threshold will apply to both the max deviation and the root mean square results for each deviation patch identified. This threshold for acceptance is based on previous studies that have indicated healthy patients without scoliosis had a standard deviation of max deviation of $3.4 \pm 0.8\text{mm}$ (31).

Chapter 2 – An Open Source Software Approach to Markerless 3D Assessment of Adolescent Idiopathic Scoliosis Using Asymmetry

The method of markerless 3D assessment of torso asymmetry using surface topography involves comparing a 3D mesh formed from 3D scan points of a patient's torso with a mirrored version of that same mesh. The maximum deviation between these two meshes, as well as the root mean square of the deviation values, is determined to produce quantifiable measurements of the degree of severity of scoliotic deformity (31). Repeated measurements can aid clinicians in tracking the progression of spinal curve development. This method comparison seeks to explore using CloudCompare, a free, open source 3D point cloud analysis program, to replace methods used in previous studies which relied on proprietary programs. The purpose of exploring this alternate method is to reduce the costs associated with the analysis of the point clouds and to develop a simplified analysis workflow.

CloudCompare was identified as a potential alternative following an online search of various 3D point cloud analysis programs using the search term "3D Point Cloud Analysis Software" on the Google search platform. CloudCompare was the only program found that was governed by the open source software license, allowing not only free use of the software but also the development of custom add-ons.

Description of Full Torso Asymmetry Analysis

The previous full torso analysis performed by Komeili et al (27) utilized a point cloud capture used in previous research by Parent et al. (38) and Emrani et al. (39) This approach involved utilizing 4 Minolta scanners to capture 3D point cloud data from the front, back and sides of the torso simultaneously. These 4 individual point clouds were then registered to form a

single amalgamated point cloud using the Konica Minolta Polygon Editing Tool (PET version 2.21) (31). The regions of the point cloud related to the torso were isolated by manually deleting areas outside of the torso itself. Points located on the neck above the spinous process C7 as well as points below the posterior superior iliac spine were deleted (31). Points along the arms were deleted by drawing a vertical line through the posterior corner of the acromion (31).

Once the torso points were isolated, a best fit plane of symmetry was determined in the software and the torso was reflected about this plane, creating two torsos superimposed on each other. The shortest distance from each point on the original torso to the reflected torso was then calculated in Geomagic using the '3D Comparison' function (32), with the resulting measurement being represented in a deviation color map (DCM) on the surface of the original

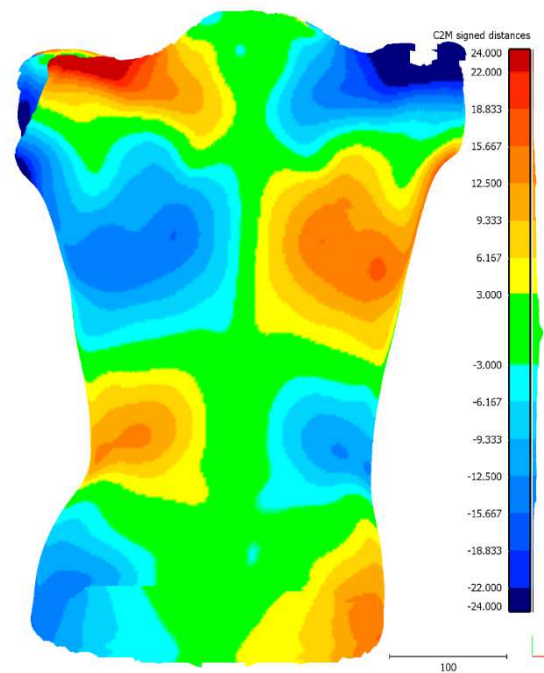


Figure 2-1 Example Deviation Color Map
torso as illustrated in Figure 2-1.

This torso analysis resulted in patches of deviation which were clearly visible in the color maps. Each zone of deviation would result in corresponding patches on the left and right side of

the plane of symmetry. Because of symmetry, only patches on the right side of the plane of symmetry were used for extracting values of maximum deviation and the root mean square of deviation within the patch.

This method of analysis has provided very promising results for markerless assessment of scoliosis using surface topography (31), but the original method relied on Geomagic, an expensive proprietary software.

CloudCompare (version 2.9.1) is an open source program for the processing and analysis of 3D point clouds and triangulated irregular network (TIN) surfaces (40). The program is well suited to analyzing the type of data produced by the capture techniques employed by Komeili et al (31). The use of this program is free for both personal and commercial use, and the development of the program and custom add-ons is governed by the GNU General Public License.

GNU is a Unix compatible software structure developed by the Free Software Foundation. The aim of GNU is to create software that is non-proprietary, and can be downloaded, modified, and distributed by anyone (41). The GNU General Public License (GNU GPL) is a license that ensures that any GNU software cannot be limited in distribution in future iterations of software, even after modifications or add ons have been created. CloudCompare was created on the GNU framework and is distributed under the General Public License (GPL), ensuring that the program will remain free to use and can be modified and redistributed by anyone.

In order to determine if CloudCompare is a viable alternative to Geomagic, the same point cloud data analyzed by Ghaneei et al. (32) was used. The first step was to create a mesh from the point cloud of the full torso. This newly created mesh was then mirrored about the

sagittal plane to create two superimposed torso meshes. The position of the mirrored torso mesh was then manipulated using the programs registration tools to find a best fit between the two torsos. The program was then able to isolate the patches and provide max deviation and root mean square (RMS) results to be compared with the results from the previous study. Appendix A contains detailed instructions on how CloudCompare was use to accomplish these steps, including explicitly listing the functions and tools used.

It is important to note that this process of analysis differed slightly from the process used in previous studies (31) (13) (27) (32) in that in the previous studies process the best fit analysis was performed on the plane of symmetry, then the torso mesh was reflected about that plane. In this analysis, the torso was reflected about the sagittal plane then the best fit analysis was performed on the mirrored torso mesh. The position of the sagittal plane was determined by physical frame that the patients stood inside and grasped with their hands, creating consistent posture from patient to patient. This method was explored by Hill et al in “Assessing asymmetry using reflection and rotoinversion in biomedical engineering applications” (35). The previous method utilized reflection, whereas this method used rotoinversion. According to the findings of Hill et al. both methods produce the same results for bilaterally symmetric objects and were found to produce similar results when applied to adolescent idiopathic scoliosis (35). A full description of the steps taken to perform the analysis with CloudCompare can be found in Appendix A.

When isolating the deviation patches for analysis a deviation boundary limit of 9.33mm deviation was used. This limit value was found to reduce instances of false negatives by removing small asymmetry instances that don't reflect true scoliotic deformities (32).

The results of the maximum deviation analysis and root mean square values will be compared using a direct comparison graph, which compares the corresponding results from each method directly, and a comparison of the average value of the two methods compared to the difference between the two values. This technique of analysis for method comparison studies is proposed by Altman et al. as a way to identify correlation and bias when comparing two different methods of measurement (42). The graph illustrating the direct comparison shows how closely the results of the two methods correspond on the same data set. The graph comparing the average value of the two methods to the difference between the two helps to identify the magnitude of disagreement and identify any bias. In this paper this second type of graph will be referred to as the Bland-Altman Plot. The bias represents systematic inaccuracies that demonstrate some level of consistency. If an acceptably consistent bias is identified, it is possible to propose a calibration to the new method to produce comparable and repeatable results (43). For instance, if the results of the isolated back analysis method were found to consistently be 5 mm higher than the full torso analysis, a calibration of 5mm would allow the isolated back results to be compared to the full torso analysis. However, if the bias indicates only that the results of the isolated back analysis are consistently positive, but vary significantly in magnitude, this bias could not be used to create a calibration for comparison.

Data used

Table 2-1- Description of Participants

Test Participants	
Total Patient Scans	67
Total Isolated Patches (Corresponding to Scoliotic Curves. Sometimes more than one per patient)	85
Age Range, years	10 - 18
Cobb Angle Range, °	13 - 60
Gender, n	

Test Participants	
Male	12
Female	55
Curve Type, n	
Lenke 1	41
Lenke 2	0
Lenke 3	4
Lenke 4	0
Lenke 5	40
Lenke 6	0

Sixty-seven back scan files were available from individual patients from previous studies. These available datasets included the patient parameters such as height, weight, and curve classification, raw point clouds, and results for the patch isolation and RMS and max deviation results for each patch.

In order to have an accurate comparison between the previous full torso analysis, the open source software torso analysis, and the isolated back analysis, 18 datapoints were excluded because the deviation was so close to the 9.33mm threshold that the RMS wasn't calculated in one of the two analysis. Only those datasets which provided clear and unambiguous results in all three sets of analysis were considered in the overall comparison.

Figure 2-2 illustrates an example of a full torso analysis where the identified patches in the full torso analysis using the open source software did not identify patches beyond the 9.33mm threshold. In order to quantify patches to compare between the three methods (Geomagic analysis, CloudCompare full torso analysis, and the CloudCompare isolated back analysis), the perimeter of the patch must be identified by the 9.33mm threshold in all three analyses. Without clear delineation provided by the 9.33mm threshold, an accurate comparison

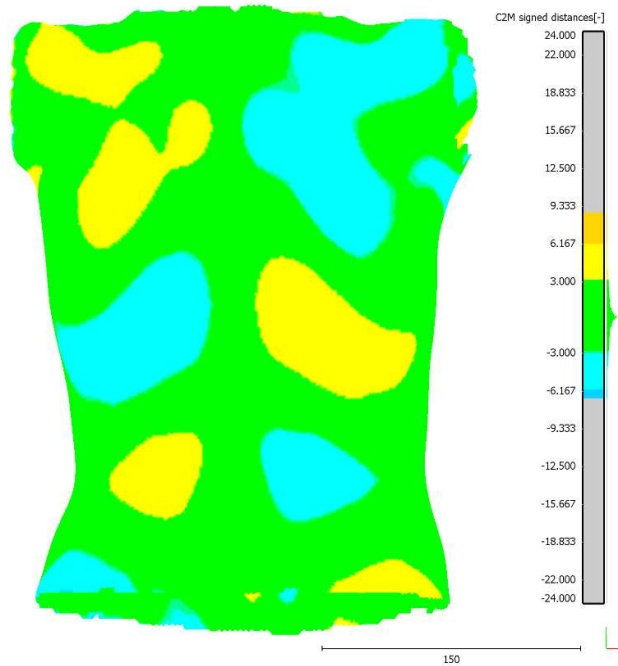


Figure 2-2 Example Of Excluded Data - Insufficient RMS for 9.33mm Threshold cannot be carried out and the patch was excluded from comparison.

Results

Comparison of maximum deviation.

The analysis of the results of the comparison of the two methods was carried out following the suggested procedure in “Design, Analysis and Interpretation of Method-Comparison Studies” (43). The measurements for max deviation from the previous study was plotted against the result

obtained from this method and plotted in Figure 2-3. Each data point is placed using the results of the previous study as the y component and the results from the CloudCompare method as the x component.

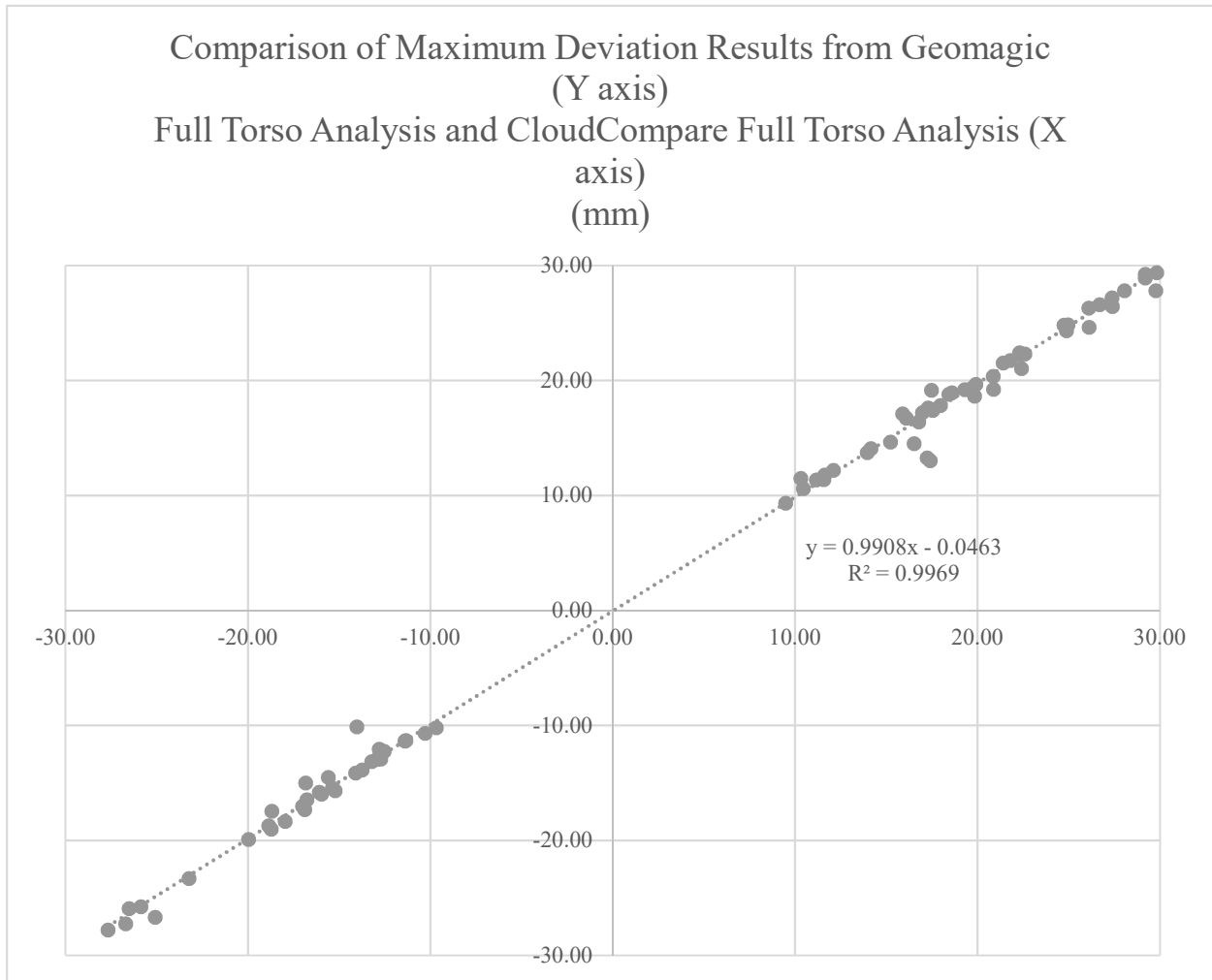


Figure 2-3 Full Torso Analysis – Scatter Plot of CloudCompare Max Deviation vs Geomagic Max Deviation

A Bland-Altman plot (42) was also prepared using the analysis results. The average of each set of results was plotted on the x axis, with the difference between the two results (the original Geomagic results minus the CloudCompare results) plotted on the Y axis. This plot is recommended by both the Bland Altman study (42) and the Hanneman study (43) as a means of

quantifying and communicating the bias and confidence limits of the two tests. The Bland-Altman plot for the analysis of the max deviation is shown in Figure 2-4.

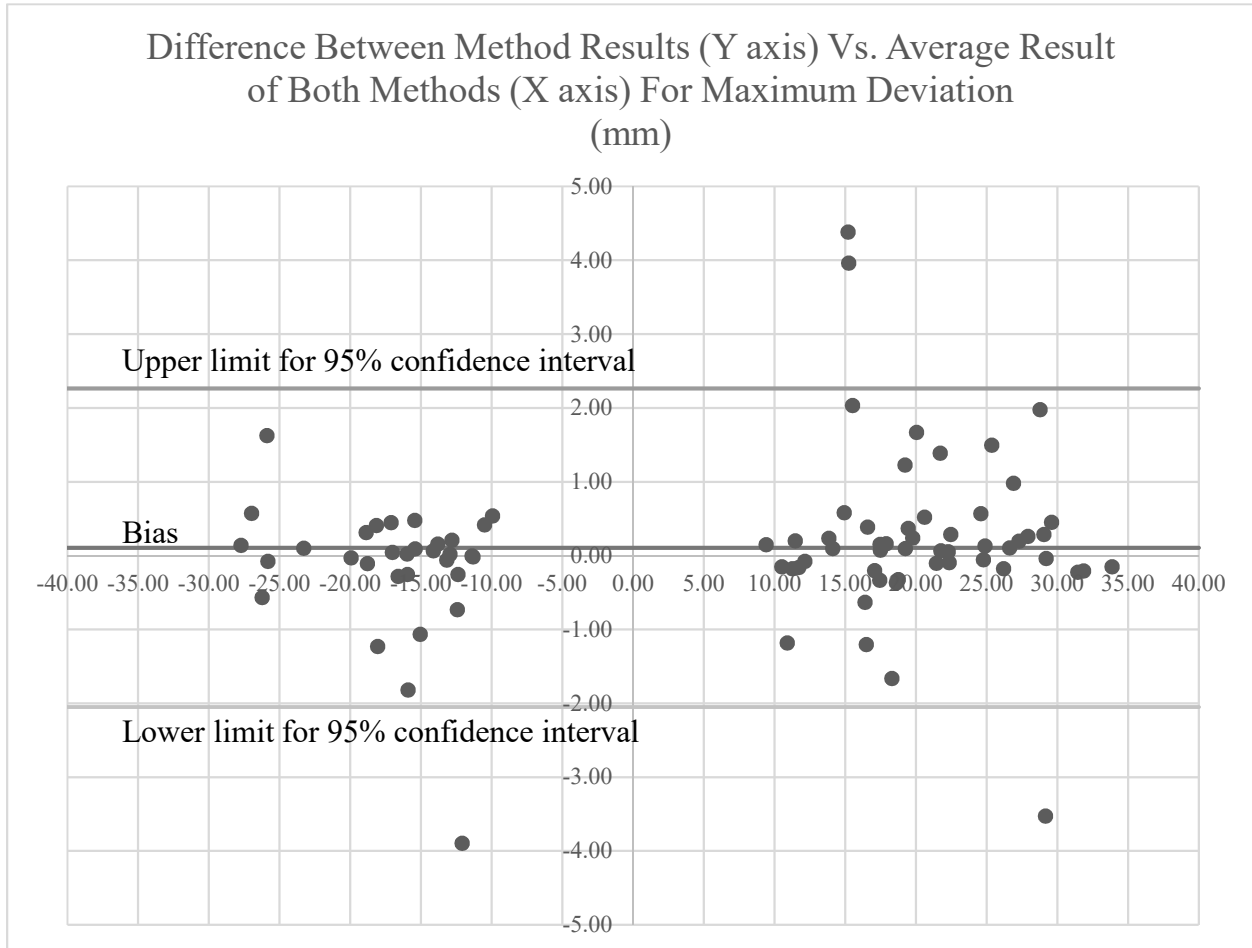


Figure 2-4 Scatter Plot of the Measured Differences Between CloudCompare Max Deviation and Geomagic Max Deviation

The Bland-Altman plot includes a horizontal line indicating the average value of the difference between the two methods, which is an indication of the bias of the method. Also shown on the plot are two horizontal lines indicating the upper and lower limits of the 95% confidence interval, calculated by determining the standard deviation of the results for the difference

between the two methods. These results are summarized in Table 2-2 Full Torso Maximum Deviation Comparison Results.

Table 2-2 Full Torso Maximum Deviation Comparison Results

Max Deviation Comparison Results	
Number of Data Points	85
Standard Deviation of the Difference	1.08 mm
95% Confidence Interval (1.96 SD)	+/- 2.115 mm
Average Difference (Measurement Bias)	+0.11 mm for Open Source Method
Precision (R^2)	0.9969
Percentage Error	3.4%

The average of the difference between the two methods on the Bland-Altman Plot indicates a bias of +0.11mm in the measurement of the maximum deviation using this new method, indicating a slight overestimation by the open source software method. The standard deviation for the difference in measurement between the two methods was 1.08 mm, giving a range of 1.08 ± 2.115 mm as the 95% confidence interval for the max deviation measurement from the new method. Komeili et al. study “Surface Topography Asymmetry Maps Categorizing External Deformity in Scoliosis” indicates that the significant deviation over the entire torso is indicative of the asymmetry. Healthy patients without scoliosis had a standard deviation (SD) of max deviation of 3.4 ± 0.8 mm (31).

Comparison of RMS

The comparison of the RMS values for the two methods was conducted in the same manner as the comparison of the max deviation results. The values for the RMS results from the previous method were plotted along the x axis, and the values from the new method were plotted along the y axis in Figure 2-5.

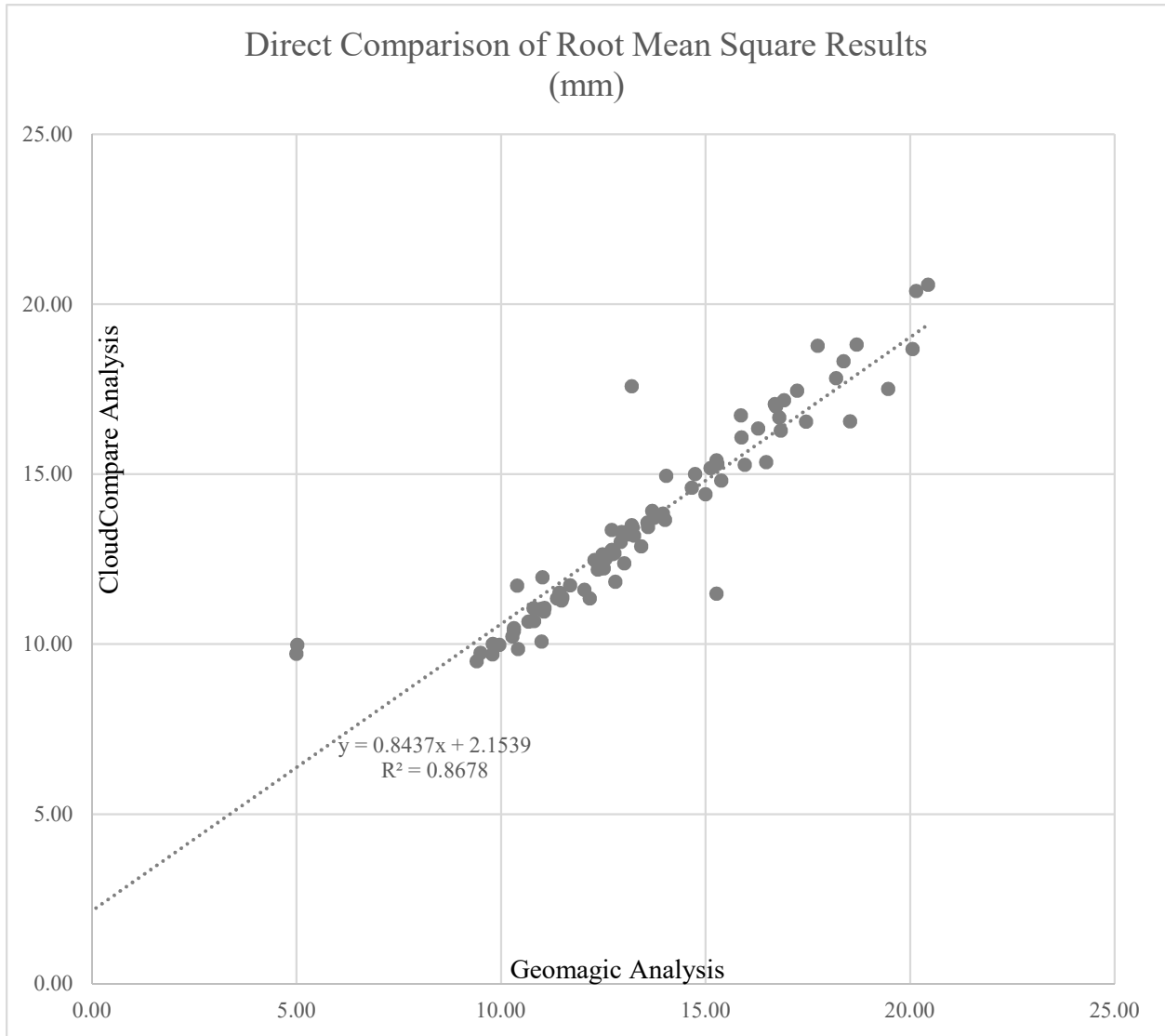


Figure 2-5 Scatter Plot of CloudCompare RMS vs Geomagic RMS

The Bland-Altman Plot was calculated in the same manner as for the max deviation analysis and is presented in Figure 2-6.

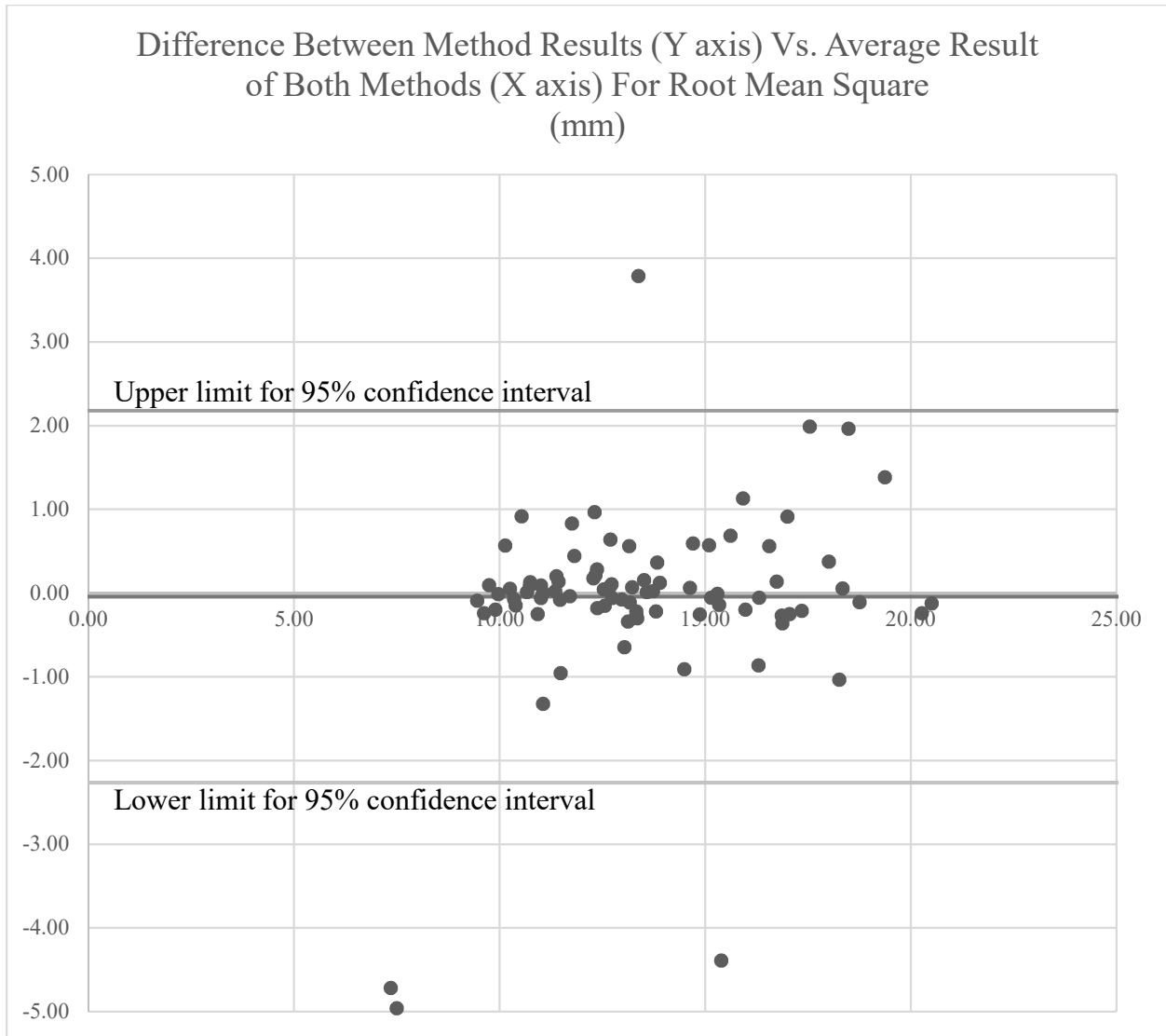


Figure 2-6 Scatter Plot of the measured differences between CloudCompare RMS and Geomagic RMS

The results of the RMS comparison between the two methods are summarized in Table

2-3

Table 2-3 Full Torso RMS Comparison Results

RMS Comparison Results	
Number of Data Points	85
Standard Deviation	1.11
95% Confidence Interval (1.96 SD)	+/- 2.18 mm
Average Difference (Measurement Bias)	-0.043 mm
Precision (R^2)	0.8678
Percentage Error	4.6%

Together, the results for the comparison of the analysis of the full torso model using the Geomagic method and the CloudCompare method show that the CloudCompare method reliably provides equivalent results and can be used as a viable alternative.

A comparison of the results between the two methods is shown in Table 2-4.

Table 2-4 Full Torso Analysis Results Comparison

	Max Deviation Comparison Results	RMS Comparison Results
Bias	0.11 mm	-0.043 mm
Confidence Limit	+/- 2.12 mm	+/- 2.18 mm
Percentage Error	3.5%	4.6%
Precision (R^2)	0.9976	0.8678
Standard Deviation	1.08 mm	1.11 mm

The average difference between the results of the two methods indicate the bias of the new method. For the measurement of the max deviation between the original back mesh and the mirrored back mesh the bias in the measurement from the new method was +0.11 mm higher than the previous method. For the measurement of the RMS of each patch the bias was -0.043mm, indicating slightly lower measurement of RMS in the new method.

The close correlation between the two methods for the value of the maximum deviation and RMS as well as the almost exact correlation for the location of the patches visible in the DCM very strongly support the conclusion that the CloudCompare method can be used as a cost effective and user-friendly method of performing the markerless surface topography analysis using symmetry as researched by Komeili et al.

Discussion

The method of markerless 3D assessment of torso asymmetry using surface topography involves comparing a 3D mesh formed from 3D scan points of a patients torso with a mirrored

version of that same mesh. The deviation between the two meshes provides valuable insight into the nature of the scoliotic deformity and repeated measurements can aid clinicians in tracking the progression of spinal curve development. This method comparison study sought to explore using CloudCompare, a free, open source 3D point cloud analysis program, to replace methods used in previous studies which relied on multiple programs with expensive licensing costs. The study compared the analysis of a full torso scan of patients diagnosed with Adolescent Idiopathic Scoliosis using the two methods to determine the reliability of the new method. The CloudCompare method of analysis proved to be a viable alternative to the previous method, with a standard deviation of 1.11 mm in the difference between the measurements of max deviation and 1.08 mm in the measurement of difference between the results of the root mean square analysis.

The viability of the open source software approach creates an opportunity to expand the use of this analysis method by lowering the barrier of entry of software costs for clinicians. It also opens the possibility of creating software add-ons for the CloudCompare program to enhance and focus the abilities of the software for 3d assessment of scoliotic symptoms. A custom tool to streamline the markerless asymmetry method could be created, as well as tools focused on other methods of 3D assessment. A suite of clinical tools could be created and freely distributed under the GNU General Public License to further the use of 3D scanning and assessment for the treatment of Adolescent Idiopathic Scoliosis.

The open source software method is able to perform the entire workflow of analysis, including initial registration of the raw point clouds, trimming the raw point cloud to isolate the torso, and analysing the torso (or isolated back) point cloud to produce the DCM. Previous studies using the proprietary software method report an analysis time of approximately 10 - 15

min for the initial preparation of the torso point cloud to the final DCM (13). The open source workflow used in the course of this study was consistently completed within 10 minutes. This workflow is also very simple to carry out with the only requirement for the operator being basic computer literacy and minimal training in the workflow.

The greatest opportunity for improvement in the time required for each analysis would be realized if the workflow used in this study was automated in the form of a program add-on. One of the biggest advantages of using an open source software approach is the opportunity to alter the program according to the GNU open source license in order to optimize workflows. As mentioned previously, the GNU license allows add-ons to be created and added to the program with the only requirement being that the add-ons must be made freely available to others. With a custom add on using the workflow developed in the course of this study the analysis time for each patient could be cut down to an estimated 3-5 min.

Licensing costs are also an advantage to using the open source method. The cost of an educational license of Geomagic is approximately \$5000. CloudCompare is completely free, and has all the capabilities of Geomagic in relation to the surface topography analysis used in this study, although there are some capabilities of Geomagic that CloudCompare does not have, mainly related to computer aided drafting and model creation. Previous studies did not indicate that these features were used in the course of this study, but if these capabilities were required in the future this would have to be taken into account. Further studies could explore using other open source software programs that specialize in this type of 3D modeling, such as a modeling program called 'Blender', that could allow research to continue in the open source framework to reduce costs and improve accessibility.

In comparing the output of Geomagic and CloudCompare within the scope of this study, the outputs are very similar, as illustrated in Figure 2-7.

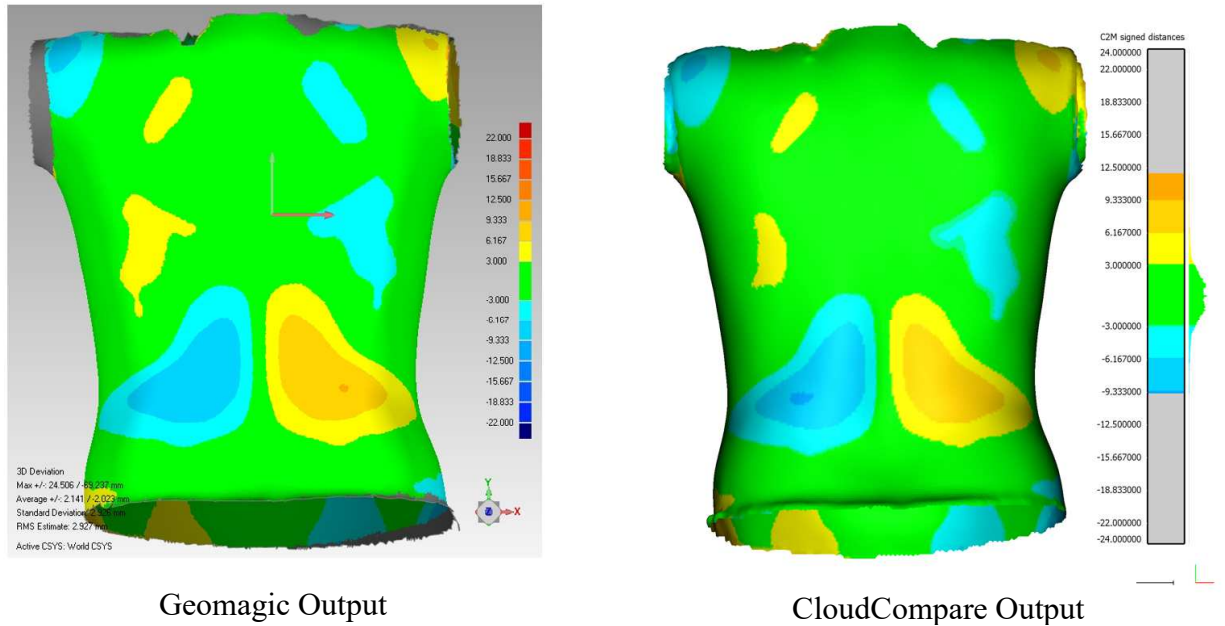


Figure 2-7 Geomagic (31) and CloudCompare Output Comparison

Both CloudCompare and Geomagic can produce customized output by adjusting options for the colours, shading, lighting, legend settings, etc.

Chapter 3 – Applying the Method of Markerless 3D Assessment of Adolescent Idiopathic Scoliosis to Isolated Back Scans

The previous chapter discussed the comparison of two different software packages in the analysis of a full torso scan. The results of that analysis indicated that the use of the open source software program CloudCompare was effective as an alternative to more expensive, proprietary software packages. In this chapter, the method of using the open source program on an isolated scan of the patients back is explored. The same data sets have been used throughout both comparisons, with the isolated back analysis performed by isolating points that are associated with the back only from the full torso scan. The criteria for determining points that are part of the patients back, and not sides or front, and the method of analyzing the isolated points, are described in the subsequent portions of this chapter.

The purpose of exploring this alternative method of markerless 3D assessment is to improve patient comfort during treatment. As mentioned previously, the majority of patients who experience adolescent idiopathic scoliosis are female, and the critical stage of monitoring and treatment of scoliotic deformity occurs during the early teenage years. To collect the full torso scan points, the patient must remove their clothing from the waist up and stand in the positioning frame with their arms raised as their torso is scanned. Understandably, this is psychologically uncomfortable for the patients. If the scan could focus solely on the back of the patient and allow them to wear an open backed robe or some other form of covering, it will greatly improve the patient experience.

Isolated Back Analysis

To analyze the isolated back, the normal vector of each point was determined using an algorithm built into CloudCompare. This algorithm determines the normal vector for any given point by

examining the location and relative orientation of neighboring points within a radius specified by the user, then anticipating the most likely surface represented by the group of points and assigning a normal vector to the examined point based on this anticipated surface. In this study a radius of 4.24mm was automatically computed by the program on the basis of the point cloud density and was found to provide consistent results. This process is repeated for every point, resulting in a field of vectors with the point cloud points as the base of each vector and their direction facing outward from the torso surface represented by the points. Then a plane is created that is parallel to the coronal plane but situated below all points in the cloud in the z direction. This positioning of the parallel plane helps to ensure a consistent reference for all points in the point cloud. The position of the coronal plane relative to the point cloud is determined by the positioning frame that the patient stands in and holds on to while the scan is performed. The frame consistently positions the arms, shoulders, and feet to provide repeatable physical restrictions on the posture that ensures reproducible positioning when the scans are performed. The position of the scanner to this frame is used to determine the x, y, z coordinates of all points in the point cloud, with the coronal plane determined as the XY plane in the point cloud coordinate system. The x coordinates indicate the position of the point perpendicular to the sagittal plane, the y coordinates indicate position perpendicular to the axial plane, and the z component indicates position perpendicular to the sagittal plane.

Once these vectors are determined, a filter is used to isolate only those points with a positive z value in relation to the offset coronal plane. Figure 3-1 illustrates this portion of the process.

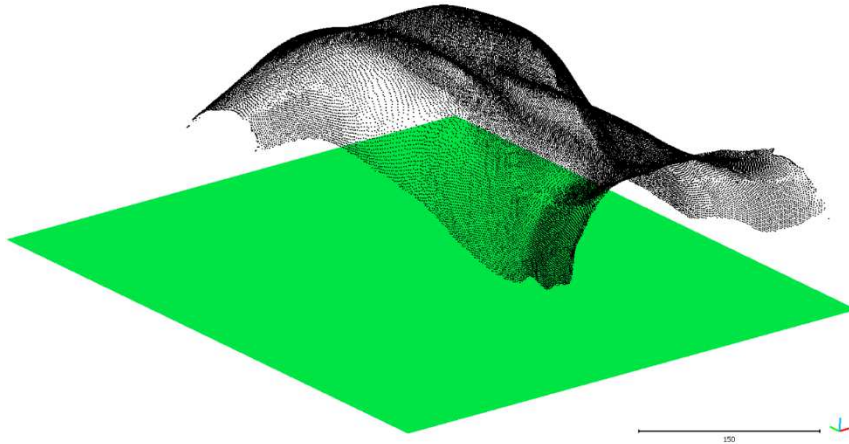


Figure 3-1 Isolated Back Points and Offset Coronal Plane

Once the points associated with the back only are isolated, a mesh is created from the points using the ‘Poisson Surface Reconstruction’ tool in CloudCompare, as demonstrated in Figure 3-2.

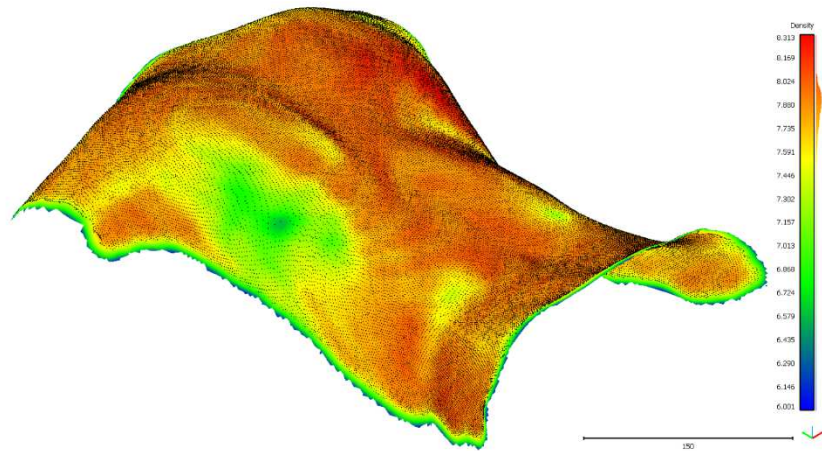


Figure 3-2 Isolated Back Mesh (Color Indicates Point Cloud Density)

This mesh is then mirrored about the sagittal plane by using the scale function and assigning a -1 scale factor to the x-axis only, to create two separate meshes as seen in Figure 3-3.

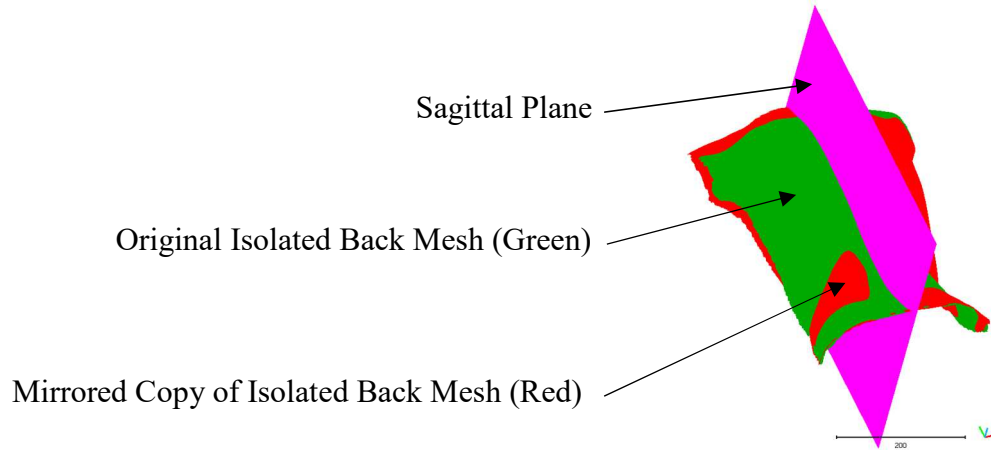


Figure 3-3 Visualization of Mirroring Mesh About Sagittal Plane

The mirrored mesh is then aligned to the original mesh using a process of best fit registration to find the closest correlation as demonstrated in Figure 3-4. This registration is done with the ‘Fine Registration’ tool in CloudCompare. The threshold for the RMS difference between the iterative steps was set to $1 \text{ e-}5$, as shown in Appendix A. This process results in a rotoinverted copy of the original mesh (35).

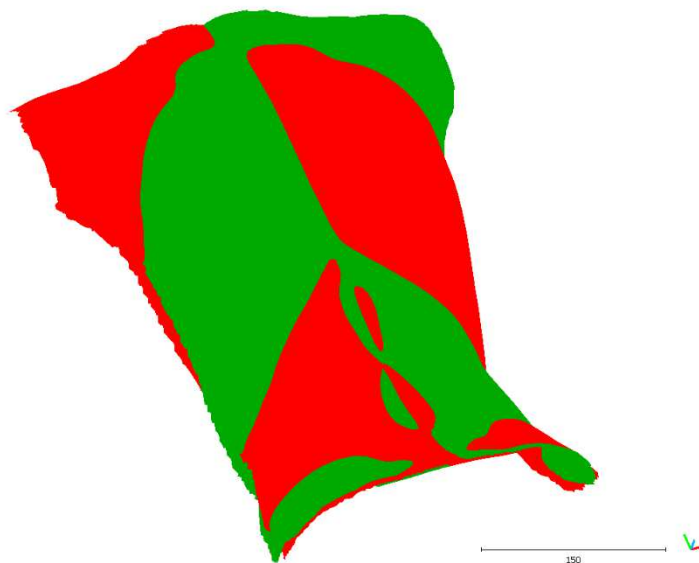


Figure 3-4 Registration of Mirrored Copy of Back Mesh

The measurement of deviation between the two meshes is then measured by the ‘Cloud/Mesh Distance’ tool in the program and applied to the original back mesh, resulting in a color deviation map as shown in Figure 3-5, Figure 3-6, and Figure 3-7.

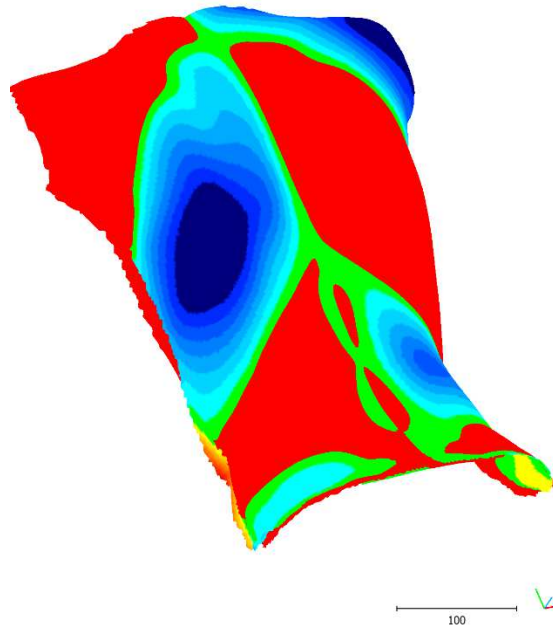


Figure 3-5 Distance Between Measured and Mirrored Meshes applied to Original as Deviation Color Map

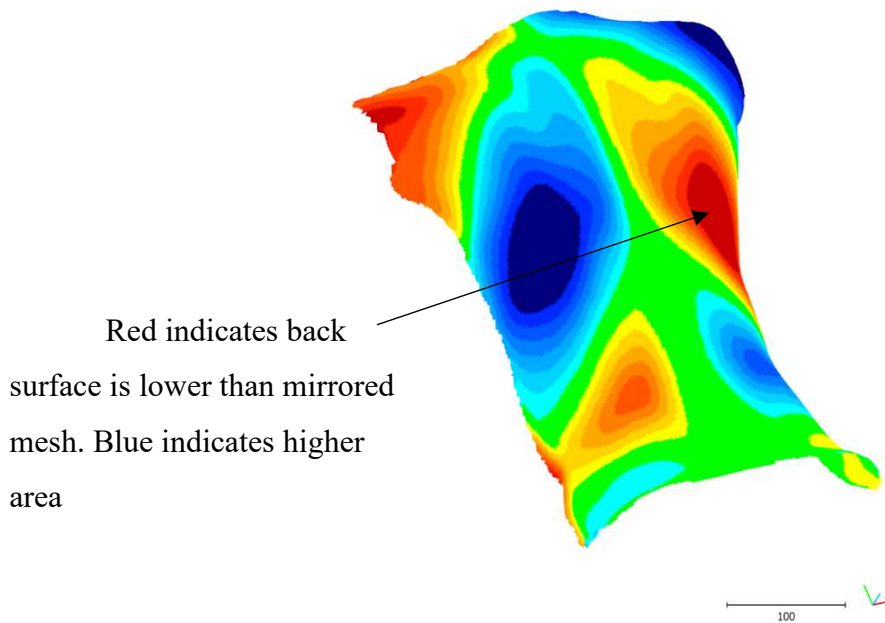


Figure 3-6 Final Colorized Isolated Back Mesh

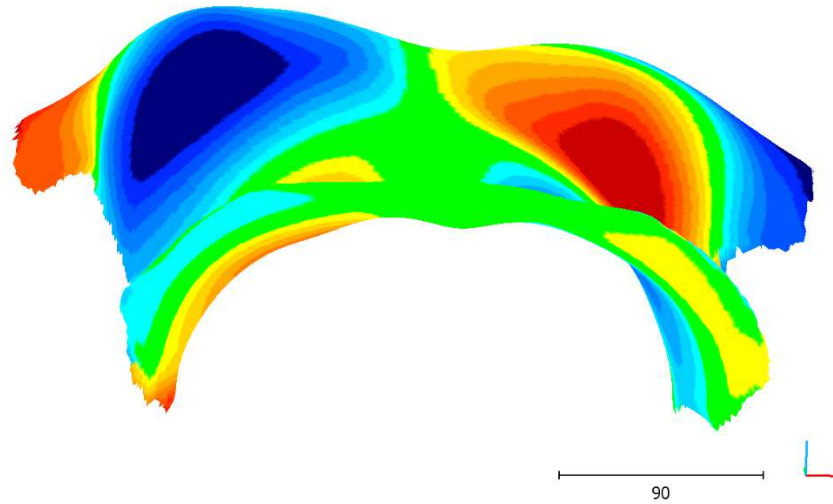


Figure 3-7 View of Colored Back Mesh, Looking Up From The Bottom Of The Mesh. Illustrates Color Mapping on Actual Contours

The results of the maximum deviation analysis and root mean square values will be compared using a direct comparison graph, and the Bland-Altman plots that were used in the previous chapter. The method of comparison and interpretation of the results will be carried out in the same manner.

A full step by step description of the method of isolating the back points using CloudCompare can be found in Appendix B.

Data used

Table 3-1- Description of Participants

Test Participants	
Total Patient Scans	67
Total Isolated Patches (Corresponding to Scoliotic Curves. Sometimes more than one per patient)	85
Age Range, years	10 - 18
Cobb Angle Range, °	13 - 60
Gender, n	
Male	12

Test Participants	
Female	55
Curve Type, n	
Lenke 1	41
Lenke 2	0
Curve Type, n (continued)	
Lenke 3	4
Lenke 4	0
Lenke 5	40
Lenke 6	0

The data used for the isolated back analysis was the exact same data set as that used in Chapter 2 for the comparison of the Geomagic analysis of the full torso point cloud and the CloudCompare analysis of the full torso point cloud. The exclusion criteria noted in Chapter 2 were designed to ensure that every patch identified would have a corresponding value in the Geomagic full torso analysis, the CloudCompare full torso analysis, and the CloudCompare isolated back analysis.

Results

Maximum Deviation

Figure 3-8 presents a direct comparison of the results of the maximum deviation analysis on the full torso scan and the isolated back scan. In each case the exact same scan was used, with the isolated back scan being performed on the scan points from the full torso scan isolated with the technique described previously.

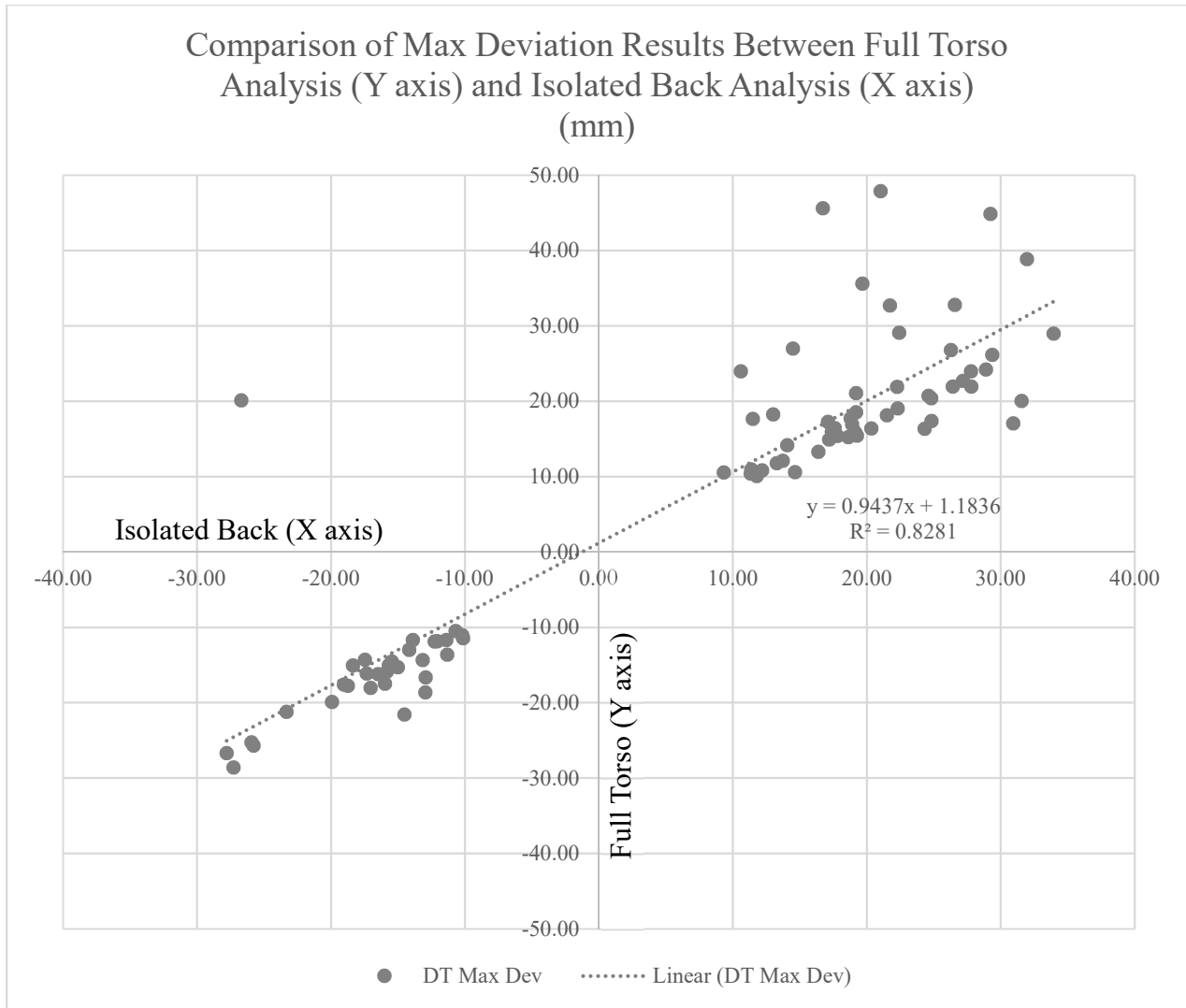


Figure 3-8 Scatter Plot of Measure Values of Maximum Deviation Between Full Torso Analysis and Isolated Back Analysis

Figure 3-9 presents the Bland-Altman plot of the average result and difference between the results for each data set. For the calculations the results of the isolated back analysis were subtracted from the full torso analysis results.

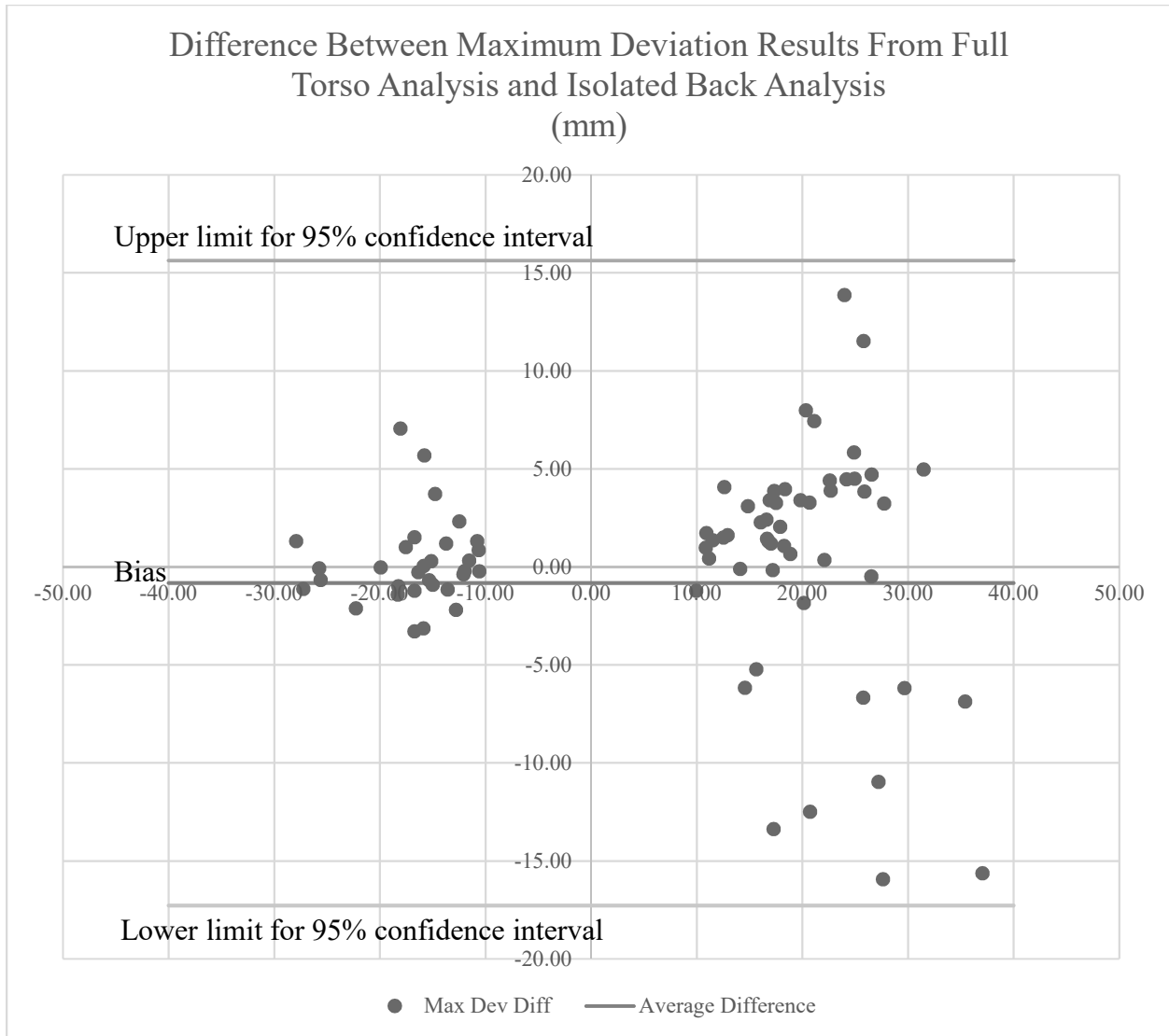


Figure 3-9 Scatter Plot of the Measured Differences Between Full Torso Max Deviation and Isolated Back Max Deviation

In Figure 3-9 the bias of -0.83mm indicates overall slightly lower estimates of the maximum deviation in the isolated back analysis than the full torso analysis.

Table 3-2 Isolated Back Max Deviation Comparison Results

Max	
Number of Data Points	85
Standard Deviation	8.22 mm
Number of Data Points within 1SD	83 (97.6%)
Number of Data Points between 1 and 2 SD	85 (100%)
Average diff/MaxDev	34.9%
Bias	-0.83 mm

Max	
Confidence Limit	± 16.12 mm

RMS

Figure 3-10 and Figure 3-11 show the same plots as were used in the maximum deviation analysis but using the results of the root mean square analysis.

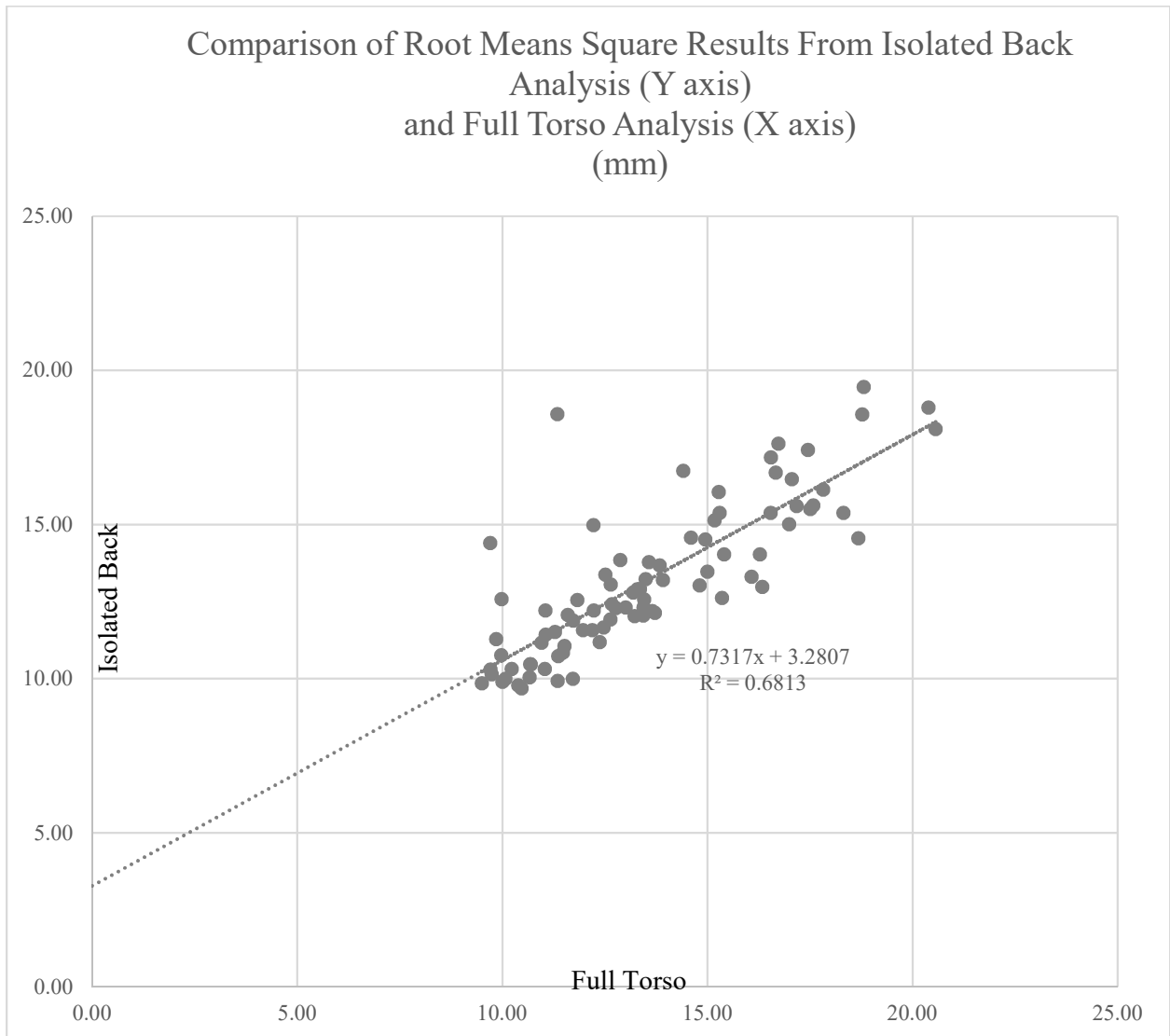


Figure 3-10 Scatter Plot of Measure Values of Root Mean Square Between Full Torso Analysis and Isolated Back Analysis

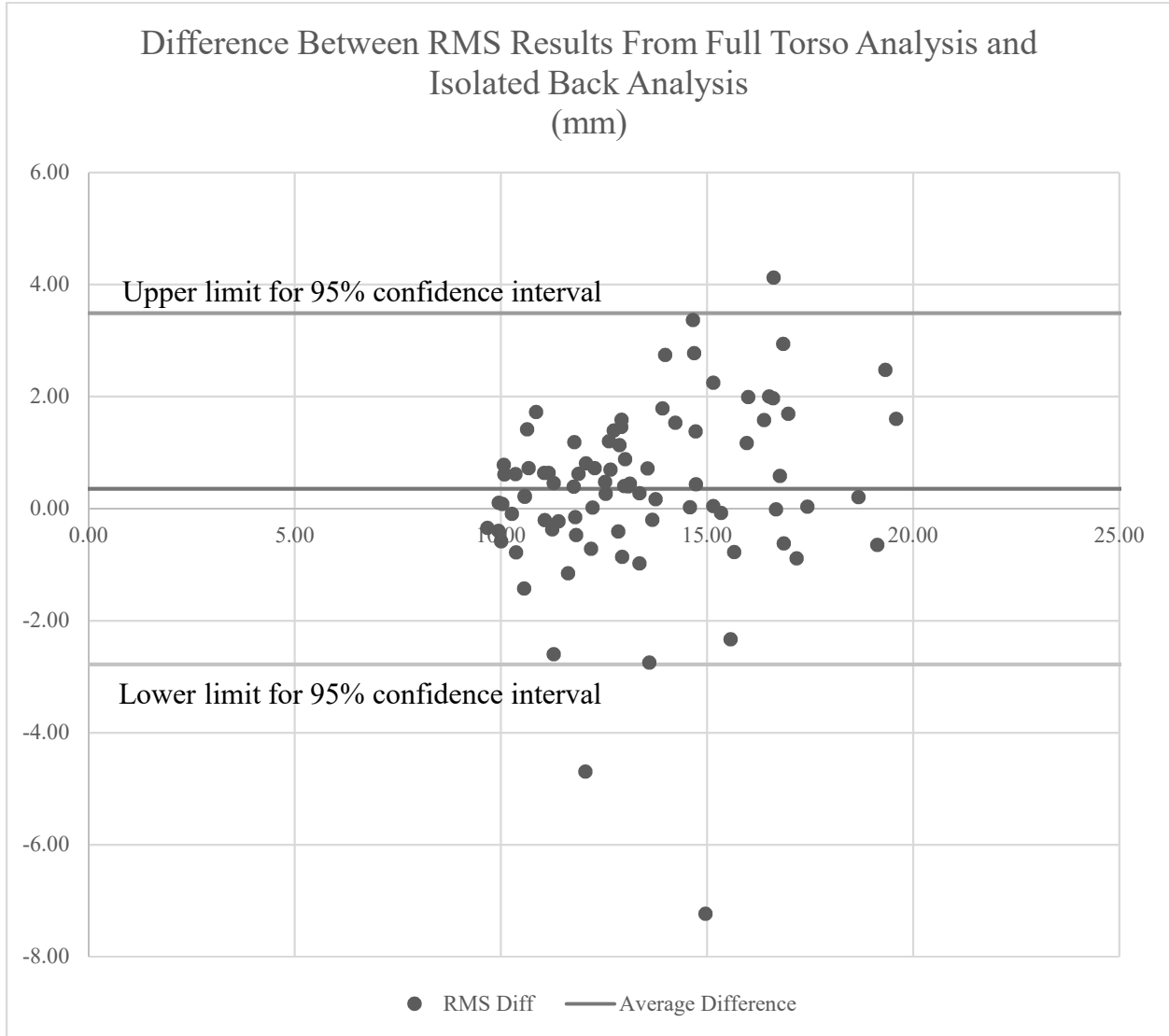


Figure 3-11 Scatter Plot of the Measured Differences Between Root Mean Square Results of Full Torso Analysis and the Isolated Back Analysis

Figure 3-11 is calculated by subtracting the isolated back analysis results from the full torso analysis results. The bias of 0.35mm indicates a higher RMS result by the isolated back analysis.

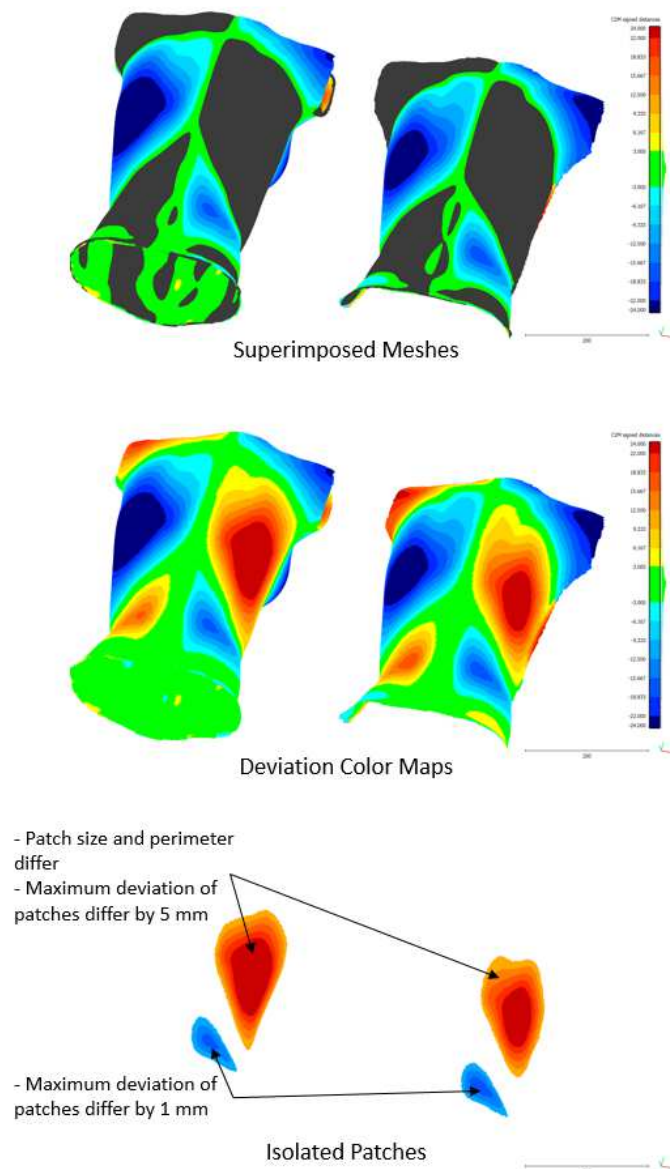
Table 3-3 Isolated Back RMS Comparison Results

Parameter	Results
Number of Data Points	85
Standard Deviation	1.56 mm
Number of Data Points within 1SD	69 (81.2%)
Number of Data Points within 2 SD	83 (97.6%)

Parameter	Results
Average Diff/RMS	8.1%
Bias	+ 0.35 mm
Confidence Limit	± 3.07 mm

Isolated Back Analysis Discussion

The full torso analysis and the isolated back analysis revealed inconsistencies in the results of the two methods. Figure 3-12 provides a visual illustration of the differences between the results for maximum deviation.



Full Torso Analysis

Isolated Back Analysis

Figure 3-12 Visual Comparison of Full Torso Analysis and Isolated Back Analysis

As observed in Figure 3-12, the two methods of comparison produce similar results in the number and general location of the patches, but dissimilar results with regards to the maximum deviation and the extents of the patch. In Figure 3-12 two patches are identified and isolated; patch 1 is an instance of a negative deviation (a depression in the back compared to the mirrored mesh) and patch 2 indicates a positive deviation (a rise in the back compared to the mirrored mesh). The larger negative patch had a difference in maximum deviation between the two patches of 5 mm, while the smaller positive patch produced a measurement difference of just 1 mm. The difference between RMS results for the two patches were 2.5 mm and 0.3 mm respectively. This case illustrates the disproportionate differences between the readings depending on the size of the identified patch and overall asymmetry of the mesh. Larger patches, or patches with larger maximum deviations, have greater disagreement in the results of the two methods than smaller patches do. This is a result of the registration process in which the program attempts to find the best fit between the two meshes by iteratively adjusting the relative orientation of the mirrored torso mesh. After each iteration of repositioning the mirrored torso, the program will measure the overall RMS of the differences between the two meshes. In each iteration, the value of the RMS analysis is compared to that of the previous iteration. Once the difference between these two measurements reaches a threshold level set by the user (1×10^{-5} for this study) the program will fix the position of the mirrored mesh and provide the results. Since the program is trying to minimize differences in the position of each point in the two meshes, the rotation and translation of the mirrored mesh will be adjusted to decrease the largest maximum deviation more than the lower magnitude deviation.

This process creates greater deviations in the measurements of the full torso than in the isolated back because the front of the torso exhibits less asymmetrical deformity due to scoliotic

deformation than the back. This causes the front of the torso to act as an anchor in the registration process. The isolated back mesh lacks this large area of greater symmetrical overlap, so the registration tends to adjust the orientation of the mirrored mesh to a greater degree.

The overall results of the method comparison between the full torso analysis and the back only analysis are summarized in Table 3-4 and Table 3-5.

Table 3-4 Comparison for Patch Max Deviation Determined Via the Full Torso Analysis and the Isolated Back Analysis

	Max Deviation Full Torso	Max Deviation Isolated Back
Bias	+0.11 mm	-0.83 mm
95% Confidence Limit	+/- 2.12 mm	+/- 16.12 mm
Percentage Error	3.5%	34.94%
Precision (R ²)	0.9976	0.8281
Standard Deviation	1.08 mm	8.23 mm

Table 3-5 Comparison for Patch RMS Values Determined Via the Full Torso Analysis and the Isolated Back Analysis

	RMS Full Torso	RMS Isolated Back
Bias	-0.043 mm	+0.35 mm
95% Confidence Limit	+/- 2.18 mm	+/- 3.07 mm
Percentage Error	4.6%	8.1%
Precision (R ²)	0.8678	0.6813
Standard Deviation	1.11 mm	1.57 mm

The results of the isolated back scan indicate a lack of correspondence between the two methods. In particular, the magnitude of the standard deviation for the maximum deviation is much higher than for the full torso comparison, which would create issues with mis-classification since the standard deviation is almost as much as the threshold deviation value for identification of a deviation patch (9.33mm). In addition, the isolated back analysis disproportionately affects the max deviation in comparison to the RMS. This is a result of the registration process described above. This process attempts to minimize the magnitude of deviation between the two meshes. If the relative position of the mirrored mesh is adjusted so that the maximum deviation is

minimized, the calculation of the root mean square will still be similar due to the absolute value produced in the squaring of the negative deviation, as illustrated in Figure 3-13.

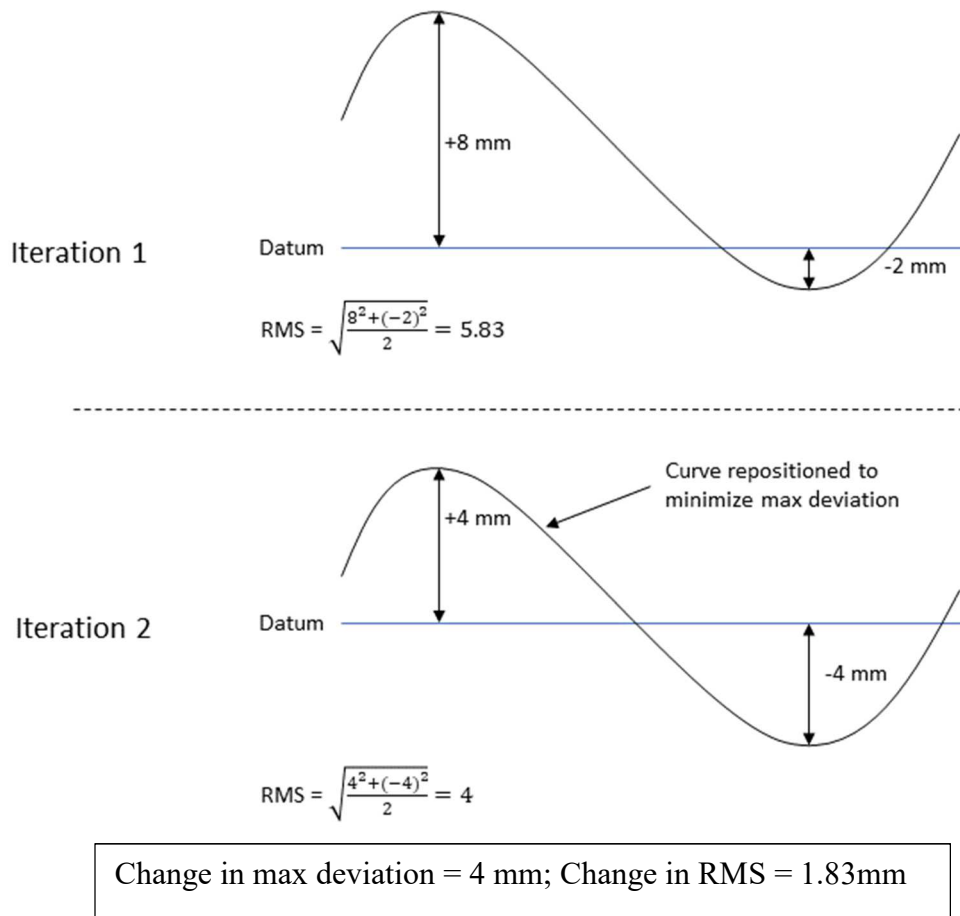


Figure 3-13 Illustration of Differences Between Maximum Deviation and RMS During Registration

Figure 3-14 illustrates this calculation as applied to the individual patches identified in the DCM, after the registration between the mesh and mirrored mesh has been completed.

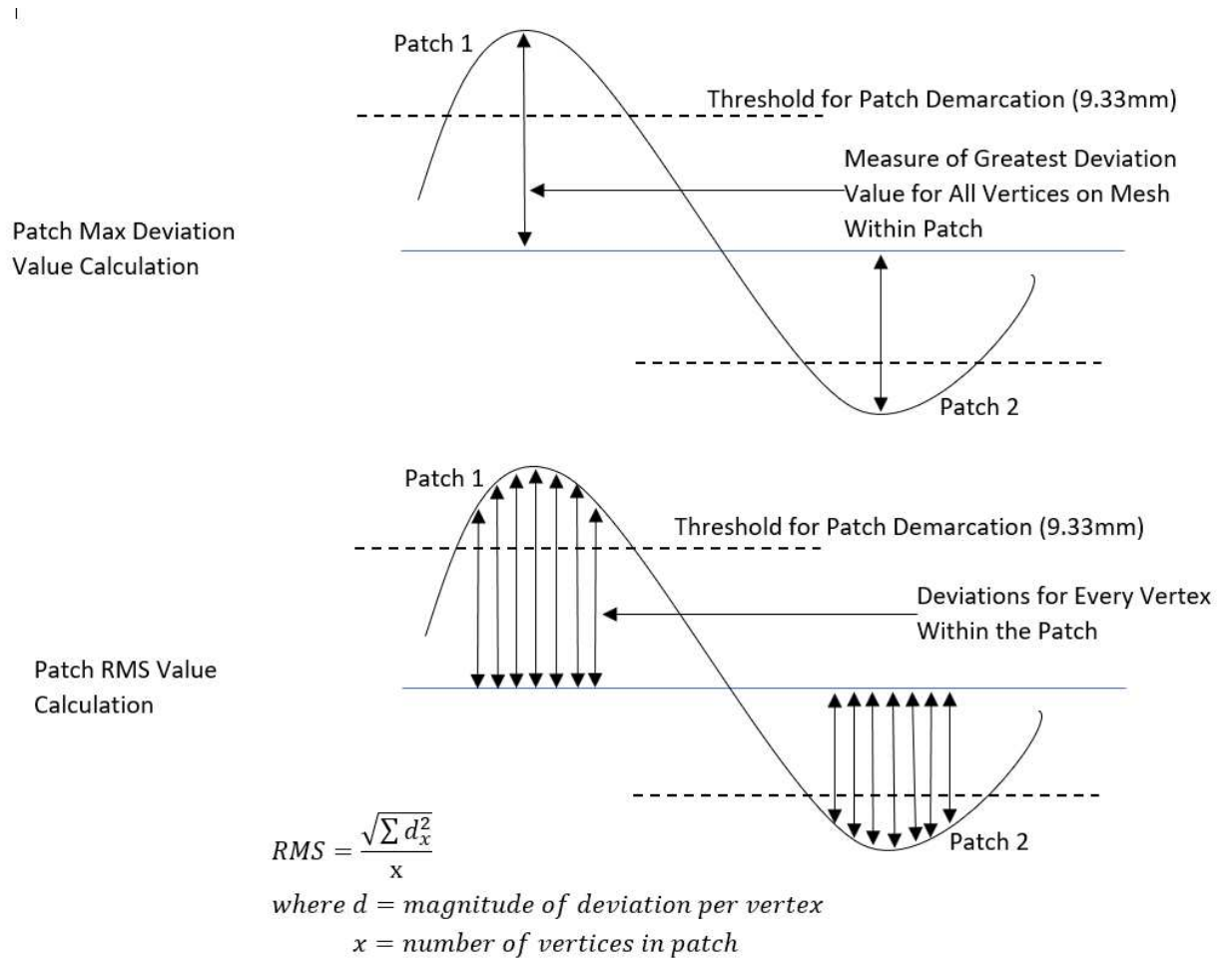


Figure 3-14 Illustration of Max Deviation and RMS Calculations Per Patch

One option with method comparison studies such as this is that one method can be calibrated to produce consistently comparable results. For instance, if the new method is consistently measuring 5% lower than the original method, the two results can be compared by simply adjusting the new method results by 5%. This would require a standard error between the two studies that could be quantified in a regression study. In this case, if there was a consistent bias on the part of the isolated back method this value could be used as a calibration constant to allow comparisons. However, the results from the analysis of the isolated back points indicate inconsistent differences between the full torso analysis and the isolated back analysis. The

Bland-Altman plots in Figure 3-9 and Figure 3-11 demonstrate this inconsistency. This clearly indicates that a calibration approach to the use of the isolated back method would not produce valid results.

The root mean square analysis demonstrated more consistency between the two methods, but when the absolute value nature of the root mean square analysis is taken into account, the discrepancy between the maximum deviation and the root means square analysis also indicate that the method of examining the isolated back scan is not a viable alternative to the analysis of the full torso scan for the markerless assessment of asymmetry method.

These results are similar to other studies that have examined the applicability of examining 3D surface topography of the isolated back. In particular, research by Parent et al. into the use of back only surface topography scans versus full torso scans indicates that only full torso scans had a significant ability to detect stable thoracic curves during 1 year follow up examinations (36). The research by Parent et al. examined various ST parameters taken from full torso scans and from back only scans to see which parameters could be used to determine which curves are not progressing (progression defined by a change of >5 degrees in the Cobb angle) in patients with a main thoracic curve (38). The researchers used 30 full torso parameters and 16 back only parameters that were based on 11 landmarks placed on the scans by evaluators. Of the 30 parameters determined for the full torso analysis, 2 were found to provide statistically significant indicators of the stability of curves. One parameter measured the angle between the principal axis of inertia of torso cross sections and the frontal plane, the other parameter measured the transverse plane angle between the anterior superior iliac spines and the sternum (36). These two parameters helped provide reliable indicators of the progression of the scoliotic curves of the patient when an initial scan was compared to a 1 year follow up scan on the same

patient. Of the 16 parameters that were determined using back only scans, none were found to provide reliable indicators of curve progression. The approach of the study by Parent et al. was similar to my study in that the ability of full torso scans vs isolated back scans were directly compared to determine the potential value of isolated back scans in the monitoring and treatment of scoliosis. In both cases, the results indicate that the additional data available in a full torso scan is needed to provide meaningful guidance to researchers and clinicians.

Other studies have also examined the use of surface topography metrics to assess the severity of scoliotic deformity and monitor progression. Some depend on specific data acquisition techniques, such as the Moiré technique (44), but many others use various indices that make use of 3D surface data such as that collected by the 3D scans used in this study. These indices often measure coordinates, angles, and distances between landmarks on the back, or the relative position of these landmarks related to the transverse, sagittal or coronal planes (45) (3) (37). The understanding of overall shape of the back and asymmetries resulting from Scoliotic deformity is extremely valuable to clinicians (37), but research indicates that it is not possible to predict the degree of curvature that the Cobb angle measures by any means of examination of the surface topography of the back (46). While studying screening techniques that relied on the examination of surface deformity through various methods and indices (such as Moiré topography, Integrated Shape Imaging Systems, Incliniometry, and others) Bunnell concluded “It has become apparent from many reports that although there is a significant correlation between clinical deformity and radiographic measurement, the standard deviation is so high that it is not possible to reliably predict the degree of curvature from surface topography in any given patient by any technique” (46).

The results of these previous studies and the results of the current study regarding the use of isolated back scans for 3D assessment of adolescent idiopathic scoliosis using surface topography consistently indicate that the isolated back scan does not contain enough data to reliably assess scoliotic deformities to reduce the frequency of x-rays required during treatment if the decision trees and indices that depend on max deviation and RMS values proposed by Komeili et al. and Ghaneei et al. are applied.

The results of this study do not indicate alternate decision trees or indices that could be used on isolated back scans. As noted previously, there was not a consistent bias found that could be used for calibration between the two methods, and the standard deviation in measurements of the max deviation for the patches indicates a significant loss of sensitivity of the analysis, where patches would not be adequately identified by the isolated back analysis. Although these results are clear that the asymmetry analysis cannot be used in the same manner on the isolated back as the full torso, it is possible that future research into the use of the isolated back scans could provided useful data. Techniques such as the Moiré method and sections of back topography have provided useful results in better understanding scoliotic deformity and reducing X-ray usage for patients (47) (34). CloudCompare is capable of providing the sections used in previous studies and also has the potential to aid in the consistent identification of landmarks for use in techniques that depend on markers. The flexibility of this tool and the value for patient comfort in using isolated back scans would make this future research worthwhile.

In order to fully realize the value for patient comfort in using isolated back scans the scans would have to not depend on the back points being isolated from the full torso scan, as was done in this study. This could be accomplished by simply positioning multiple scanners around the back of the patient, and allowing them to wear an open backed robe that exposed their

shoulders, sides and back. Multiple scanners would still be necessary, since the scanners can only capture data points in their direct line of sight. If only one scanner is used, the scans tend to have shadows where there is an absence of points. Multiple scanners can provide the simultaneous viewpoints necessary to ensure adequate point density over the entire surface of the back. At least 2 scanners would be required, situated behind the patient standing in the frame and to either side of the sagittal plane.

Chapter 4 – Conclusion

Patients who suffer from scoliosis have an abnormal curvature in their spine that can cause physical discomfort and psychological suffering. This abnormal curvature, referred to as scoliotic deformity, can include abnormal curvature in the coronal plane, the sagittal plane, or both, as well as twisting of the spine along the vertical axis.

The most common method for diagnosing and monitoring scoliosis is the measurement of the Cobb angle from radiometric measurements. Measuring the Cobb angle involves identifying the vertebrae at the start and apex of lateral curvature in the coronal plane, then measuring the angle between straight lines drawn at the base of each of these vertebrae. This measurement of the severity of scoliosis has been in use for many years and is accepted as the gold standard for quantifying the severity of scoliotic deformity.

Because the Cobb angle only measures the deviation from the expected axis of symmetry in one plane, it does not give the clinician a full understanding of the 3-dimensional nature of the scoliotic deformity. It also requires extensive use of radiometric monitoring, which can be harmful to the health of the patient during long term monitoring and treatment (24) (6) (11) (27) (32) (28). For these reasons, alternate methods for diagnosing and monitoring scoliosis have been devised with varying results.

One such method involves the use of surface topography measurements taken from 3D scans of the patient's torso. Multiple 3D scanners are situated around the patient as they stand in a frame that controls their posture and defines a coordinate system that the scan will be captured in. The 3D scan can then be analyzed, as with the system of 3D markerless assessment using asymmetry that has been explored in this thesis. As demonstrated by Komeili et al. the point cloud can be duplicated and mirrored, allowing for a detailed analysis of the asymmetry caused

by scoliotic deformity. The max deviation between the original and mirrored point cloud, as well as the root mean square in the differences measured at the vertices of the point cloud mesh, give a good indication as to the severity of the scoliotic deformity and can provide reliable indications as to the progression when a single patients subsequent scans are compared. Gahneei et al. (32) demonstrated that the sensitivity of decision trees for monitoring curve progression can be improved by employing a knn nearest neighbor algorithm. Together, these approaches have shown promising results in efforts to reduce the amount of radiometric tests necessary during the treatment and monitoring of progression for scoliosis patients.

This research sought to contribute to this body of knowledge by testing the applicability of open source software to the method of 3D markerless surface topography assessment and to explore the use of the is technique on an isolated back scan of the patient. The reason for exploring these methods was to lower the software costs associated with surface topography analysis, and to improve the patient experience by allowing the patient to only have the scan performed on their back rather than the entire torso.

The results for using an open source software approach demonstrated that the open source software selected (CloudCompare) could provide reliable analysis results using the asymmetry analysis method. The method of applying this specific analytical method to an isolated back scan did not provide adequate max deviation and root mean square results that Komeili et al. (31) (13) (27) and Gahneei et al. (32) have explored in their research.

Future Work

Although the specific parameters used in the 3D markerless assessment of surface topography using asymmetry were not reliable when the analysis was limited to the isolated back

scan, many other parameters can be determined from both the isolated back scan and full torso scan that can be used with a variety of indices of scoliotic classification. Many of these indices could benefit from the use of open source software such as that used in this study to make analysis more economical and accessible to clinics. Pazos et al. mention that the sensitivity of many of the surface analysis techniques can be a limiting factor in the usefulness of these measurements and indices for monitoring curve progression in a patient (45). Programs such as CloudCompare are capable of much more sensitive analysis than older programs have been capable of and 3D point cloud capture hardware has become much more accessible and affordable in recent years. Further research is warranted to examine if the use of recent advances in hardware and software provide enough sensitivity to use these point clouds to a greater extent. With open source programs such as CloudCompare, researchers could easily program toolsets to help automate analysis techniques to improve reliability and repeatability. Toolbars could be created that would contain a different button for each type of measurement or index, creating an affordable and easily shareable toolkit for clinicians to use. Although this study into the use of isolated back scans for markerless 3D assessment of asymmetry indicates that the use of isolated back scans for this specific technique is not effective, the testing of open source software for 3D surface topography analysis could open up exciting opportunities for the development of economical toolsets to aid in the treatment of patients suffering from scoliosis.

References

1. *Automatic Quantification of Spinal Curvature in Scoliotic Radiograph using Image Processing.* **H, Anitha and Prabhu, G.K.** 2012, Journal of Medical Systems, Vol. 36, pp. 1943-1951.
2. **Woloschuk, Christopher.** *A Wireless 3D Posture Monitor for Adolescent Idiopathic Scoliosis.* Department of Electrical and Computer Engineering, University of Alberta. Edmonton : University of Alberta, 2013.
3. *State of the art of current 3-D Scoliosis classifications: a systematic review from a clinical perspective.* **Donzeli, Sabrina, et al.** 91, 2015, Journal of NeuroEngineering and Rehabilitation, Vol. 12, pp. 1-11.
4. **Life Science Integrated Database Center.** s.l., Japan : CC Display.
5. *Comparison of scoliosis measurements based on three-dimensional vertebra vectors and conventional two-dimensional measurements: Advantages in evaluation of prognosis in surgical results.* **Illes, Tamas and Somoskeoy, Szabolcs.** 2013, European Spine Journal, Vol. 22, pp. 1255-1263.
6. *Scoliosis Imaging: What Radiologists Should Know.* **Kim, Hana, et al.** 7, 2010, RadioGraphics, Vol. 30, pp. 1823-1842.
7. *Spontaneous regression of curve in immature idiopathic scoliosis - does spinal column play role in imbalance? An observation with literature review.* **Hitesh, Modi, et al.** 80, 2010, Journal of Orthopaedic Surgery and Research, Vol. 5.
8. *Predictors of spine deformity progression in adolescent idiopathic scoliosis: A systematic review with meta-analysis.* **Noshchenko, Andriy, et al.** 7, August 18, 2015, World Journal of Orthopedics, Vol. 6, pp. 537-558.

9. *Adolescent Idiopathic Scoliosis*. **Ekinci, Safak and Ersen, Omer.** 3, 2014, Archive of Clinical Experimental Surgery, Vol. 3, pp. 174-182.
10. *Optimal management of idiopathic scoliosis in adolescence*. **Kotwicki, Tomasz, et al.** July 22, 2013, Adolescent Health, Medicine and Therapeutics, pp. 59-73.
11. **Knott, Patrick, et al.** SOSORT 2012 consensus paper: reducing x-ray exposure in pediatric patients with scoliosis. *scoliosis journal*. [Online] 9 4, 2014.
<http://www.scoliosisjournal.com/content/9/1/4>.
12. *Breakthrough in three-dimensional scoliosis diagnosis: Significance of horizontal plane view and vertebra vectors*. **Illes, Tamas, Tunyogi-Csapo, Miklos and Somoskeoy, Szabolcs.** 2011, European Spine Journal, Vol. 20, pp. 135-143.
13. *Correlation Between a Novel Surface Topography Asymmetry Analysis and Radiographic Data in Scoliosis*. **Komeili, Amin, et al.** 2015, Spine Deformity, Vol. 3, pp. 303-311.
14. *Idiopathic scoliosis in children and adolescents: assessment with a biplanar X-ray device*. **Amzallag-Bellenger, Elisa, et al.** 2014, Insights Imaging, Vol. 5, pp. 571-583.
15. *The Pathogenesis of Idiopathic Scoliosis: Biplanar Spinal Asymmetry*. **Dickson, R. A., et al.** 1, Leeds : British Editorial Society of Bone and Joint Surgery, January 1984, Journal of Bone and Joint Surgery, Vols. 66-B.
16. *A review of the trunk surface metrics used as Scoliosis and other deformities evaluation indices*. **Patias, Petros, et al.** 12, s.l. : Scoliosis Journal, 2010, Vol. 5.
17. *Reliability Analysis for Digital Adolescent Idiopathic Scoliosis Measurements*. **Kuklo, Timothy, et al.** 2, 2005, Journal of Spinal Disorders and Techniques, Vol. 18, pp. 152 - 159.

18. *Adolescent Idiopathic Scoliosis: A new classification to determine extent of spinal arthrodesis.* **Lenke, Lawrence G, et al.** A, 2001, The Journal of Bone and Joint Surgery, Vol. 83, pp. 1169-1181.
19. *The selection of fusion levels in thoracic idiopathic scoliosis.* **King, H A, et al.** 1983, The Journal of Bone and Joint Surgery, Vol. 65, pp. 1302-1313.
20. *Classification of Adolescent Idiopathic Scoliosis.* **Ovadia, Dror.** 2013, Journal of Child Orthopaedics, Vol. 7, pp. 25 - 28.
21. **Ann Arbor Spine Center at Michigan Brain and Spine St. Joe's Medical Group.**
Harrington Rod. *Ann Arbor Spine Centre.* [Online] [Cited: 01 06, 2019.]
<http://www.annarborspinecenter.com/scoliosis/harrington.html>.
22. **Harms Study Group.** Lenke Classification. *Setting Scoliosis Straight.* [Online] 2017. [Cited: May 21, 2018.] <http://hsg.settingscoliosisstraight.org/lenke-classification/>.
23. *Adolescent idiopathic scoliosis – to operate or not? A debate article.* **Hans-Rudolf, Weiss, et al.** 25, September 30, 2008, Patient Safety in Surgery, Vol. 2.
24. **Hoffman, Daniel A, et al.** Breast Cancer in Women With Scoliosis. *Journal of the National Cancer Institute.* September 6, 1989, Vol. 81, 17, pp. 1307-1312.
25. *Adolescent Idiopathic Scoliosis - to Operate or Not? A Debate Article.* **Wiess, Hans-Rudolf, et al.** 25, Sept 2008, Patient Safety in Surgery, Vol. 2.
26. *Did the Lenke Classification Change Scoliosis Treatment.* **Clements, David H, et al.** 14, 2011, Spine, Vol. 36, pp. 1142 - 1145.
27. *Monitoring for idiopathic scoliosis curve progression using surface topography asymmetry analysis of the torso in adolescents.* **Komeili, Amin, et al.** January 2015, The Spine Journal, Vol. 15, pp. 743-751.

28. **U.S. Food and Drug Administration.** Reducing Patient Exposure During Scoliosis Radiography. *FDA Homepage*. [Online] 12 12, 2017. [Cited: 12 16, 2018.]
<https://www.fda.gov/Radiation-EmittingProducts/ResourcesforYouRadiationEmittingProducts/ucm252765.htm>.
29. *Three-Dimensional Classification of Thoracic Scoliotic Curves.* **Sangole, Archana P, et al.** 1, 2009, *Spine*, Vol. 34, pp. 91-99.
30. *Classification of scoliosis deformity 3-D spinal shape by cluster analysis.* **Stokes, Ian A.F., Sangole, Archana P. and Aubin, Carl-Eric.** 6, *Spine (Phila Pa 1976)*, Vol. 34, pp. 584-590.
31. *Surface topography asymmetry maps categorizing external deformity.* **Komeili, Amin, et al.** 2014, *The Spine Journal*, Vol. 14, pp. 973-983.
32. **Ghaneei, Maliheh.** *Algorithms for Adolescent Idiopathic Scoliosis Classification Based on Surface Topography Analysis.* s.l. : University of Alberta, 2017.
33. *Moire Topography in Scoliosis.* **Daruwalla, J.S. and Balasubramaniam, P.** 2, s.l. : *Journal of Bone and Joint Surgery*, 1985, Vols. 67-B.
34. *Development of a 3-Dimensional Back Contour Imaging System for Monitoring Scoliosis Progression in Children.* **Liu, Xue-Cheng, et al.** 2013, *Spine Deformity*, pp. 102-107.
35. *Assessing asymmetry using reflection and rotoinversion in biomedical engineering applications.* **Hill, Shannon, et al.** 5, 2014, *Journal of Engineering in Medicine*, Vol. 228, pp. 523-529.
36. *The ability of surface topography postural measurements to detect cobb angle progression in adolescents with idiopathic scoliosis (AIS) and a main thoracic curve: full torso scans*

- compared to back only parameters.* **Parent, Eric C, et al.** Wiesbaden : Scoliosis Journal, 2014. 11th International Conference on Conservative Management of Spinal Deformities.
37. *A review of the trunk surface metrics used as scoliosis and other deformities evaluation indices.* **Patias, Petros, et al.** 12, 2010, Scoliosis, Vol. 5, pp. 1-20.
38. *Sensitivity to change of Full Torso Surface Topography Measurements in Adolescents with Idiopathic Scoliosis and a Main Thoracic Curve.* **Parent, Eric C, et al.** 2012, Studies in Health Technology and Informatics, Vol. 176, p. 484.
39. *Surface Reconstruction of Torsos With and Without Scoliosis.* **Emrani, M, et al.** 13, Sept 2009, Journal of Biomechanics, Vol. 42, pp. 2200 - 2204.
40. CloudCompare. *CloudCompare.* [Online] 2018. <https://www.cloudcompare.org/>.
41. GNU. *Webopedia.* [Online] [Cited: July 25, 2018.]
<https://www.webopedia.com/TERM/G/GNU.html>.
42. *Measurement in Medicine: The Analysis of Method Comparison Studies.* **Altman, D. G. and Bland, J. T.** 3, Sept 1983, Journal of the Royal Statistical Society. Series D (The Statistician), Vol. 32, pp. 307-317.
43. *Design, Analysis and Interpretation of Method-Comparison Studies.* **Henneman, Sandra K.** 2, s.l. : National Institutes of Health, 2008, AACN Advanced Critical Care, Vol. 19, pp. 223-234.
44. *Moire Topography for the Study of Multiple Curves of the Spine.* **Kamal, Syed Arif.** Mont Sainte Marie : Surface Topography and Spinal Deformity: Proceedings of the 4th International Symposium, 1987.
45. *Reliability of trunk shape measurements based on 3-D surface reconstructions.* **Pazos, Valerie, et al.** 16, s.l. : European Spine Journal, 2007.

46. *Selective Screening for Scoliosis*. **Bunnell, WP.** May 2005, *Clinical Orthopedics and Related Research*, Vol. 434.
47. *Topography of Surface and Spinal Deformity*. **Zawieska, Dorota.** B5, s.l. : International Archives of Photogrammetry and Remote Sensing, 2000, Vol. 33.
48. National Scoliosis Foundation. *Information and Support*.
49. **Wegner, Joanne.** *Measurement of Scoliosis Deformity Using Moire Topography*. Edmonton : University of Alberta, 1985.
50. *Shadow Moire Technique for Postural Assessment: Qualitative Assessment Protocol by Intra- and Inter-rater Evaluation* . **Nunes Da Silva Filho, Jose, et al.** 2, s.l. : Journal of Physical Therapy Science, 2017, Vol. 29.
51. *Statistics Corner: A guide to appropriate use of correlation coefficient in medical research*. **Mukaka, M M.** 3, 2012, *Malawi Medical Journal*, Vol. 24, pp. 69-71.
52. *Cancer Risks Associated with External Radiation From Diagnostic Imaging Procedures*. **Linnet, Martha S, et al.** 2, August 3, 2013, *CA Cancer Journal for Clinicians*, Vol. 62, pp. 75-100.
53. *Workflow of CAD / CAM Scoliosis Brace Adjustment in Preparation Using 3D Printing*. **Hans-Rudolf, Weiss, et al.** 2017, *The Open Medical Informatics Journal*, Vol. 11, pp. 44-51.
54. **Carter, Olivia D and Haynes, Suzanne G.** Prevalence Rates for Scoliosis in US Adults: Results from the First National Health and Nutrition Examination Survey. *International Journal of Epidemiology*. September 1, 1987, Vol. 16, 4, pp. 537-544.
55. *Adolescent idiopathic scoliosis and back pain*. **Balagué, Federico and Pellisé, Ferran.** 27, 2016, *Scoliosis and Spinal Disorders*, Vol. 11.

56. **Asher, M, et al.** The reliability and concurrent validity of the scoliosis research society-22 patient questionnaire for idiopathic scoliosis. *Spine*. January 1, 2003, Vol. 28, 1, pp. 63-69.


57. *The reliability and concurrent validity of the scoliosis research society-22 patient questionnaire for idiopathic scoliosis. Asher, M, et al.* 2003, *Spine*, pp. 63-69.

58. *Multisurgeon assessment of surgical decision-making in adolescent idiopathic scoliosis: curve classification, operative approach, and fusion levels. Lenke, LG, et al.* 21, 2001, *Spine*, Vol. 26, pp. 2347 - 2353.

Appendix A - Markerless Assessment of Surface Topography Asymmetry Using CloudCompare

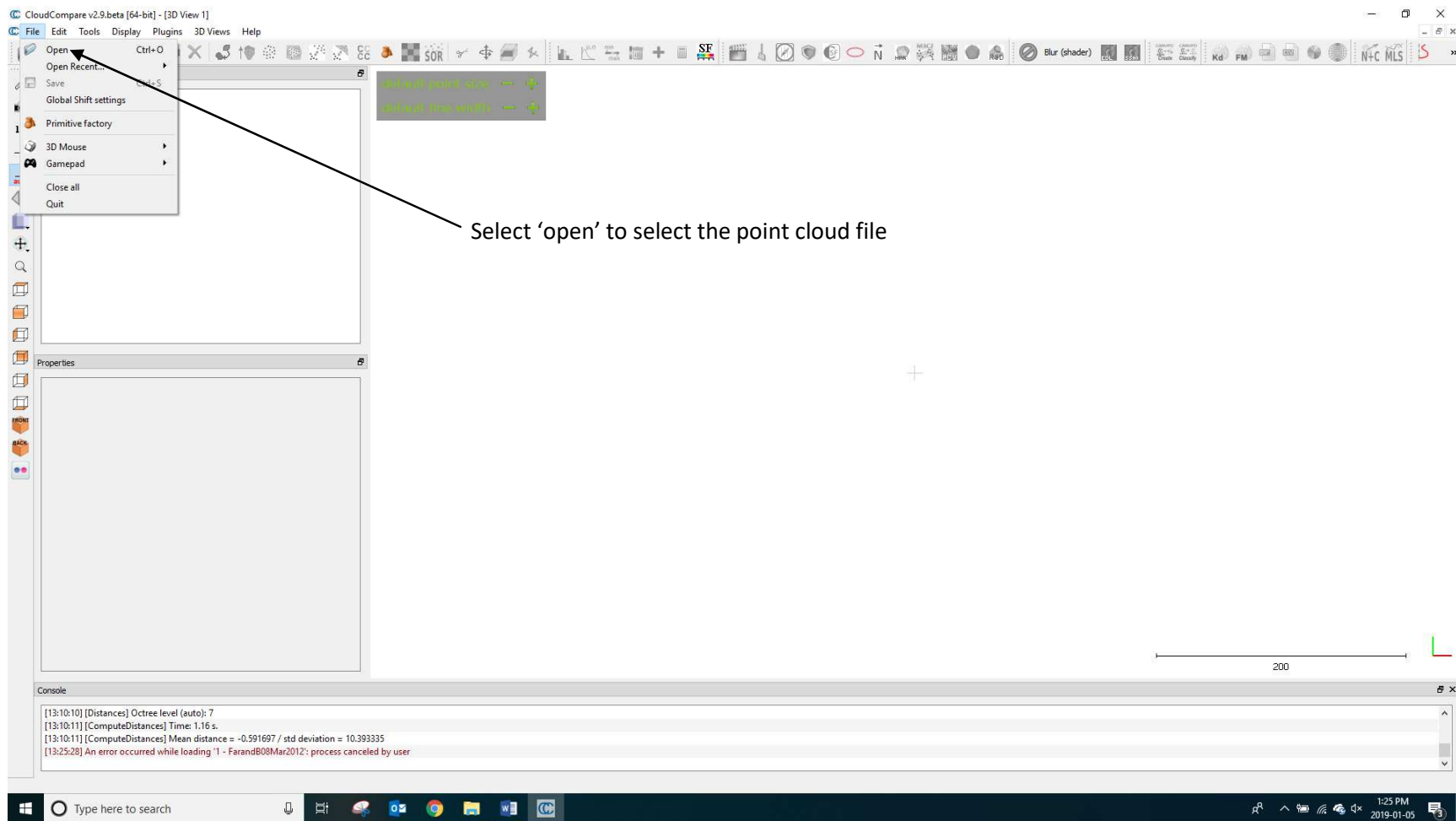
Contents

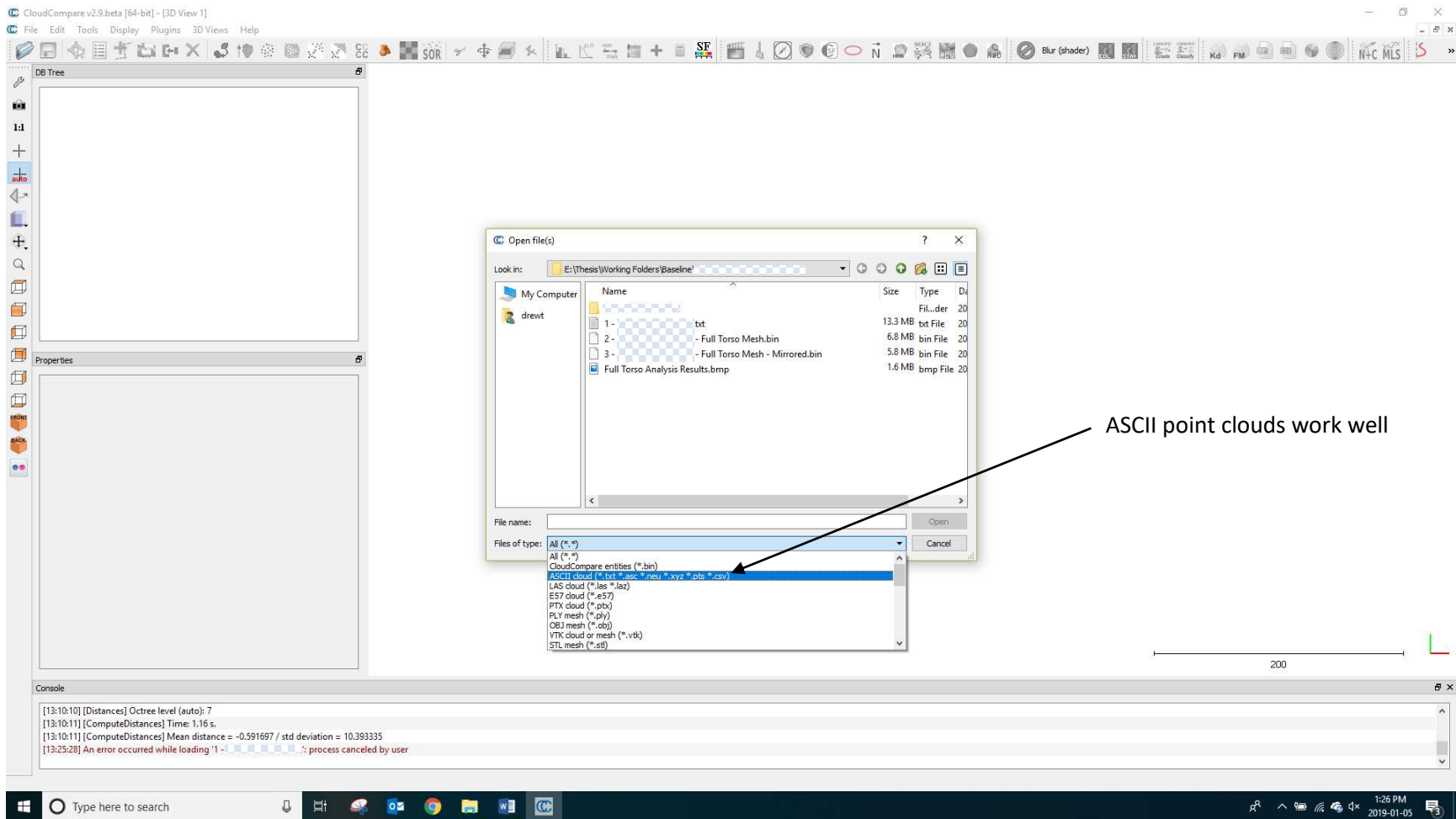
Appendix A - Markerless Assessment of Surface Topography Asymmetry Using CloudCompare	66
Step 1 – Import the Point Cloud	67
Step 2 – Mesh Creation.....	71
Step 3 – Create a Reflected Cloned Mesh.....	79
Step 4 – Registration of Cloned Mesh.....	82
Step 5 – Measurement of Deviation	85
Step 6 – Create Deviation Color Map.....	90
Step 7 – Isolate Patches	94
Step 8 – Calculate RMS and Max Deviation for Each Patch.....	102
References	105

Note: The masking shown has been inserted to cover file names where required for patient confidentiality → 

Step 1 – Import the Point Cloud

Cloudcompare can import many 3D pointcloud file types. ASCII text files work well, and give the opportunity to specify how each column in the file is interpreted.





CloudCompare v2.9.0 beta [64-bit] - [3D View 1]

File Edit Tools Display Plugins 3D Views Help

DB Tree

Open ASCII File

Filename: E:/Thesis/Working Folders/Baseline/31 - 1.txt

Here are the first lines of this file. Choose each column attribution (one cloud at a time):

Header: X,Y,Z,R,G,B,Scalar field #2,Scalar field #3,Scalar field #4,Scalar field #5,Scalar field #6,Scalar field #7,Nx,Ny,Nz

1	2	3	4	5	6	7	8	9	10	11	12	13	14	15	16
coord. X	coord. Y	coord. Z	Red (0-255)	Green (0-255)	Blue (0-255)	Scalar	Scalar	Scalar	Scalar	Scalar	Scalar	Scalar	Nx	Ny	Nz
-104.71370697	103.57020569	-1804.38867188	125	62	237	-104.674553	104.758179	-1806.381470	0.039154	1.187972	-1.992739	2.320306	-0.014859	-0.509265	0.860482
120.31002808	142.10516357	-1788.21716309	167	50	221	113.379623	155.756775	-1804.617676	-6.930406	13.651615	-16.400427	22.435932	0.310956	-0.600967	0.736305
66.29096222	-142.02503967	-1834.69384766	36	133	216	71.085526	-142.309265	-1839.514038	4.794568	-0.284225	-4.820228	6.804650	-0.712082	0.044061	0.700712
66.99311066	-143.51937866	-1833.85083008	36	134	216	71.808258	-143.956573	-1838.637573	4.815149	-0.437200	-4.786725	6.803642	-0.715853	0.058818	0.695769
-142.09344482	-134.78282166	-1766.65441895	240	158	76	-148.331146	-136.511383	-1763.704468	-6.237704	-1.72561	2.949948	7.113302	0.882767	0.243471	-0.401801
-81.05876923	-218.73524475	-1853.50683594	184	143	240	-81.293251	-218.801010	-1853.967896	-0.234475	-0.065760	-0.461111	0.521466	0.448726	0.126783	0.884631
-147.47674561	-24.64217567	-1800.69494629	234	119	195	-143.726746	-24.941313	-1798.330078	3.749993	-0.299137	2.364862	-4.443478	0.841267	-0.063412	0.536889
-6.35850811	169.90051270	-1820.45666504	85	205	218	-10.377638	176.786743	-1812.480713	-4.019130	6.886222	7.976030	-11.277878	-0.332490	0.614700	0.715258
14.70086384	-84.83874512	-1868.50000000	100	99	248	13.771098	-85.722466	-1864.681763	-0.929766	-0.883724	3.818222	-4.027934	-0.212584	-0.220709	0.951891
-42.04277420	69.99320221	-1677.81555176	53	125	23	-45.892120	69.876549	-1683.166992	-3.849344	-0.116647	-5.351462	-6.593117	-0.580102	-0.017913	-0.814347
4.82255983	-197.33570862	-1861.22802734	96	139	250	5.608505	-197.667130	-1864.496216	0.785945	-0.331434	-3.268143	3.377620	-0.242984	0.092868	0.965575
-14.97659302	-137.63807678	-1873.54125977	131	144	253	-14.980603	-137.661224	-1873.710327	-0.004010	-0.023142	-0.169044	0.170668	0.028110	0.133805	0.990609
50.54074860	73.78087885	-1821.37243652	145	84	246	-60.411452	75.606108	-1826.616042	-0.870705	1.006321	-5.244615	5.647847	0.144446	-0.334200	0.921325

Separator: , (ASCII code: 44) ESP TAB

Skip lines: 1 extract scalar field names from first line

Max number of points per cloud: 2000.00 Million

Apply Apply all Cancel

Console

```
[13:10:10] [Distances] Octree level (auto): 7
[13:10:11] [ComputeDistances] Time: 1.16 s.
[13:10:11] [ComputeDistances] Mean distance = -0.591697 / std deviation = 10.393335
[13:25:28] An error occurred while loading '1' - process canceled by user
```

CloudCompare gives an opportunity to specify the interpretation of each column in the point cloud file. The default will interpret the first three columns as x, y, z coordinates. Other values can be assigned to each point in other columns, such as colors, measurements, etc. For the purpose of the asymmetry analysis, only the first 3 columns (the x,y,z coordinates) are required. The rest can be ignored or deleted. These columns offer the opportunity for storing custom analysis values if desired.

The screenshot displays the CloudCompare v2.9.beta [64-bit] - [3D View 1] application window. The interface includes a menu bar (File, Edit, Tools, Display, Plugins, 3D Views, Help), a toolbar with various 3D manipulation tools, and a left sidebar with icons for file operations and view settings. The main 3D view shows a point cloud model of a human torso, rendered in a greenish-grey color. A scale bar at the bottom right of the 3D view indicates a length of 250 units. On the left, the 'DB Tree' panel shows a hierarchical view of the scene, with a point cloud entity labeled '1 - Cloud' selected and highlighted. An arrow points from this entity to the text: 'The point cloud entity is shown here. It is now ready for analysis'. Below the DB Tree is the 'Properties' panel, which is currently empty. At the bottom, the 'Console' window displays the following log messages:

```
[13:10:11] [ComputeDistances] Mean distance = -0.591697 / std deviation = 10.393335  
[13:25:28] An error occurred while loading '1 - ...': process canceled by user  
[13:31:46] [I/O] File 'E:/Thesis/Working Folders/Baseline/...' .bt' loaded successfully  
[13:31:46] [VBO] VBO(s) (re)initialized for cloud '1 - ... - Cloud' (1.30 Mb = 100.00% of points could be loaded)
```

The Windows taskbar at the bottom shows the system clock as 1:31 PM on 2019-01-05.

Step 2 – Mesh Creation

The screenshot displays the CloudCompare v2.9.0 beta [64-bit] interface. The DB Tree on the left shows a point cloud selected. The Properties panel on the left shows the selected object's details, including its name, visibility, and box dimensions. The 3D View window shows a mesh reconstruction of the point cloud. The Poisson Surface Reconstruction tool is highlighted in the toolbar. A scale bar at the bottom right indicates 250 units.

Select Point Cloud

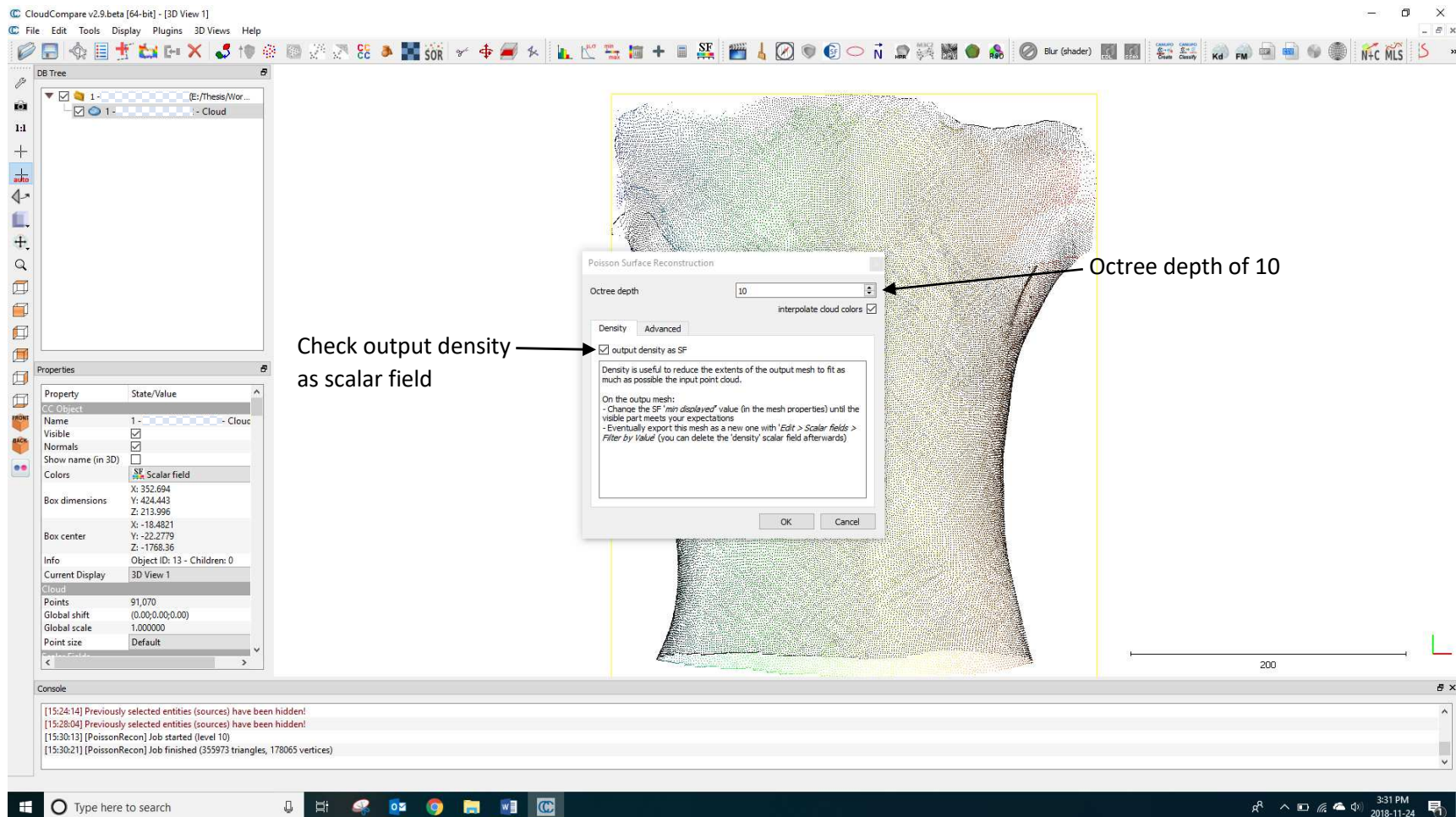
Poisson Surface Reconstruction

Property	State/Value
CC Object	
Name	1 - Cloud
Visible	<input checked="" type="checkbox"/>
Normals	<input checked="" type="checkbox"/>
Show name (in 3D)	<input type="checkbox"/>
Colors	Scalar field
Box dimensions	X: 352.694 Y: 424.443 Z: 213.996
Box center	X: -18.4821 Y: -22.2779 Z: -1768.36
Info	Object ID: 13 - Children: 0
Current Display	3D View 1
Cloud	
Points	91,070
Global shift	(0.00;0.00;0.00)
Global scale	1.000000
Point size	Default

```

[15:00:46] [I/O] File 'E:/Thesis/Working Folders/Baseline/36 - .txt' loaded successfully
[15:00:46] [VBO] VBO(s) (re)initialized for cloud '1 - Cloud' (1.46 Mb = 100.00% of points could be loaded)
[15:02:49] [I/O] File 'E:/Thesis/Working Folders/Baseline/31 - .txt' loaded successfully
[15:02:49] [VBO] VBO(s) (re)initialized for cloud '1 - Cloud' (1.30 Mb = 100.00% of points could be loaded)
  
```

The Poisson Surface Reconstruction tool creates a mesh using the program's native mesh tool which creates a triangular mesh by connecting points in the point cloud. The added value of the Poisson Surface Reconstruction tool is it provides the opportunity to attach a scalar field value to the mesh facets that corresponds to the point cloud density. This provides the opportunity to restrict the limits of the mesh to only those areas of the point cloud with a certain density, thus eliminating mesh edges that extend beyond the edge of the point cloud.



Using 'output density as SF' will provide a parameter to use to filter out portions of the mesh that are extrapolations beyond the point cloud that result from the surface reconstruction algorithm.

The 'Octree Depth' parameter refers to the 3-dimensional grid used to subdivide the point cloud into parts for analysis by the software functions. A higher octree depth will increase the analysis time, but produce more accurate results for any functions that require estimation. In this case, lower octree values will result in bridging of the mesh between separate parts of the mesh. An octree depth of 10 was found to provide the best results with reasonable analysis time.

CloudCompare v2.9.beta [64-bit] - [3D View 1]

File Edit Tools Display Plugins 3D Views Help

DB Tree

- 1 - bt (E:/Thesis/Wor...
- 1 - Cloud

Properties

Property	State/Value
Object	1 - Cloud
Name	1 - Cloud
Visible	<input checked="" type="checkbox"/>
Normals	<input checked="" type="checkbox"/>
Show name (in 3D)	<input type="checkbox"/>
Colors	Scalar field
Box dimensions	X: 352.694 Y: 424.443 Z: 213.996
Box center	X: -18.4821 Y: -22.2779 Z: -1768.36
Info	Object ID: 13 - Children: 0
Current Display	3D View 1
Cloud	
Points	91,070
Global shift	(0.00;0.00;0.00)
Global scale	1.000000
Point size	Default

Poisson Surface Reconstruction

Octree depth: 10

interpolate cloud colors

Density Advanced

samples per node: 1.50

full depth: 5

point weight: 4.00

boundary: Free

OK Cancel

Select advanced parameters

Choose free boundary to avoid having the software try and close in the holes at the arms, neck and waist.

200

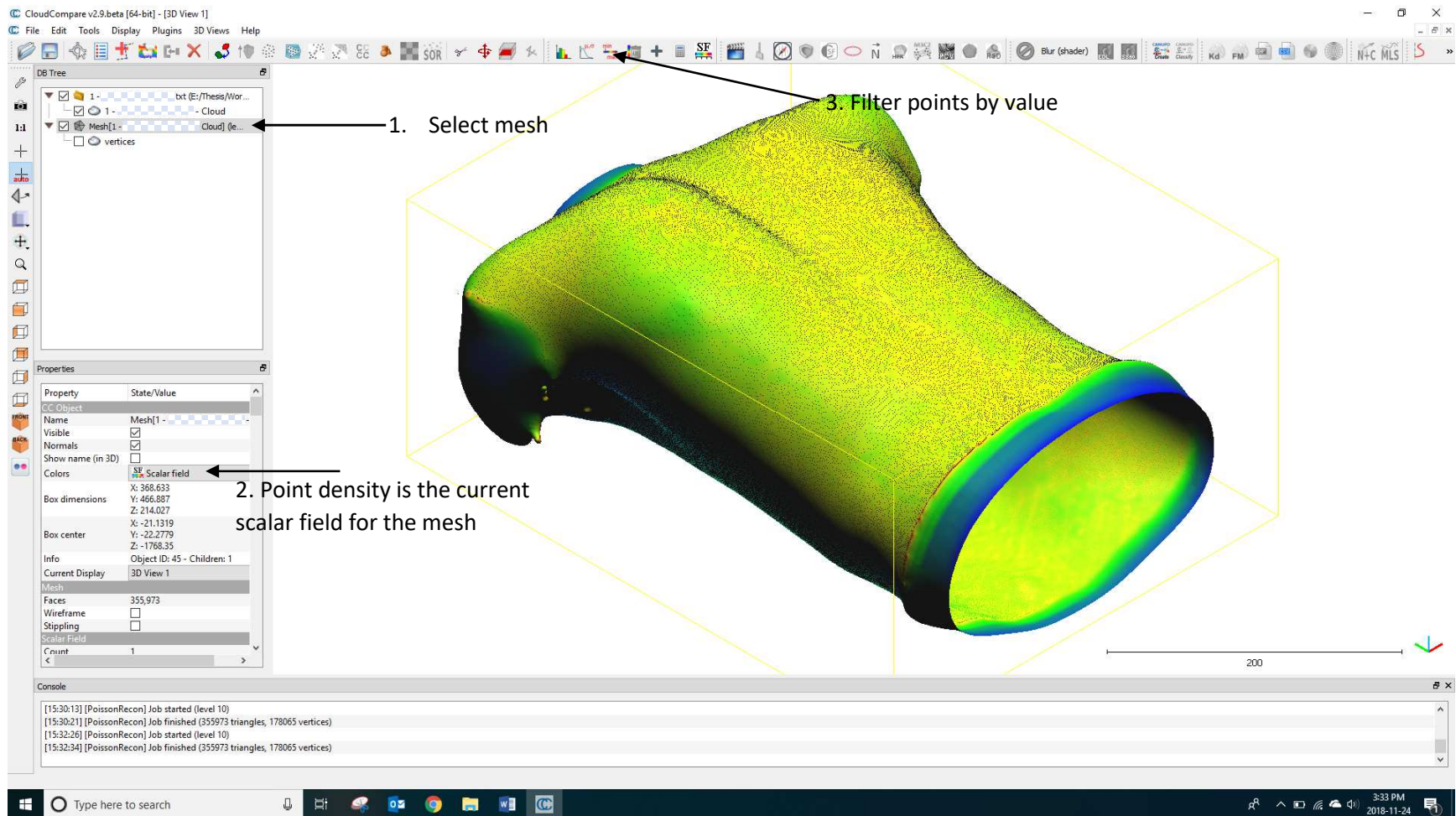
Console

```
[15:24:14] Previously selected entities (sources) have been hidden!
[15:28:04] Previously selected entities (sources) have been hidden!
[15:30:13] [PoissonRecon] Job started (level 10)
[15:30:21] [PoissonRecon] Job finished (355973 triangles, 178065 vertices)
```

Type here to search

3:32 PM 2018-11-24

The free boundary setting prevents the program from trying to close the surface. If this is not selected, the program will try and close the hole at the neck, arms and waist.



Delete all vertices in the mesh that have a density scalar value of less than 6 points/mm^2 by using the filter points by value field. The point clouds consistently have a point density of 6 points/mm^2 , so choosing this value mitigates the risk of unintentionally measuring differences in surface topography that are extrapolations of the collected data.

The screenshot displays the CloudCompare v2.9.0 beta interface. The main 3D view shows a point cloud of a mechanical part, colored by density. A yellow wireframe bounding box is visible around the object. A dialog box titled "Filter by value" is open, showing a range from 6.00000000 to 10.10023689. Two text annotations with arrows point to the dialog box: "Select 6 points/mm² as the minimum density to keep" and "The maxim density of the point cloud will automatically be entered in the maximum range". The Properties panel on the left shows the object is a Mesh with 355,973 faces. The Console at the bottom shows log messages for PoissonRecon jobs.

CloudCompare v2.9.0.beta [64-bit] - [3D View 1]

File Edit Tools Display Plugins 3D Views Help

DBTree

- 1 - bt (E:/Thesis/Wor...
- Cloud
- Mesh[1 - Cloud] (e...
- vertices

Properties

Property	State/Value
Object	
Name	Mesh[1 - ...
Visible	<input checked="" type="checkbox"/>
Normals	<input checked="" type="checkbox"/>
Show name (in 3D)	<input type="checkbox"/>
Colors	Scalar field
Box dimensions	X: 368.633 Y: 466.887 Z: 214.027
Box center	X: -21.1319 Y: -22.2779 Z: -1768.35
Info	Object ID: 45 - Children: 1
Current Display	3D View 1
Mesh	
Faces	355,973
Wireframe	<input type="checkbox"/>
Stippling	<input type="checkbox"/>
Scalar Field	
Count	1

Filter by value

Range: 6.00000000 - 10.10023689

Export Split Cancel

Select 6 points/mm² as the minimum density to keep

The maxim density of the point cloud will automatically be entered in the maximum range

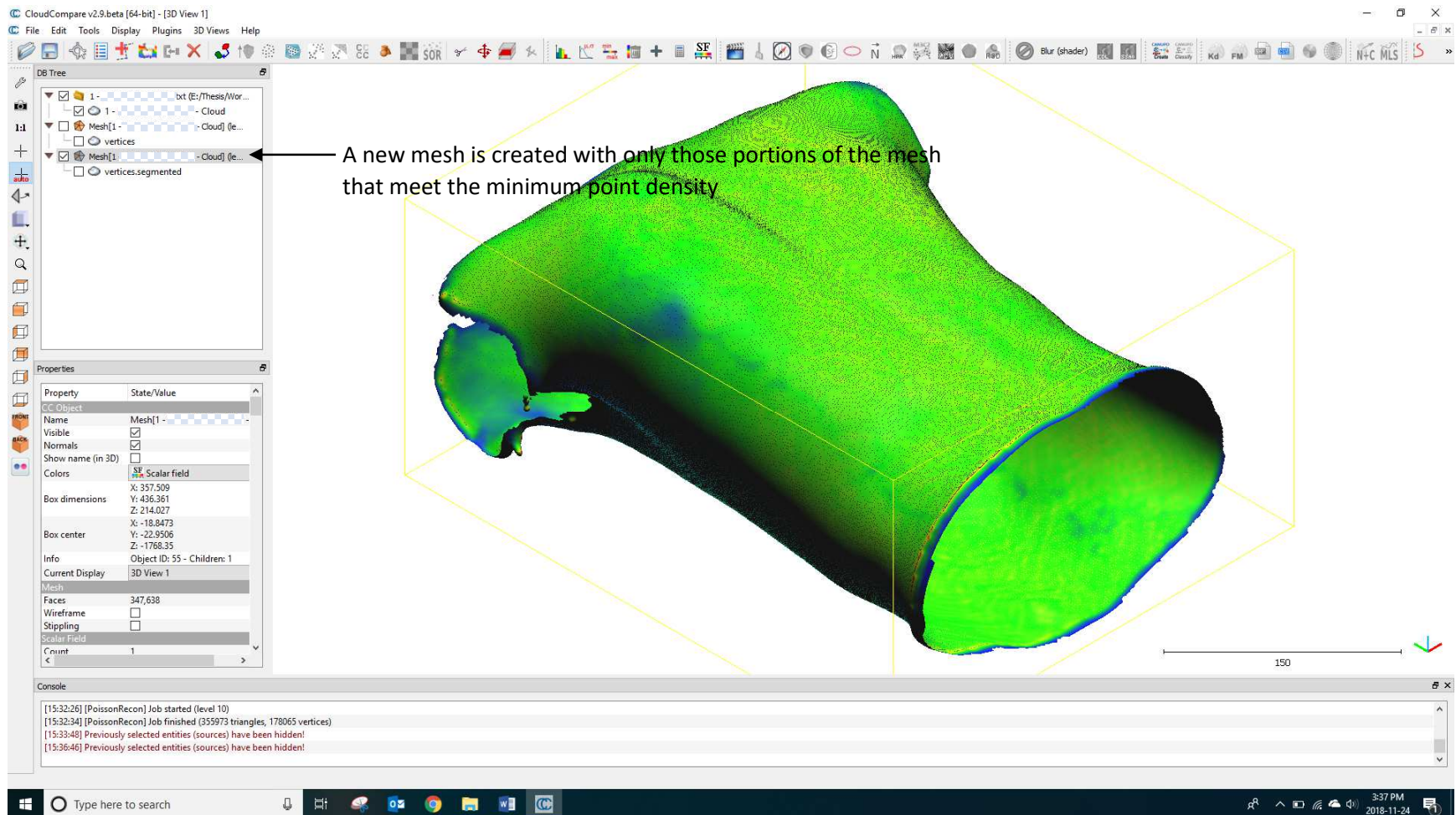
150

Console

```
[15:30:21] [PoissonRecon] Job finished (355973 triangles, 178065 vertices)
[15:32:26] [PoissonRecon] Job started (level 10)
[15:32:34] [PoissonRecon] Job finished (355973 triangles, 178065 vertices)
[15:33:48] Previously selected entities (sources) have been hidden!
```

Type here to search

3:36 PM 2018-11-24



A new mesh is created with only those portions of the mesh that meet the minimum point density

Use the 'Segment' tool to delete areas of the mesh that result from stray points

CloudCompare v2.9.0.beta [64-bit] - [3D View 1]

File Edit Tools Display Plugins 3D Views Help

DB Tree

- 1 - [bt (E:/Thesis/Wor...]
- 1 - Cloud
- Mesh[1 - Cloud] (e...
- vertices
- Mesh[1 - Cloud] (e...
- vertices.segmented

Properties

Property	State/Value
Active	Density
Color Scale	
Current	Blue>Green>Yellow>Red
Steps	256
Visible	<input type="checkbox"/>

SF display params

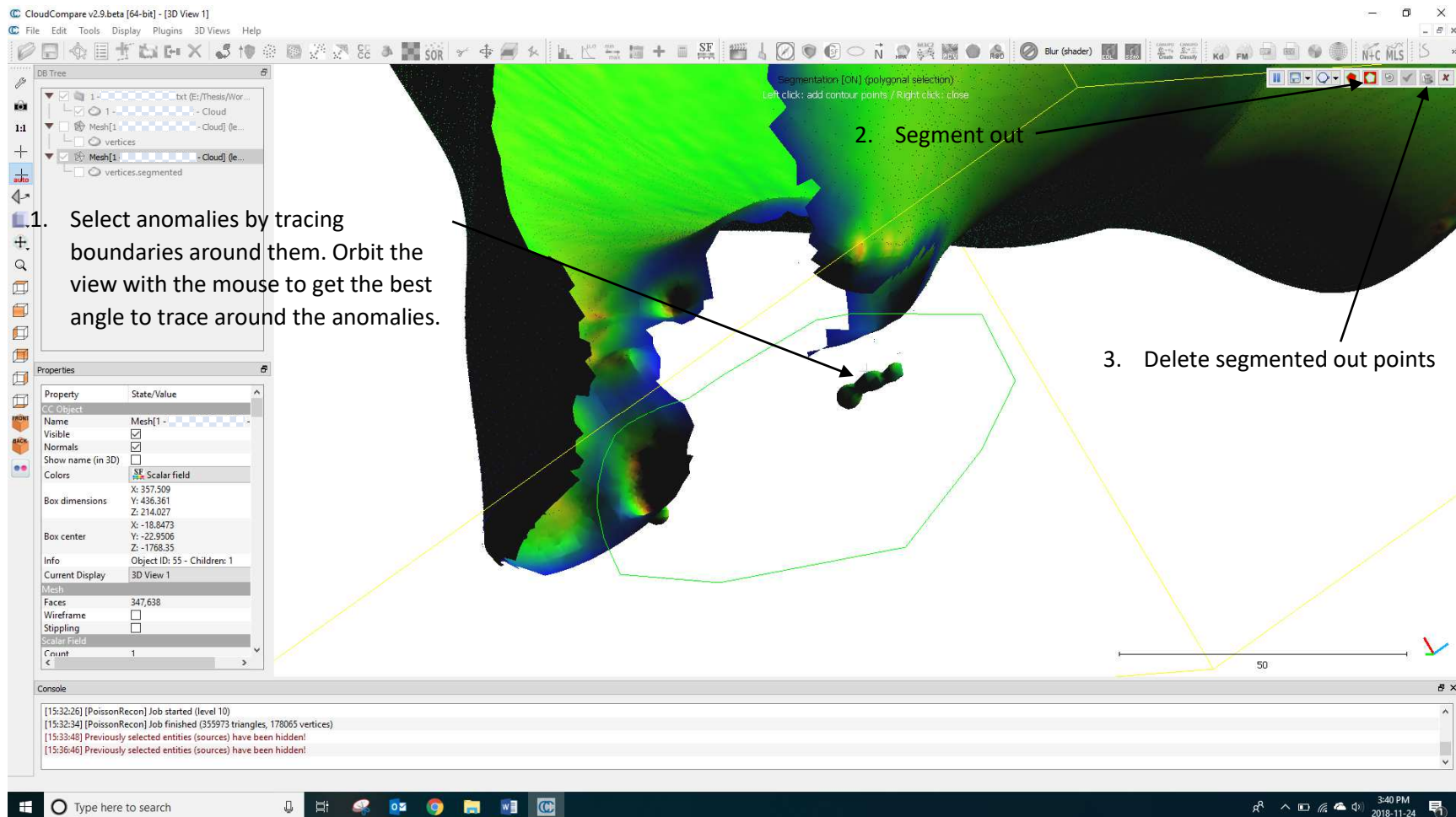
Display ranges	Parameters
6.00056171	displayed 8.36781788

Transformation history

Console

```
[15:11:47] [PoissonRecon] Job finished (266328 triangles, 133243 vertices)
[15:18:56] Previously selected entities (sources) have been hidden!
[15:19:25] Previously selected entities (sources) have been hidden!
[15:24:14] Previously selected entities (sources) have been hidden!
```

Delete areas of mesh that result from stray points using the 'Segment' tool



Segmenting out anomalies means selecting those areas that are obviously not meant to be part of the analysis. These anomalies can result from stray points in the point cloud, which can be caused by several factors such as reflections of the laser, dust or hair that reflects the laser, etc.

Step 3 – Create a Reflected Cloned Mesh

The screenshot displays the CloudCompare v2.9.0 beta interface. The main 3D view shows a bone mesh with a color map ranging from blue to red. The DB Tree on the left shows a hierarchy of objects, with 'Mesh[1]' selected. The Properties panel on the left shows the selected object's details, including its name, visibility, and box dimensions. The Console at the bottom shows the results of a PoissonRecon job. An arrow points to the 'Clone' icon in the toolbar with the text 'Clone selected mesh'.

Clone selected mesh

Property	State/Value
CC Object	
Name	Mesh[1] -
Visible	<input checked="" type="checkbox"/>
Normals	<input checked="" type="checkbox"/>
Show name (in 3D)	<input type="checkbox"/>
Colors	Scalar field
Box dimensions	X: 357.509 Y: 436.361 Z: 214.027
Box center	X: -18.8473 Y: -22.9506 Z: -1768.35
Info	Object ID: 65 - Children: 1
Current Display	3D View 1
Mesh	
Faces	345,478
Wireframe	<input type="checkbox"/>
Stippling	<input type="checkbox"/>
Scalar field	
Count	1

```
[15:32:26] [PoissonRecon] Job started (level 10)
[15:32:34] [PoissonRecon] Job finished (355973 triangles, 178065 vertices)
[15:33:48] Previously selected entities (sources) have been hidden!
[15:36:46] Previously selected entities (sources) have been hidden!
```

CloudCompare v2.9.0.beta [64-bit] - [3D View 1]

File Edit Tools Display Plugins 3D Views Help

Normals
Octree
Grid
Mesh
Plane
Sensors
Scalar fields
Waveform

Clone
Merge
Subsample
Apply transformation Ctrl+I
Multiply/Scale
Translate/rotate
Segment
Crop
Edit global shift and scale
Toggle (recursive)

Delete Del

Name Mesh[1]
Visible
Normals
Show name (in 3D)
Colors SF Scalar field
X: 357.509
Y: 436.261
Z: 214.027
Box dimensions
X: -18.8473
Y: -22.9506
Z: -1768.35
Box center
Info Object ID: 69 - Children: 1
Current Display 3D View 1

Mesh
Faces 345,478
Wireframe
Stippling
Scalar Field
Print 1

Console

[15:32:26] [PoissonRecon] Job started (level 10)
[15:32:34] [PoissonRecon] Job finished (355973 triangles, 178065 vertices)
[15:33:48] Previously selected entities (sources) have been hidden!
[15:36:46] Previously selected entities (sources) have been hidden!

Select second mesh. Select Multiply/Scale tool

200

3:46 PM
2018-11-24

Uncheck "same scale for all dimension"

Scale / multiply

Scale(x) -1 Scale(y) 1.00000000 Scale(z) 1.00000000

Same scale for all dimensions

Keep entity in place

Rescale Global shift

OK Cancel

Scale -1 in x direction to mirror the mesh about the xy plane

200

Properties

Property	State/Value
Object	
Name	Mesh[1] -
Visible	<input checked="" type="checkbox"/>
Normals	<input checked="" type="checkbox"/>
Show name (in 3D)	<input type="checkbox"/>
Colors	Scalar field
X	357.509
Y	436.361
Z	214.027
Box dimensions	
X	-18.8473
Y	-22.9506
Z	-1768.35
Box center	
Info	Object ID: 69 - Children: 1
Current Display	3D View 1
Mesh	
Faces	345,478
Wireframe	<input type="checkbox"/>
Stippling	<input type="checkbox"/>
Scalar Field	
Count	1

Console

```
[15:32:26] [PoissonRecon] Job started (level 10)
[15:32:34] [PoissonRecon] Job finished (355973 triangles, 178065 vertices)
[15:33:48] Previously selected entities (sources) have been hidden!
[15:36:46] Previously selected entities (sources) have been hidden!
```

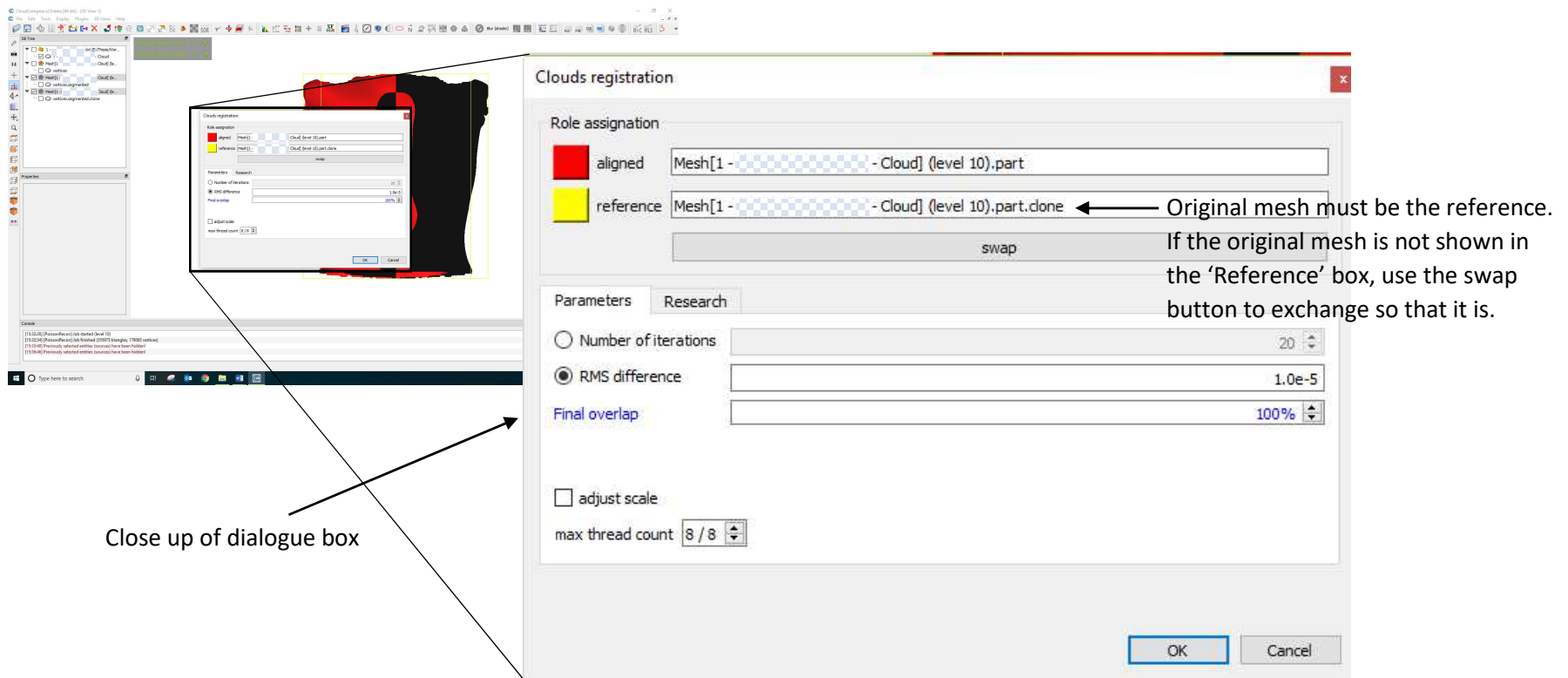
Step 4 – Registration of Cloned Mesh

1. Select both meshes.

2. Use the fine registration tool to adjust position of cloned mesh to match original mesh as close as possible

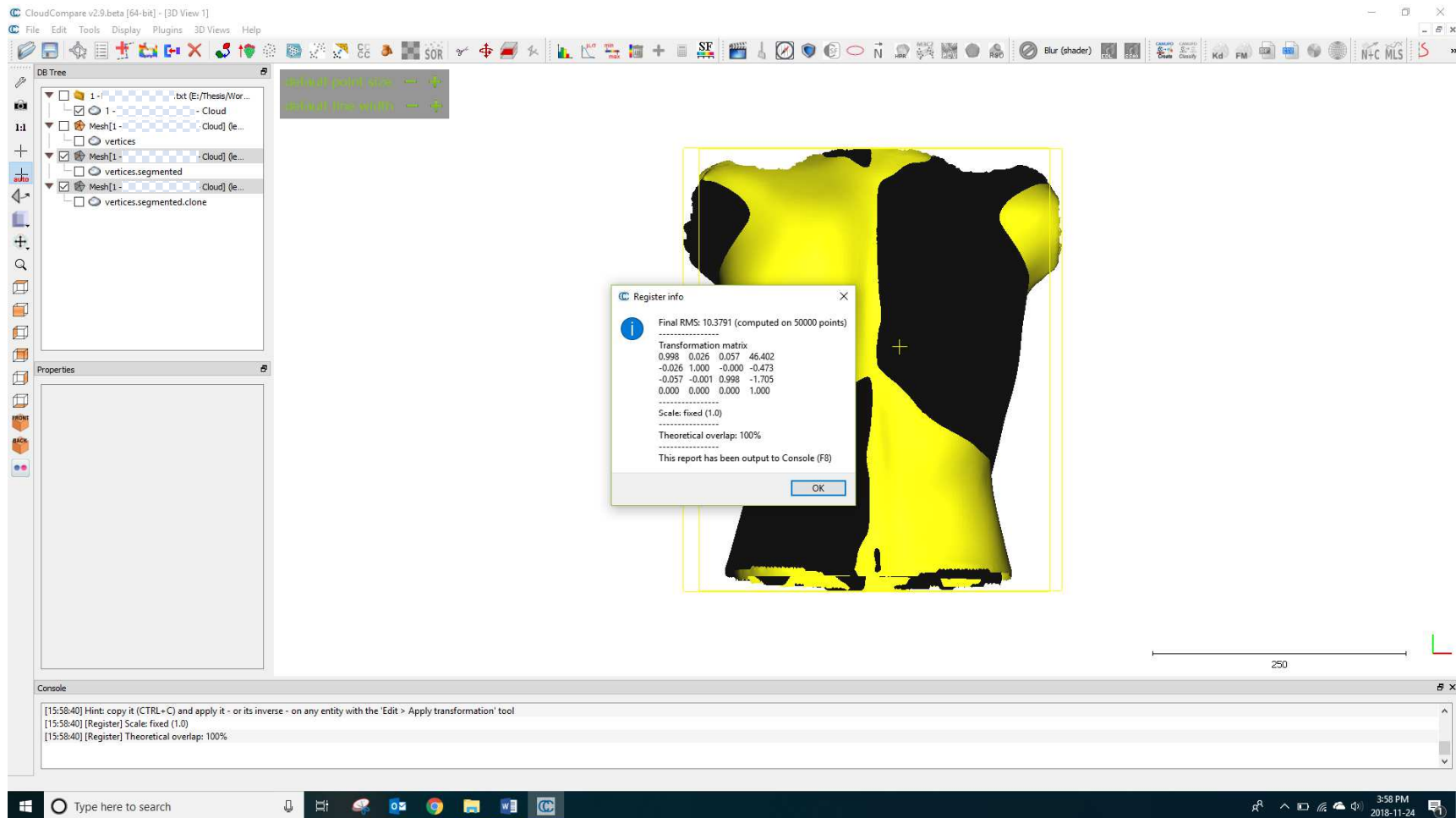
Console:

```
[15:32:26] [PoissonRecon] Job started (level 10)
[15:32:34] [PoissonRecon] Job finished (35973 triangles, 178065 vertices)
[15:33:48] Previously selected entities (sources) have been hidden!
[15:36:46] Previously selected entities (sources) have been hidden!
```



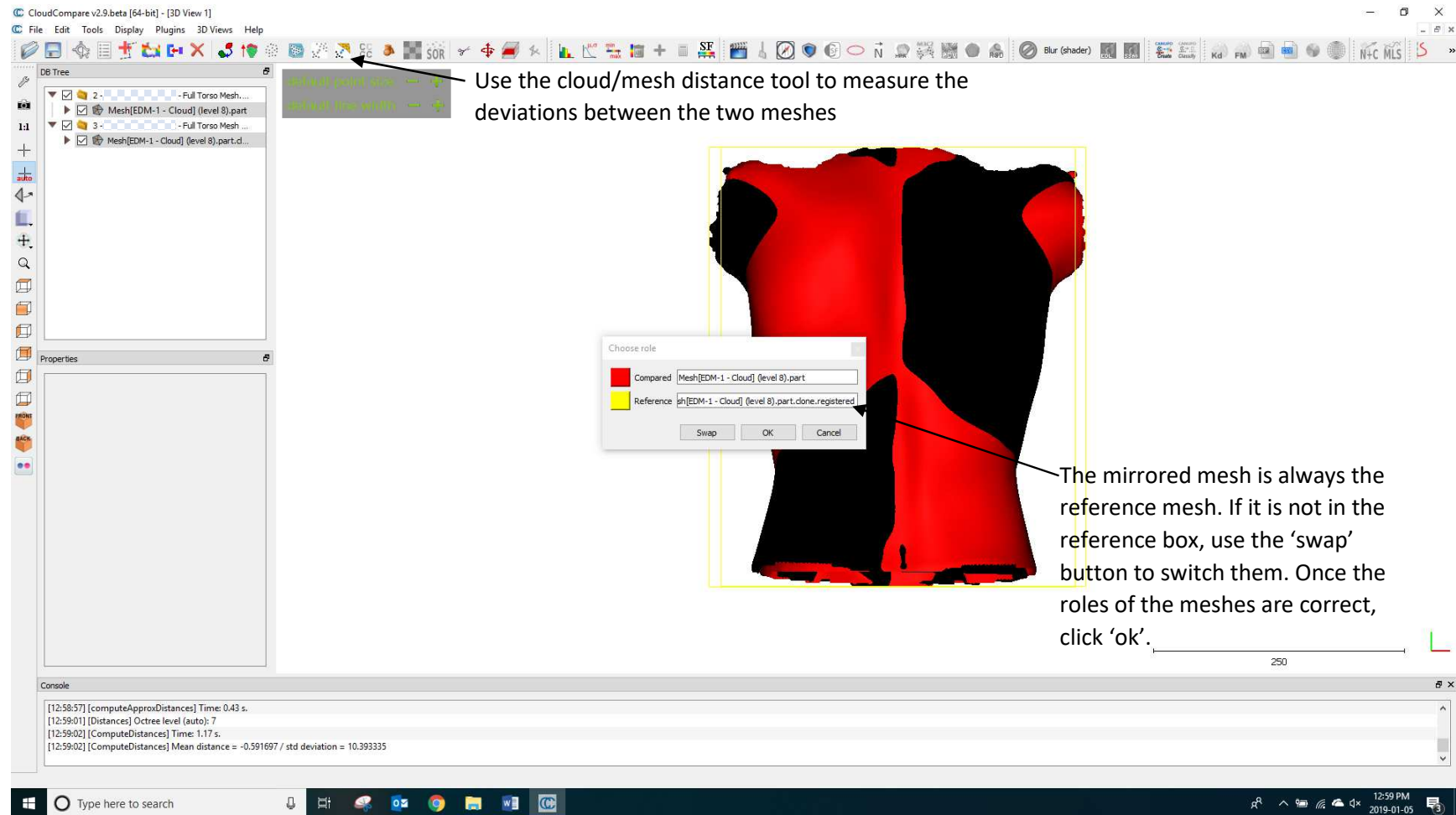
Once threshold of RMS difference between iterations is reached, transformation matrix that has been applied to the cloned mesh is displayed. The final RMS displayed in this pop up is not the RMS for any of the patches identified in the mesh, this is for the overall registration of the point clouds.

The registration is an iterative process of the computer trying to find the best fit between the two meshes. The iterations can be limited to a specific number of iterations, or they can continue until the root mean square of the differences between each successive iteration reaches a certain threshold. Using the 'RMS Difference' option brings the aligned mesh as close as possible to the reference. The threshold of 1 E-05 is the default threshold and provided consistent results throughout the study. Because this value is so small compared to the threshold of 3.4mm used in his study but didn't cause issues with the performance of the registration, it was not changed from the default.



The next step is to measure the deviations between the two meshes at each vertex on the meshes. This creates thousands of deviation measurements that are applied to the original scan mesh as a deviation color map (DCM).

Step 5 – Measurement of Deviation



Setting the mirrored mesh as the reference causes all measured deviations to be applied to the original mesh, which has been set as the 'Compared' mesh.

The screenshot displays the CloudCompare v2.9.beta [64-bit] interface. The main 3D view shows a torso model with a color-coded distance map. A 'Distance computation' dialog box is open, allowing for the configuration of distance calculation parameters. The console window at the bottom provides a log of the process, including the time taken for distance and approximate distance computations.

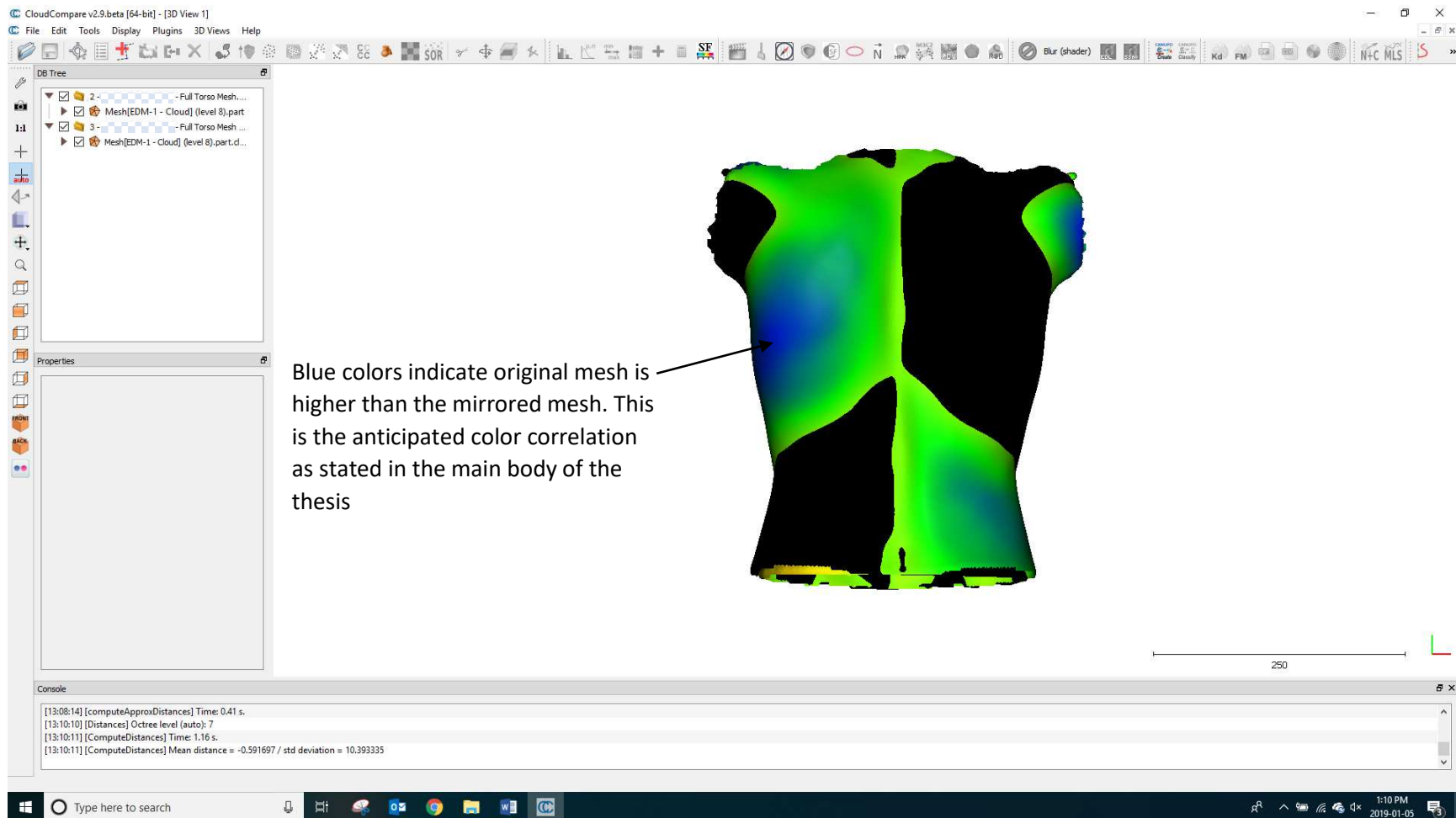
Distance computation dialog box details:

- Compared: Mesh[EDM-1 - Cloud] (level 8).part
- Reference: Mesh[EDM-1 - Cloud] (level 8).part.done.registered
- Precise results:
 - General parameters: Octree level: AUTO, max. distance: 27.826561
 - Local modeling: signed distances (checked), flip normals (unchecked), split X,Y and Z components (unchecked), multi-threaded (checked)
 - Approx. results: max thread count: 8 / 8
- Buttons: Compute, OK, Cancel

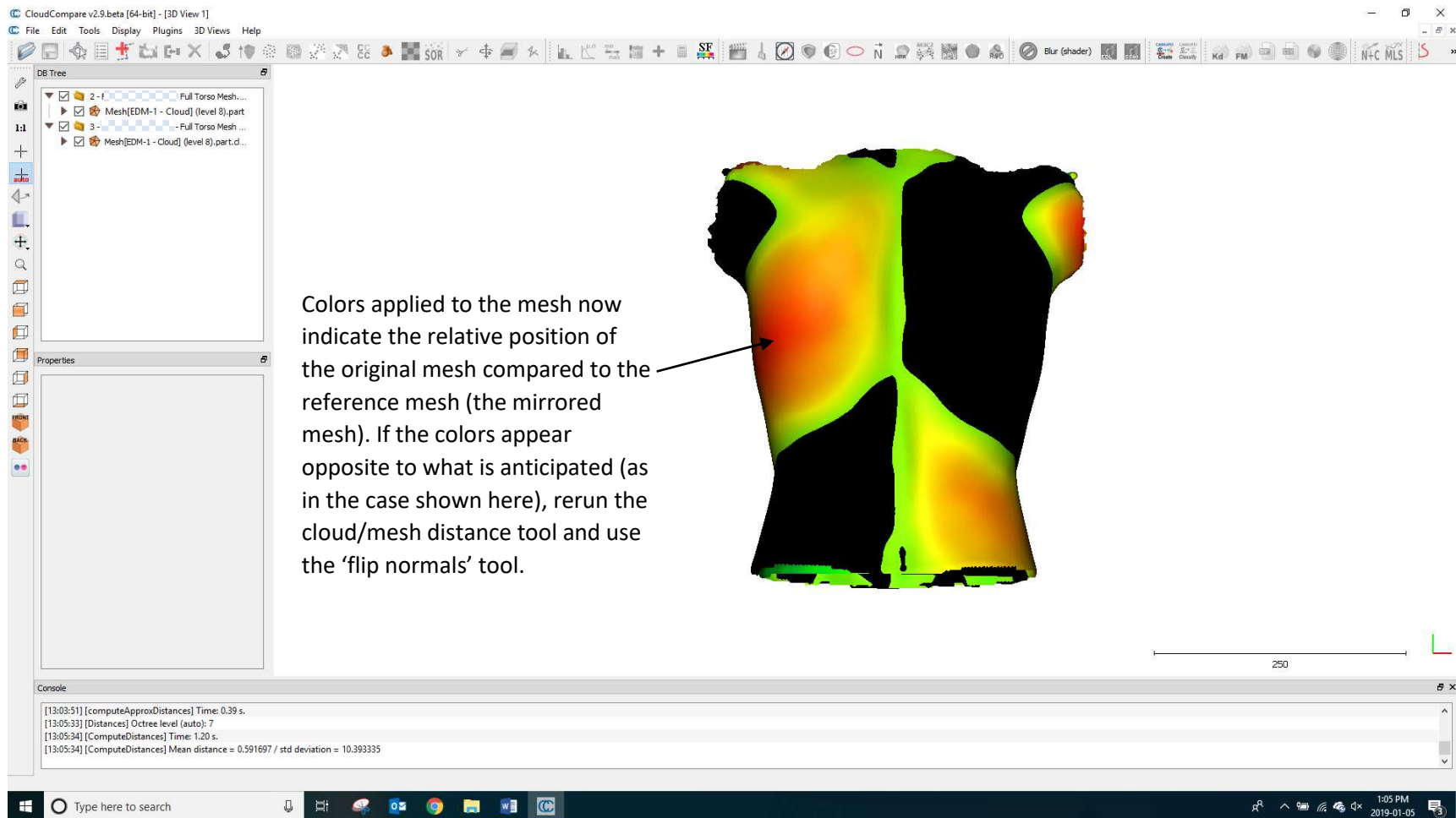
Console log:

```
[12:59:01] [Distances] Octree level (auto): 7  
[12:59:02] [ComputeDistances] Time: 1.17 s.  
[12:59:02] [ComputeDistances] Mean distance = -0.591697 / std deviation = 10.393335  
[13:03:51] [computeApproxDistances] Time: 0.39 s.
```

Although the colors on the meshes will change once this dialogue box appears, the deviation have not been determined until 'compute' is clicked. Once the compute cycle is done, click 'ok'.



As mentioned in the main body of the thesis, red colors indicate that the mirrored mesh is above the original mesh, and blue colors indicate that the original mesh is higher. If the colors are reversed, with areas of the original mesh that are visibly higher than the mirrored mesh colored red, use the following steps to correct the coloring.



CloudCompare v2.9.0.beta [64-bit] - [3D View 1]

File Edit Tools Display Plugins 3D Views Help

DB Tree

- 2-f Full Torso Mesh...
- Mesh[EDM-1 - Cloud] (level 8).part
- 3 - Full Torso Mesh...
- Mesh[EDM-1 - Cloud] (level 8).part.d...

Properties

Console

```
[13:03:51] [computeApproxDistances] Time: 0.39 s.  
[13:05:33] [Distances] Octree level (auto): 7  
[13:05:34] [ComputeDistances] Time: 1.20 s.  
[13:05:34] [ComputeDistances] Mean distance = 0.591697 / std deviation = 10.393335
```

Colors applied to the mesh now indicate the relative position of the original mesh compared to the reference mesh (the mirrored mesh). If the colors appear opposite to what is anticipated (as in the case shown here), rerun the cloud/mesh distance tool and use the 'flip normals' tool.

250

Type here to search

1:05 PM
2019-01-05

Distance computation

Compared Mesh[EDM-1 - Cloud] (level 8).part
Reference Mesh[EDM-1 - Cloud] (level 8).part.done.registered

Precise results

General parameters Local modeling Approx. results

Octree level AUTO

max. distance 27.826561

signed distance flip normals

split world Z components

multi-threaded max thread count 8 / 8

Compute

Ok Cancel

Rerun the distance computation with 'flip normals' selected. This step is only necessary if the deviation colors are reversed.

Console

```
[13:05:33] [Distances] Octree level (auto): 7  
[13:05:34] [ComputeDistances] Time: 1.20 s.  
[13:05:34] [ComputeDistances] Mean distance = 0.591697 / std deviation = 10.393335  
[13:08:14] [computeApproxDistances] Time: 0.41 s.
```

Step 6 – Create Deviation Color Map

The screenshot shows the CloudCompare v2.9.beta interface. The DB Tree on the left lists several meshes, with an arrow pointing to the 'Mesh[EDM-1 - Cloud] (level 8).part.d...' entry. The 3D view in the center displays a torso model with a color map representing deviation. A scale bar at the bottom right indicates a length of 250 units. The Console at the bottom shows the following log entries:

```
[13:08:14] [computeApproxDistances] Time: 0.41 s.  
[13:10:10] [Distances] Octree level (auto): 7  
[13:10:11] [ComputeDistances] Time: 1.16 s.  
[13:10:11] [ComputeDistances] Mean distance = -0.591697 / std deviation = 10.393335
```

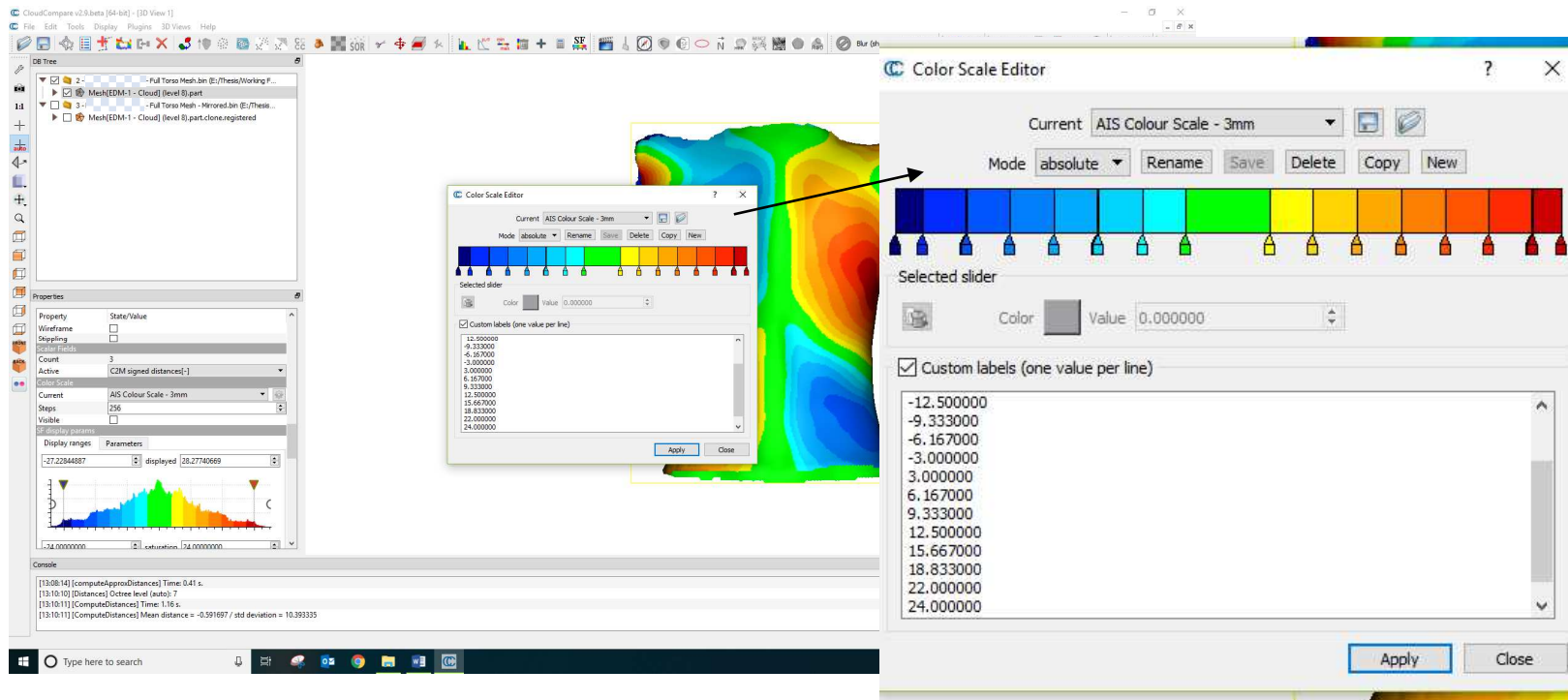
Uncheck boxes next to the mirrored meshes to hide them, leaving only the original back mesh with the deviation color map applied.

Current color scheme uses default color legend. The color legend can be customized to reflect the desired legend.

The screenshot displays the CloudCompare v2.9.0 beta interface. The DB Tree on the left shows a hierarchy of objects, with 'Mesh[EDM-1 - Cloud] (level 8).part' selected. The Properties panel below it shows the 'Color Scale' settings for the selected mesh, with the 'Current' scale set to 'Blue>Green>Yellow>Red'. A 3D view of the torso mesh is shown on the right, colored according to the selected scale. A scale bar below the mesh indicates a length of 250 units. The Console at the bottom shows log messages related to distance calculations.

Select the mesh to activate the properties dialog

The color scale dialog gives an opportunity to choose different color scales. Click the settings gear next to 'current' to have an opportunity to create a custom scale.



Use the color scale editor to create a custom color scale that will provide the correct deviation color map, using the colors and thresholds used in this thesis and previous studies (see main body of thesis for description and references of previous studies). The values for the color thresholds are show in this screenshot and are also listed in the Figure 1-5 of the thesis body. Save this customized color scale for use with other meshes.

The screenshot displays the CloudCompare v2.9.0 beta interface. The main 3D view shows a torso model with a color-coded signed distance field. The color scale legend on the right is titled "C2M signed distances[-]" and ranges from -24.000000 to 24.000000. The Properties panel on the left shows the "Visible" checkbox checked under the "SF display: params" section. A text annotation points to this checkbox with the text: "To show the legend, click 'visible' in the color scale tab". The console window at the bottom shows the following log entries:

```
[13:08:14] [computeApproxDistances] Time: 0.41 s.  
[13:10:10] [Distances] Octree level (auto): 7  
[13:10:11] [ComputeDistances] Time: 1.16 s.  
[13:10:11] [ComputeDistances] Mean distance = -0.591697 / std deviation = 10.393335
```

Step 7 – Isolate Patches

The screenshot displays the CloudCompare v2.9.beta interface. The DB Tree on the left shows the hierarchy: '2 - Full Torso Mesh.bin (E:/Thesis/Working F...)' containing 'Mesh[EDM-1 - Cloud] (level 8).part'. The Properties panel below it shows the selected object's details, including 'Scalar field' set to 'C2M signed distances[-]'. The main 3D view shows a torso mesh with a color gradient representing signed distances. A color scale legend on the right side of the 3D view shows the range from -24.000000 (dark blue) to 24.000000 (dark red), with intermediate values at -22.000000, -18.833000, -15.667000, -12.500000, -9.333000, -6.167000, 3.000000, 6.167000, 9.333000, 12.500000, 15.667000, 18.833000, and 22.000000. A scale bar at the bottom right of the 3D view indicates a length of 250 units. The console window at the bottom shows the following log entries:

```
[13:46:50] [BIN] Opening file 'E:/Thesis/Working Folders/Baseline/31 - ... - Full Torso Mesh.bin'...  
[13:46:50] [BIN] Version 4.7 (coords: float / scalar: float)  
[13:46:50] [I/O] File 'E:/Thesis/Working Folders/Baseline/31 - ... - Full Torso Mesh.bin' loaded successfully  
[13:47:28] Previously selected entities (sources) have been hidden!
```

Select the mesh, then select the 'filter points by value' tool

CloudCompare v2.9.0.beta [64-bit] - [3D View 1]

File Edit Tools Display Plugins 3D Views Help

DB Tree

- 2 - Full Torso Mesh.bin (E:/Thesis/Working F...
- MeshEDM-1 - Cloud (level 8).part

Properties

Property	State/Value
CC Object	
Name	MeshEDM 1 Cloud (level 8).part
Visible	<input checked="" type="checkbox"/>
Normals	<input checked="" type="checkbox"/>
Show name (in 3D)	<input type="checkbox"/>
Colors	Scalar field
Box dimensions	X: 363.064 Y: 436.376 Z: 214.032
Box center	X: -21.284 Y: -22.9433 Z: -1768.35
Info	Object ID: 243318 - Children: 1
Current Display	3D View 1
Mesh	
Faces	259,065
Wireframe	<input type="checkbox"/>
Stippling	<input type="checkbox"/>
Scalar Fields	
Count	3
Active	C2M signed distances[-]

Filter by value

Range 9.33 - 28.27740669

Export Split Cancel

Set the minimum threshold value to match the patch threshold. In this case any points with a deviation of over 9.33mm will be isolated

C2M signed distances[-]

24.000000
22.000000
18.833000
15.667000
12.500000
9.333000
6.167000
3.000000
-3.000000
-6.167000
-9.333000
-12.500000
-15.667000
-18.833000
-22.000000
-24.000000

250

Console

```
[13:46:50] [BIN] Opening file 'E:/Thesis/Working Folders/Baseline/31 - Full Torso Mesh.bin'...  
[13:46:50] [BIN] Version 4.7 (coords: float / scalar: float)  
[13:46:50] [I/O] File 'E:/Thesis/Working Folders/Baseline/31 - Full Torso Mesh.bin' loaded successfully  
[13:47:28] Previously selected entities (sources) have been hidden!
```

Type here to search

1:49 PM 2019-01-05

The screenshot displays the CloudCompare interface. The DB Tree on the left shows a hierarchy of objects, with 'Mesh[EDM-1 - Cloud] (level 8).part' selected. The Properties panel below it shows the 'Colors' property set to 'Scalar field'. The 3D Viewport in the center shows a 3D model of a torso with a highlighted section of the mesh. The console at the bottom shows the following messages:

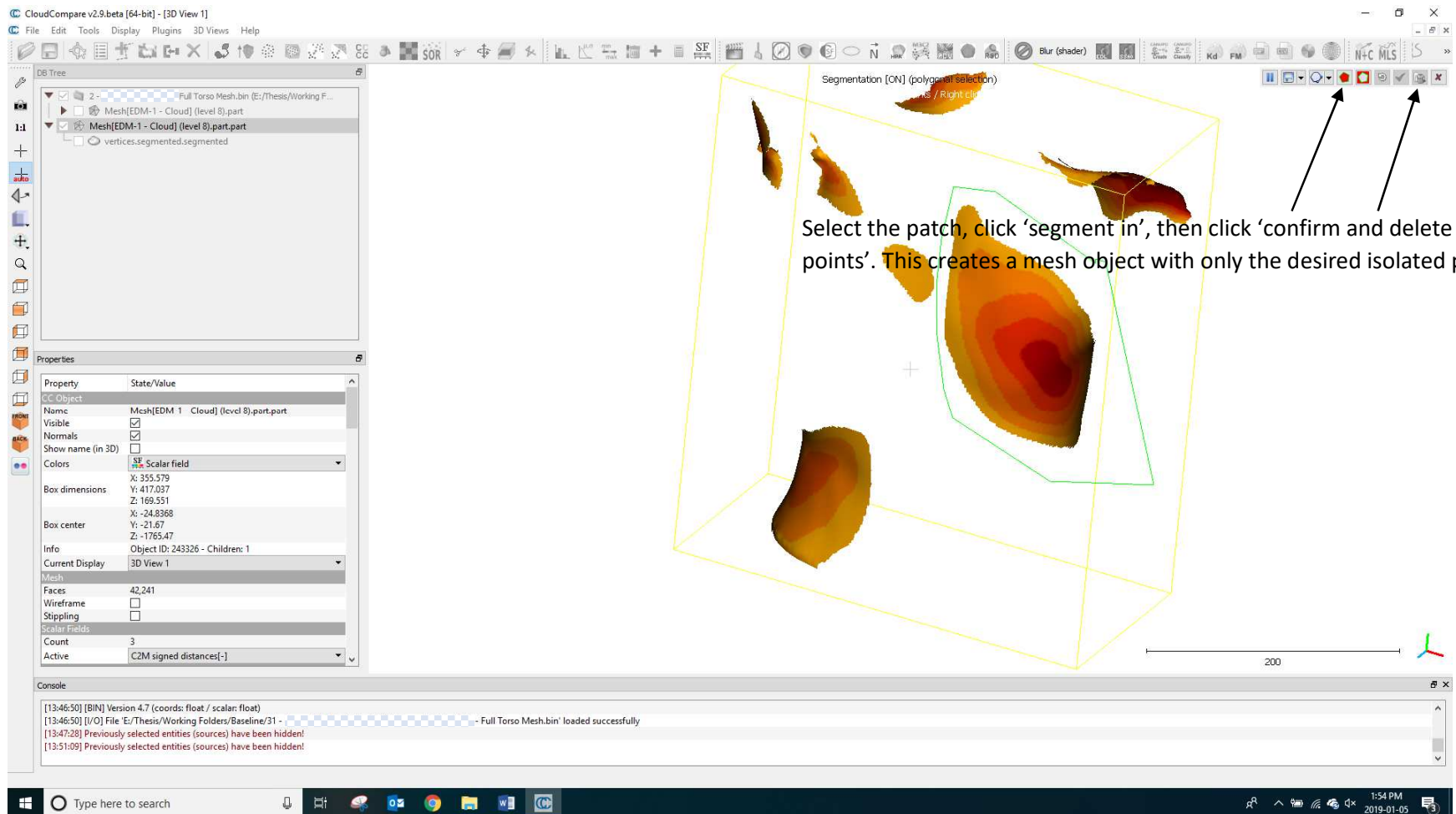
```
[13:46:50] [BIN] Version 4.7 (coords: float / scalar: float)
[13:46:50] [I/O] File 'E:/Thesis/Working Folders/Baseline/31 - Full Torso Mesh.bin' loaded successfully
[13:47:28] Previously selected entities (sources) have been hidden!
[13:51:09] Previously selected entities (sources) have been hidden!
```

A new mesh object has been created, containing only copies of those portions of the mesh which met the filter criteria (deviation greater than 9.33mm). The original mesh is still there, but has been hidden by default. It can be shown again by checking the box beside the object.

The 9.33mm threshold used is the threshold identified in the main body of the thesis and was determined by Ghaneei et. al (1) in a previous study as a threshold at which patches are clearly delineated.

The screenshot displays the CloudCompare v2.9.0 beta interface. The main 3D view shows a torso mesh with several segmented patches in a color gradient from yellow to red. A coordinate system with red, green, and blue axes is visible. A scale bar at the bottom right of the 3D view indicates a length of 200 units. The DB Tree on the left shows the hierarchy of the mesh, including 'Full Torso Mesh.bin', 'Mesh[EDM-1 - Cloud] (level 8).part', and 'vertices.segmented.segmented'. The Console at the bottom shows log messages: '[13:46:50] [BIN] Version 4.7 (coords: float / scalar: float)', '[13:46:50] [I/O] File 'E:/Thesis/Working Folders/Baseline/31 - ...' - Full Torso Mesh.bin' loaded successfully', and two messages about hidden entities at 13:47:28 and 13:51:09. The Windows taskbar at the bottom shows the search bar and system tray with the time 1:53 PM on 2019-01-05.

Orbit the mesh to clearly see the patches. Use the segment tool to isolate the desired patches for measurement of Max Deviation and RMS per patch.



Select the patch, click 'segment in', then click 'confirm and delete hidden points'. This creates a mesh object with only the desired isolated patch.

The 'segment in' tool allows you to choose objects that you wish to keep, the get rid of everything else. The opposite tool is the 'segment out' tool, which will remove the selected object and keep everything else.

Full Torso Mesh.bin (E:/Thesis/Working F...)

- 2 - Mesh[EDM-1 - Cloud] (level 8).part
- Mesh[EDM-1 - Cloud] (level 8).part.part
- vertices.segmented.segmented

Properties

Property	State/Value
CC Object	
Name	Mesh[EDM 1 Cloud] (level 8).part.part
Visible	<input checked="" type="checkbox"/>
Normals	<input checked="" type="checkbox"/>
Show name (in 3D)	<input type="checkbox"/>
Colors	SR Scalar field
Box dimensions	X: 106.698 Y: 225.031 Z: 113.199
Box center	X: 60.5135 Y: 20.9339 Z: -1737.29
Info	Object ID: 243336 - Children: 1
Current Display	3D View 1
Mesh	
Faces	18,830
Wireframe	<input type="checkbox"/>
Stippling	<input type="checkbox"/>
Scalar Fields	
Count	3
Active	C2M signed distances[-]

Console

```
[13:46:50] [BIN] Version 4.7 (coords: float / scalar: float)
[13:46:50] [I/O] File 'E:/Thesis/Working Folders/Baseline/31 - Full Torso Mesh.bin' loaded successfully
[13:47:28] Previously selected entities (sources) have been hidden!
[13:51:09] Previously selected entities (sources) have been hidden!
```

200

The patch item now contains only those mesh faces and vertices that meet the threshold for patch identification

CloudCompare v2.9.0.beta [64-bit] - [3D View 1]

File Edit Tools Display Plugins 3D Views Help

DB Tree

- 2 - Full Torso Mesh bin (E:/Thesis/Working F...
- Mesh[EDM-1 - Cloud] (level 8).part
- Mesh[EDM-1 - Cloud] (level 8).part.part
 - vertices.segmented.segmented

Properties

Property	State/Value
Current Display	3D View 1
Mesh	
Faces	259,065
Wireframe	<input type="checkbox"/>
Stippling	<input type="checkbox"/>
Scalar Fields	
Count	3
Active	C2M signed distances[-]
Color Scale	
Current	AIS Colour Scale - 3mm
Steps	256
Visible	<input checked="" type="checkbox"/>
SF display params	
Display ranges	Parameters
-27.22844887	displayed 28.27740669

Filter by value

Range: -27.22844887 to -9.33

Export Apply Cancel

C2M signed distances[-]

24.000000
22.000000
18.833000
15.667000
12.500000
9.333000
6.167000
3.000000
-3.000000
-6.167000
-9.333000
-12.500000
-15.667000
-18.833000
-22.000000
-24.000000

200

Console

```
[14:00:05] Scalar field RMS = 16.2769  
[14:01:55] [Distribution fitting] Gauss: mean = 15.720667 / std.dev. = 4.218752  
[14:01:55] [Distribution fitting] Gauss: Chi2 Distance = 2834.422247  
[14:01:55] Scalar field RMS = 16.2769
```

Type here to search

2:06 PM
2019-01-05

Perform the same procedure to identify negative value patches. Just use -9.33mm as the maximum value

The screenshot displays the CloudCompare v2.9.0 beta [64-bit] - [3D View 1] interface. The main 3D view shows a segmented mesh of a torso, rendered with a blue color map. The mesh is composed of several distinct parts, including a large central section and several smaller, separate pieces. A scale bar at the bottom right of the 3D view indicates a length of 200 units. The interface includes a DB Tree panel on the left, a Properties panel, and a Console panel at the bottom. The Console panel shows the following log entries:

```
[14:01:55] [Distribution fitting] Gauss: mean = 15.720667 / std.dev. = 4.218752  
[14:01:55] [Distribution fitting] Gauss: Chi2 Distance = 2834.422247  
[14:01:55] Scalar field RMS = 16.2769  
[14:07:27] Previously selected entities (sources) have been hidden!
```

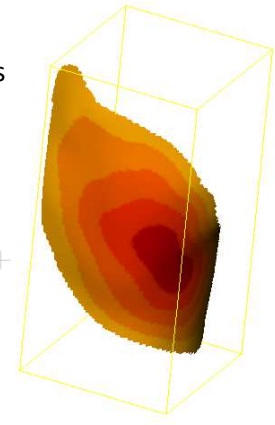
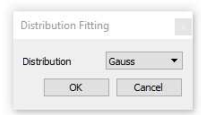
Step 8 – Calculate RMS and Max Deviation for Each Patch

The screenshot shows the CloudCompare v2.9.beta interface. The main 3D view displays a yellow wireframe box containing a torso mesh with a scalar field visualization in a color gradient from blue to red. A 'Distribution Fitting' dialog box is open, showing 'Gauss' as the selected distribution. The console window at the bottom displays the following log entries:

```
[13:59:53] Scalar field RMS = 16.2769
[14:00:05] [Distribution fitting] Weibull: a = 1.372450 / b = 6.923103 / shift = 9.330556
[14:00:05] [Distribution fitting] Weibull: Chi2 Distance = 1641.163587
[14:00:05] Scalar field RMS = 16.2769
```

The Properties panel on the left shows the active object is 'Mesh[EDM-1 - Cloud] (level 8).part.port' with a scalar field named 'C2M signed distances[-]'. The console window also shows the RMS value of 16.2769.

Select the 'distribution fitting' tool to perform a statistical analysis on the active scalar field. In this case, that's the deviation.



The screenshot displays the CloudCompare v2.9.0 beta interface. The main 3D view shows a yellow wireframe bounding box around a mesh object. A color-coded scalar field is applied to the mesh, with a color gradient from blue to red. A 'Distribution fitting' window is open, showing a histogram of 'C2M signed distances[-]' with a Gaussian fit curve. The histogram's x-axis ranges from 10 to 22.5, and the y-axis (Count) ranges from 0 to 180. The Gaussian fit parameters are: Gauss: mean = 15.720667 / std.dev. = 4.218752 [99 classes].

The 'Properties' panel on the left shows the following details for the selected object:

Property	State/Value
CC Object	
Name	Mesh[EDM 1 - Cloud] (level 8).part
Visible	<input checked="" type="checkbox"/>
Normals	<input checked="" type="checkbox"/>
Show name (in 3D)	<input type="checkbox"/>
Colors	Scalar field
Box dimensions	X: 108.698 Y: 225.031 Z: 113.199
Box center	X: 60.5135 Y: 20.9339 Z: -17.729
Info	Object ID: 243336 - Children: 1
Current Display	3D View 1
Mesh	
Faces	18,830
Wireframe	<input type="checkbox"/>
Stippling	<input type="checkbox"/>
Scalar Fields	
Count	3
Active	C2M signed distances[-]

The 'Console' at the bottom shows the following log entries:

```
[14:00:05] Scalar Field RMS = 16.2769
[14:01:55] [Distribution fitting] Gauss: mean = 15.720667 / std.dev. = 4.218752
[14:01:55] [Distribution fitting] Gauss: Chi2 Distance = 2834.422247
[14:01:55] Scalar Field RMS = 16.2769
```

An arrow points from the console log to the 'Active' property in the Properties panel.

The text below the screenshot reads: "The mean, standard deviation, Chi2 distance and RMS are all shown in the console line for the active scalar field for the selected object. The active scalar field is always the field that is determining the color of the mesh, in this case the deviation."

The screenshot displays the CloudCompare v2.9.beta [64-bit] - [3D View 1] interface. The main 3D view shows a mesh of a torso with a color-coded deviation map. The mesh is displayed within a yellow wireframe bounding box. The Properties panel on the left shows the 'SF display params' dialog box with a 'displayed' value of 24.61533928. A scale bar at the bottom right indicates 100 units. The console at the bottom shows log messages including 'Scalar Field RMS = 16.2769' and 'Gauss: mean = 15.720667 / std.dev. = 4.218752'.

The maximum deviation for the patch is the largest deviation value in the 'SF display params' dialog box.

This concludes the markerless asymmetry analysis of the 3D scanned surface topography. With practise, this analysis can be completed in ~ 10 minutes. The open source license that governs use of CloudCompare allows an add-on to be programed that would enable a custom add-on that could automate this process. Many of the available tools in the toolbar are add-ons that have been created by the CloudCompare user community and freely shared.

References

1. **Ghaneei, Maliheh.** *Algorithms for Adolescent Idiopathic Scoliosis Classification Based on Surface Topography Analysis*. s.l. : University of Alberta, 2017.

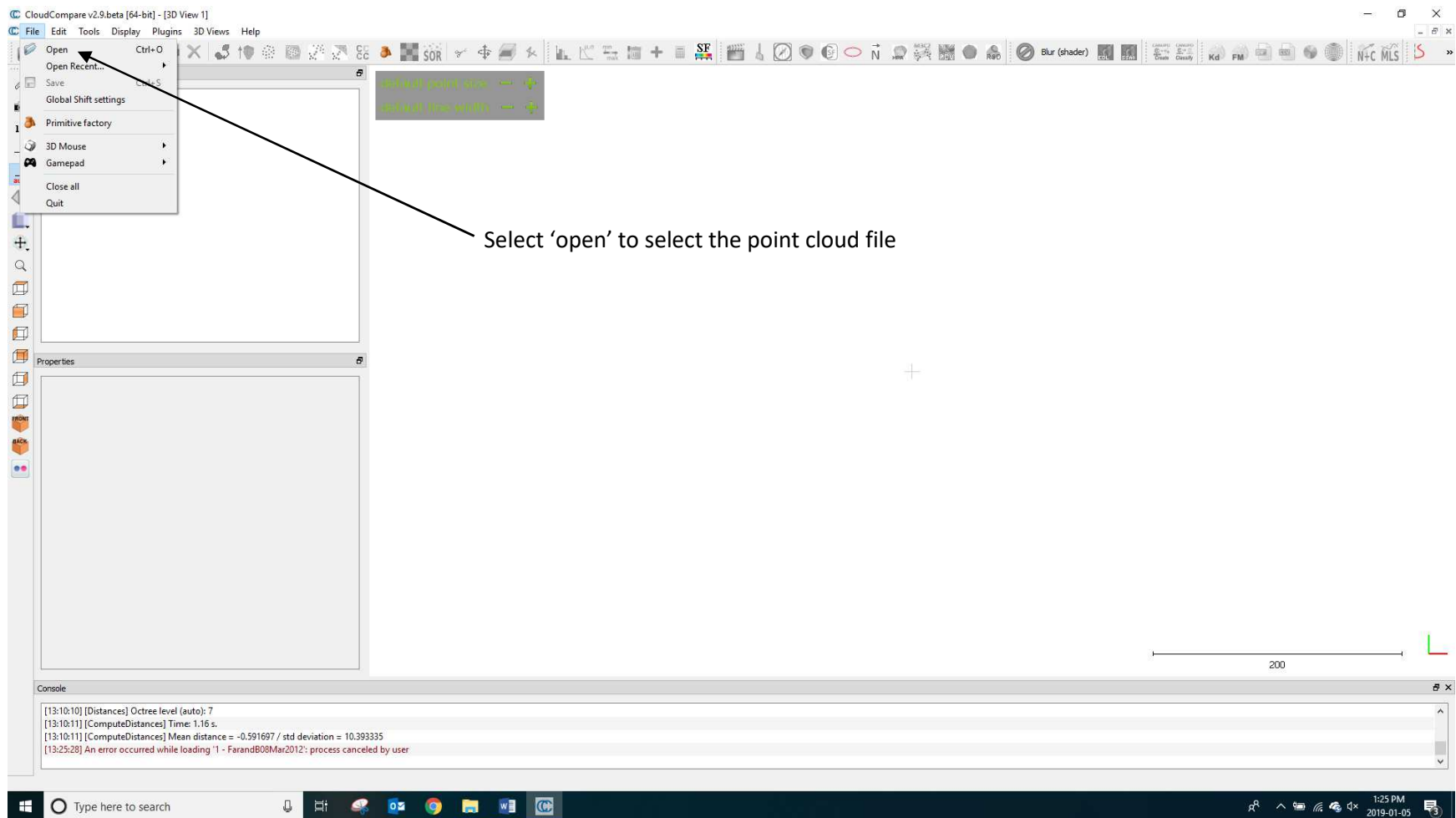
Appendix B – Isolation of Back Only Points Using CloudCompare

Contents

Appendix B – Isolation of Back Only Points Using CloudCompare	106
Step 1 – Import the Point Cloud	107
Step 2 – Calculate Normal Vectors for Each Point	111
Step 3 – Isolate Back Only Points	115

Step 1 – Import the Point Cloud

Cloudcompare can import many 3D pointcloud file types. ASCII text files work well, and give the opportunity to specify how each column in the file is interpreted.



CloudCompare v2.9.0 beta [64-bit] - [3D View 1]

File Edit Tools Display Plugins 3D Views Help

DB Tree

1:1

Properties

Console

Open file(s)

Look in: E:\Thesis\Working Folders\Baseline\31 -

Name	Size	Type	D4
1 -	13.3 MB	txt File	20
2 -	6.8 MB	bin File	20
3 -	5.8 MB	bin File	20
Full Torso Analysis Results.bmp	1.6 MB	bmp File	20

File name:

Files of type: All (*.*)

- CloudCompare entities (*.bin)
- ASCII cloud (*.asc *.neu *.xyz *.pts *.csv)
- LAS cloud (*.las *.laz)
- E57 cloud (*.e57)
- PTX cloud (*.ptx)
- PLY mesh (*.ply)
- OBJ mesh (*.obj)
- VTK cloud or mesh (*.vtk)
- STL mesh (*.stl)

ASCII point clouds work well

200

[13:10:10] [Distances] Octree level (auto): 7
[13:10:11] [ComputeDistances] Time: 1.16 s.
[13:10:11] [ComputeDistances] Mean distance = -0.591697 / std deviation = 10.393335
[13:25:28] An error occurred while loading '1 -' process canceled by user

Type here to search

1:26 PM 2019-01-05

CloudCompare v2.9.0 beta [64-bit] - [3D View 1]

File Edit Tools Display Plugins 3D Views Help

DB Tree

Open Ascii File

Filename: E:\Thesis\Working Folders\Baseline\31 -txt

Here are the first lines of this file. Choose each column attribution (one cloud at a time):

Header: X,Y,Z,R,G,B,Scalar field #1,Scalar field #2,Scalar field #3,Scalar field #4,Scalar field #5,Scalar field #6,Scalar field #7,Nx,Ny,Nz

1	2	3	4	5	6	7	8	9	10	11	12	13	14	15	16
coord. X	coord. Y	coord. Z	Red (0-255)	Green (0-255)	Blue (0-255)	Scalar	Scalar	Scalar	Scalar	Scalar	Scalar	Scalar	Nx	Ny	Nz
-104.71370697	103.57020569	-1804.38867188	125	62	237	-104.674553	104.758179	-1806.381470	0.039154	1.187972	-1.992739	2.320306	-0.014859	-0.509265	0.860482
120.31002808	142.10516357	-1788.21716309	167	50	221	113.379623	155.756775	-1804.617676	-6.930406	13.651615	-16.400427	22.435932	0.310956	-0.600967	0.736305
66.29096222	-142.02503967	-1834.69384766	36	133	216	71.085526	-142.309265	-1839.514038	4.794568	-0.284225	-4.820228	6.804650	-0.712082	0.044061	0.700712
66.99311066	-143.51937866	-1833.85083008	36	134	216	71.808258	-143.956573	-1838.637573	4.815149	-0.437200	-4.786725	6.803642	-0.715853	0.058818	0.695769
-142.09344482	-134.78282166	-1766.65441895	240	158	76	-148.331146	-136.511383	-1763.704468	-6.237704	-1.728561	2.949948	7.113302	0.882767	0.243471	-0.401801
-81.05876923	-218.73524475	-1853.50683594	184	143	240	-81.293251	-218.801010	-1853.967896	-0.234475	-0.065760	-0.461111	0.521466	0.448726	0.126783	0.884631
-147.47674561	-24.64217567	-1800.69494629	234	119	195	-143.726746	-24.941313	-1798.330078	3.749993	-0.299137	2.364862	-4.443478	0.841267	-0.063412	0.536889
-6.35850811	169.90051270	-1820.45666504	85	205	218	-10.377638	176.786743	-1812.480713	-4.019130	6.886222	7.976030	-11.277878	-0.332490	0.614700	0.715258
14.70086384	-84.83874512	-1868.50000000	100	99	248	13.771098	-85.722466	-1864.681763	-0.929766	-0.883724	3.818222	-4.027934	-0.212584	-0.220709	0.951891
-42.04277420	69.99320221	-1677.81555176	53	125	23	-45.892120	69.876549	-1683.166992	-3.849344	-0.116647	-5.351462	-6.593117	-0.580102	-0.017913	-0.814347
4.82255983	-197.33570862	-1861.22802734	96	139	250	5.608505	-197.667130	-1864.496216	0.785945	-0.331434	-3.268143	3.377620	-0.242984	0.092868	0.965575
-14.97659302	-137.63807678	-1873.54125977	131	144	253	-137.689603	-137.661224	-1873.710327	-0.004010	-0.023142	-0.169044	0.170668	0.028110	0.133805	0.990609
-50.54074860	72.78087885	-1821.37743652	145	84	246	-60.411452	75.686108	-1826.616842	-0.870705	1.906321	-5.246615	5.647847	0.144446	-0.324200	0.921235

Separator: , (ASCII code: 44) ESP TAB

Skip lines: 1 extract scalar field names from first line

Max number of points per cloud: 2000.00 Million

Apply Apply all Cancel

Console

```
[13:10:10] [Distances] Octree level (auto): 7
[13:10:11] [ComputeDistances] Time: 1.16 s.
[13:10:11] [ComputeDistances] Mean distance = -0.591697 / std deviation = 10.393335
[13:25:28] An error occurred while loading '1' - process canceled by user
```

Type here to search

1:28 PM 2019-01-05

CloudCompare gives an opportunity to specify the interpretation of each column in the point cloud file. The default will interpret the first three columns as x, y, z coordinates. Other values can be assigned to each point in other columns, such as colors, measurements, etc. For the purpose of the asymmetry analysis, only the first 3 columns (the x,y,z coordinates) are required. The rest can be ignored or deleted. These columns offer the opportunity for storing custom analysis values if desired.

The screenshot displays the CloudCompare v2.9.beta interface. The main 3D View shows a point cloud of a bone, rendered with a green-to-yellow color gradient. A scale bar at the bottom right of the 3D view is labeled '250'. On the left, the DB Tree panel shows a hierarchy where a point cloud entity is selected and highlighted with a blue checkmark. An arrow points from the text 'The point cloud entity is shown here. It is now ready for analysis' to this selected entity. The Console at the bottom shows several log messages, including a successful load of the point cloud: '[13:31:46] [VBO] VBO(s) (re)initialized for cloud '1' - Cloud' (1.30 Mb = 100.00% of points could be loaded)'. The Windows taskbar at the bottom shows the system time as 1:31 PM on 2019-01-05.

CloudCompare v2.9.beta [64-bit] - [3D View 1]

File Edit Tools Display Plugins 3D Views Help

DB Tree

- 1 - [E:/Thesis/Working Folders/Baseline/31...]
- 1 - Cloud

1:1

The point cloud entity is shown here. It is now ready for analysis

Properties

Console

```
[13:10:11] [ComputeDistances] Mean distance = -0.591697 / std deviation = 10.393335  
[13:25:28] An error occurred while loading '1' - : process canceled by user  
[13:31:46] [I/O] File 'E:/Thesis/Working Folders/Baseline/31 - .bt' loaded successfully  
[13:31:46] [VBO] VBO(s) (re)initialized for cloud '1' - Cloud' (1.30 Mb = 100.00% of points could be loaded)
```

250

Type here to search

1:31 PM
2019-01-05

Step 2 – Calculate Normal Vectors for Each Point

The screenshot displays the CloudCompare v2.9.beta software interface. The 'Edit' menu is open, and the 'Normals' option is selected, which has opened a sub-menu. In this sub-menu, the 'Compute' option is highlighted with a black arrow. A text box with the instruction 'With the point cloud selected, click 'Edit' -> 'Normals' -> 'Compute'' is positioned over the 'Compute' option. To the right of the menu, a point cloud of a human torso is displayed within a yellow rectangular frame. The software's interface includes a top toolbar, a left sidebar with various tool icons, a central 3D view area, and a bottom console window showing system logs. The Windows taskbar at the bottom indicates the time as 2:15 PM on 2019-01-05.

CloudCompare v2.9.beta [64-bit] - [3D View 1]

File Edit Tools Display Plugins 3D Views Help

Normals

- Compute
- Invert
- Orient normals
- Convert to
- Clear

With the point cloud selected, click 'Edit' -> 'Normals' -> 'Compute'

250

Console

```
[14:01:55] Scalar field RMS = 16.2769
[14:07:27] Previously selected entities (sources) have been hidden!
[14:15:31] [I/O] File 'E:/Thesis/Working Folders/Baseline/31 - ... .dxt' loaded successfully
[14:15:31] [VBO] VBO(s) (re)initialized for cloud '1 - ... - Cloud' (1.30 Mb = 100.00% of points could be loaded)
```

CloudCompare v2.9.beta [64-bit] - [3D View 1]

File Edit Tools Display Plugins 3D Views Help

DB Tree

- 1 - (E:/Thesis/Wor...)
- 1 - Cloud

Properties

Property	State/Value
Object	Cloud
Name	1
Visible	<input checked="" type="checkbox"/>
Normals	<input checked="" type="checkbox"/>
Show name (in 3D)	<input type="checkbox"/>
Colors	Scalar field
Box dimensions	X: 352.694 Y: 424.443 Z: 213.996
Box center	X: -18.4821 Y: -22.2779 Z: -1768.36
Info	Object ID: 4 - Children: 1
Current Display	3D View 1
Cloud	
Points	91,070
Global shift	(0.00;0.00;0.00)
Global scale	1.000000
Point size	Default
Scalar Fields	

Compute normals

Surface approximation
Local surface model: Plane

Neighbors
 use scan grid(s) whenever possible min angle: 1.00
 use octree radius: 4.244427 Auto

Orientation
 Use scan grid(s) whenever possible
 Use preferred orientation +2
 Use Minimum Spanning Tree knn = 6

OK Cancel

Keep default settings and click 'ok'

200

Console

```
[14:19:18] [I/O] File: 'E:/Thesis/Working Folders/Baseline/31 - ... .bt' loaded successfully
[14:19:18] [VBO] VBO(s) reinitialized for cloud '1 - Cloud' (1.30 Mb = 100.00% of points could be loaded)
[14:19:24] [ComputeCloudNormals] Timing: 0.28 s.
[14:19:25] [ResolveNormalsWithMST] Patches = 11 / Inversions: 51830
```

Type here to search

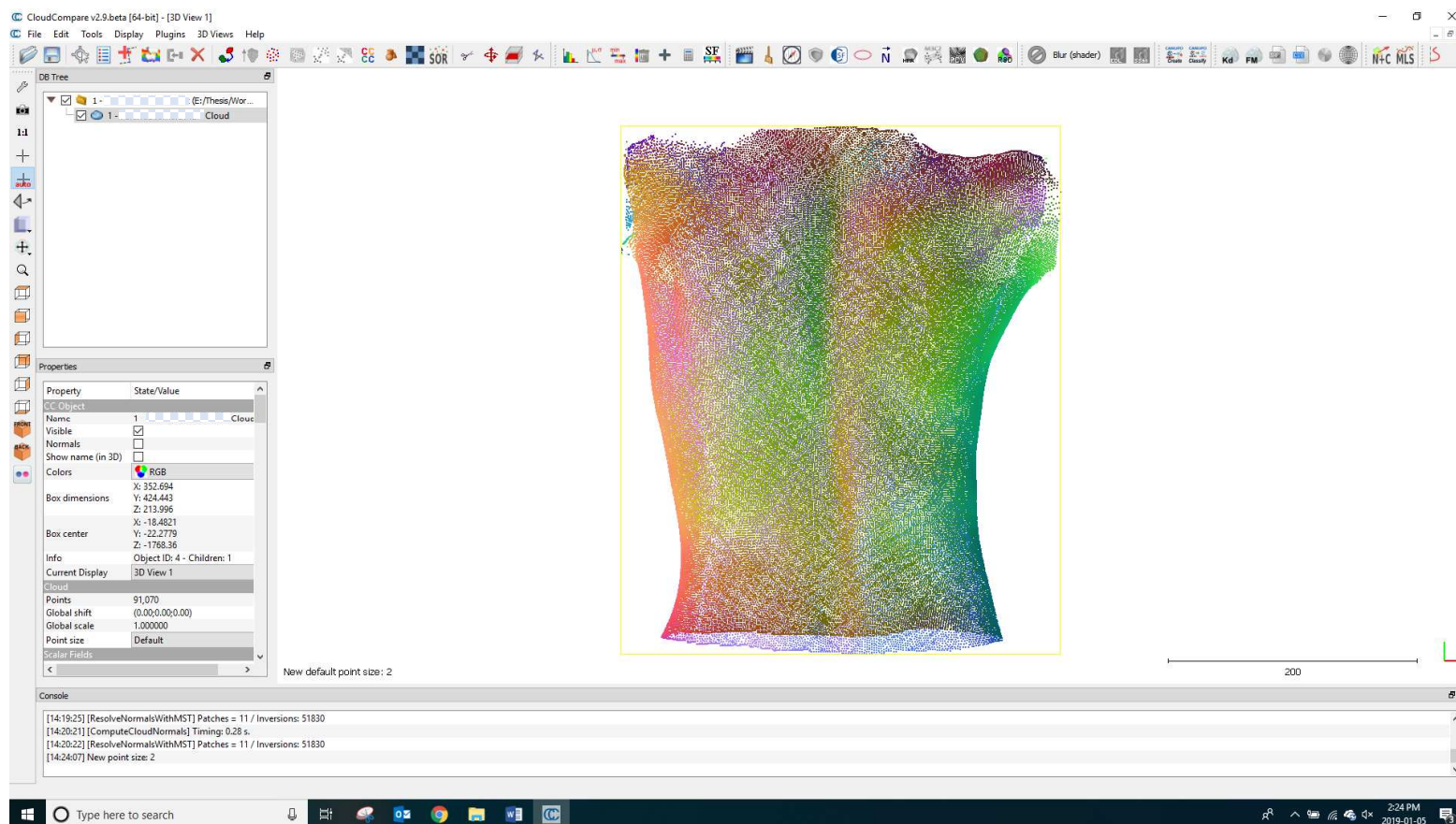
2:19 PM 2019-01-05

The screenshot displays the CloudCompare v2.9.0 beta interface. The 'Normals' menu is open, showing the path: Edit -> Normals -> Convert to -> HSV colors. A yellow box highlights a 3D model of a bone, which is rendered with a color gradient representing the HSV values of its normal vectors. The console at the bottom shows the following log entries:

```
[14:19:24] [ComputeCloudNormals] Timing: 0.28 s.
[14:19:25] [ResolveNormalsWithMST] Patches = 11 / Inversions: 51830
[14:20:21] [ComputeCloudNormals] Timing: 0.28 s.
[14:20:22] [ResolveNormalsWithMST] Patches = 11 / Inversions: 51830
```

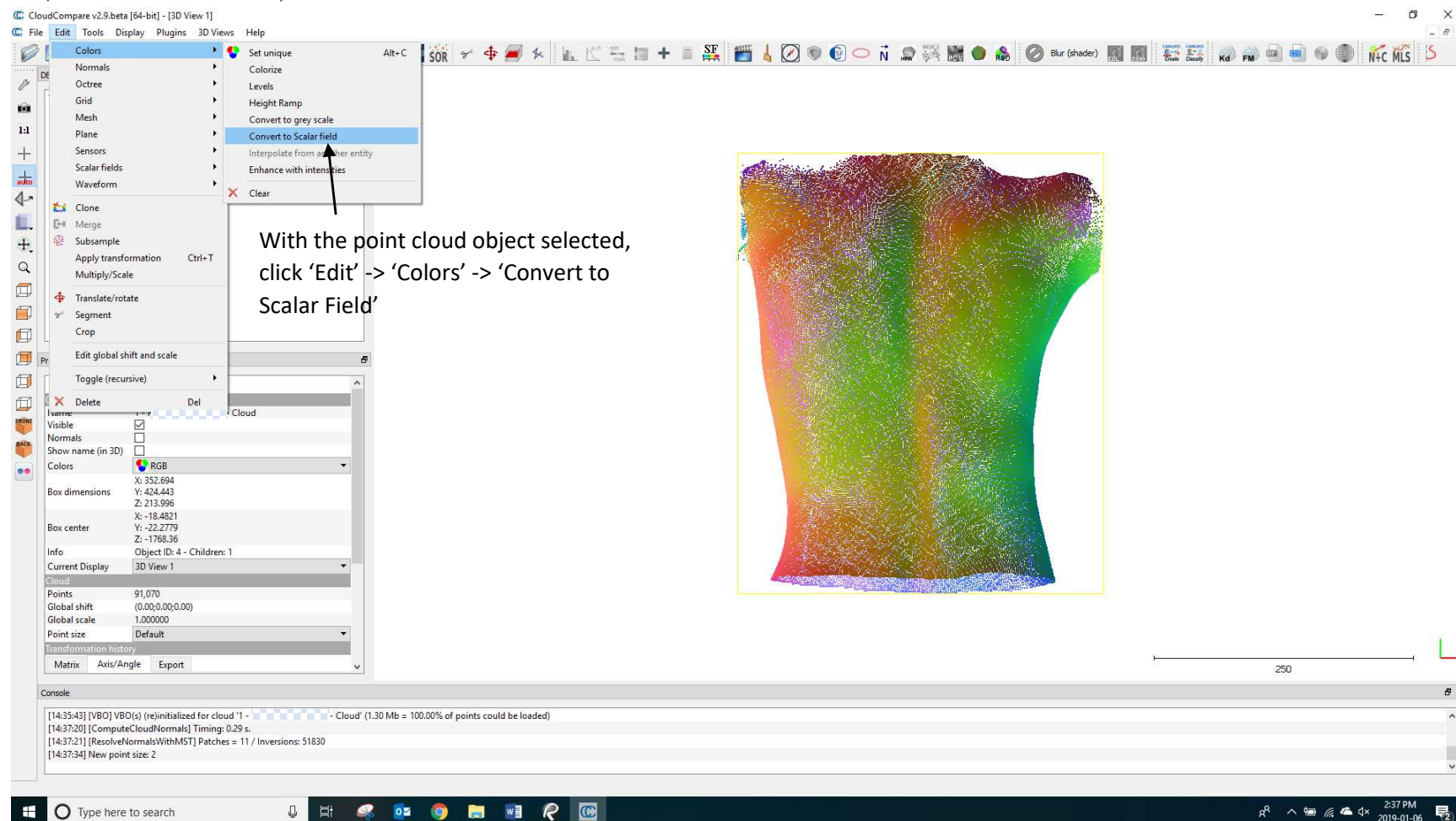
Once normals are calculated, select 'Edit' -> 'Normals' -> 'Convert to' -> 'HSV colors'

HSV colors are colors designated with numerical values for Hue, Saturation, and Value (HSV). Converting the normal vectors to HSV values just change the x, y, z values of the vectors to H, S, V values for the color. The actual H,S,V values are not important, the important part is that the z values are now attached to the points as a V value which can be selectively filtered.



The previous steps have calculated the normal vectors for each point, then translated the x,y,z direction coordinates for each normal into a HSV color value. This HSV color is then interpreted as a red, green, blue (RGB) color value that was then assigned to the points. This means that the visible RGB point colors indicate the direction of the normal vector for each point. The normal vectors have been stored as 3 scalar fields attached to each point, with one field each for the x, y, z direction coordinates for each normal vector. The x coordinate is mapped to the R (red) value, the y coordinate is mapped to the G (green) value, and the z coordinate is mapped to the B (blue). In the next step the B (blue) color value, which corresponds to the z vector direction, will be used to filter out only those points which have a positive vector direction. This means that the vector points “up” from the coronal plane. This is the criteria used to determine a point that is part of the back and not the front of the torso.

Step 3 – Isolate Back Only Points

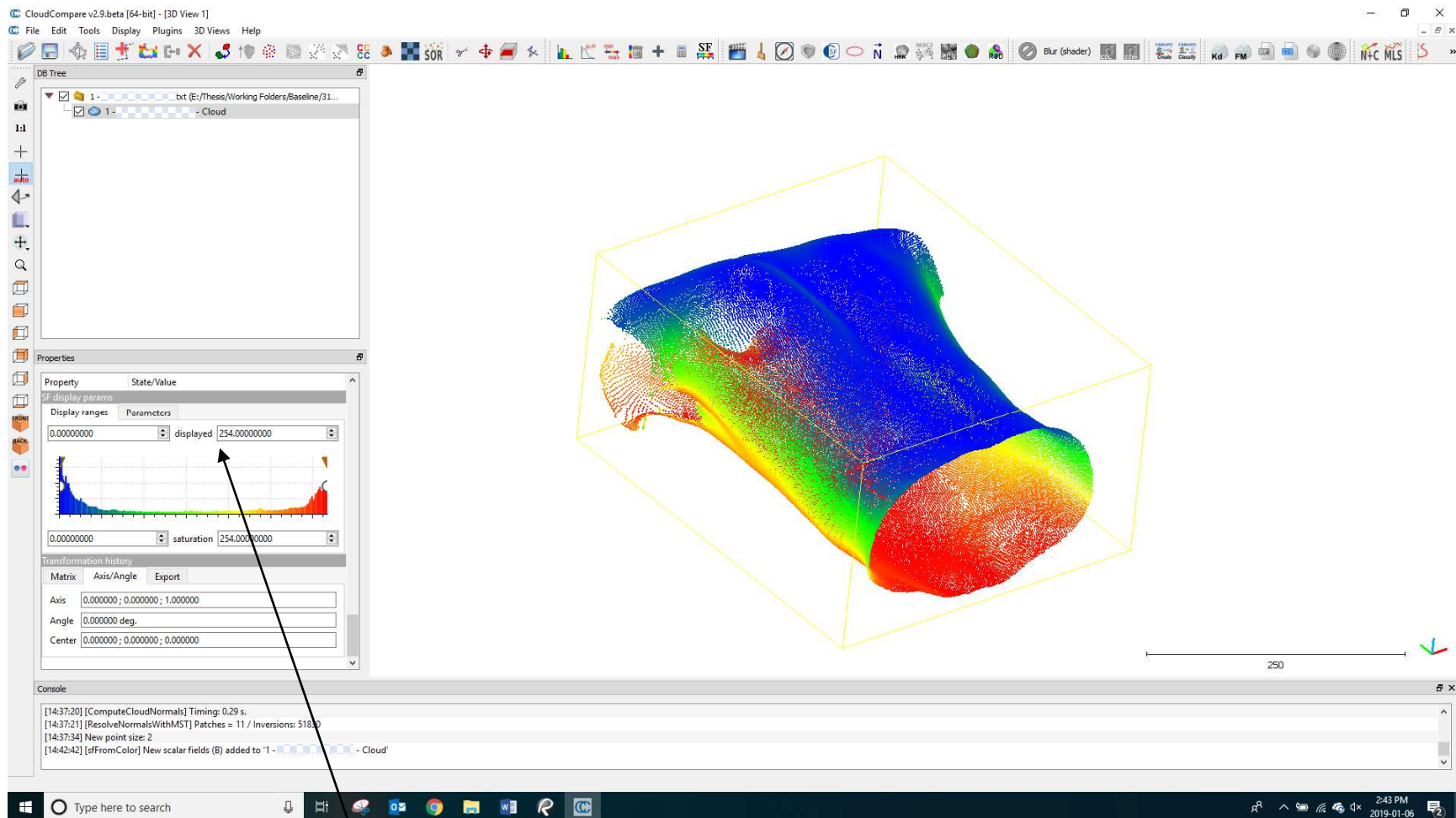


The screenshot displays the CloudCompare v2.9.0 beta interface. The 'Colors' menu is open, and the 'Convert to Scalar field' option is highlighted. A yellow box highlights the point cloud object in the 3D view. A text box with an arrow points to the 'Convert to Scalar field' option, stating: 'With the point cloud object selected, click 'Edit' -> 'Colors' -> 'Convert to Scalar Field''. The console window at the bottom shows the following log entries:

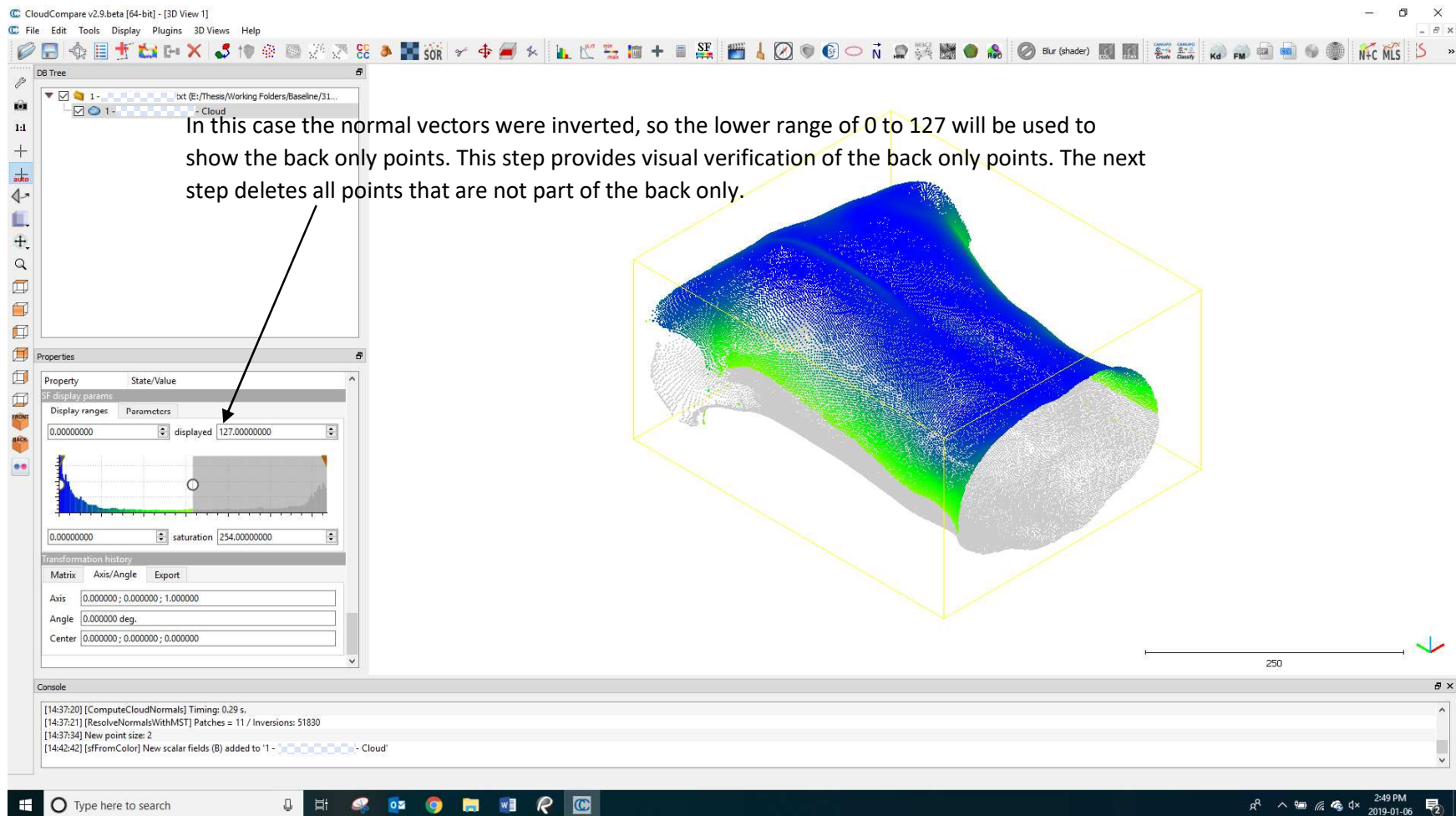
```
[14:35:43] [VBO] VBO(s) (re)initialized for cloud '1 - Cloud' (1.30 Mb = 100.00% of points could be loaded)
[14:37:20] [ComputeCloudNormals] Timing: 0.29 s.
[14:37:21] [ResolveNormalsWithMST] Patches = 11 / Inversions: 51830
[14:37:34] New point size: 2
```

The screenshot displays the CloudCompare v2.9.0 beta interface. The main 3D view shows a point cloud of a skull, colored by a scalar field. A dialog box titled "SF from RGB" is open, with the "B Channel" option checked. The Properties panel on the left shows the object's name as "1 - Cloud" and its bounding box dimensions. The console at the bottom shows logs for VBO initialization, normal computation, and point size setting.

The x,y,z fields have been translated to R,G,B color values. The 'z' coordinate has been translated from a degree value between -90 to 90 into blue hues (the 'B' channel) from 0 to 256. By translating the blue color value into a scalar field, the values can be used to selectively filter out only those vectors whose 'z' direction is away from the coronal plane.



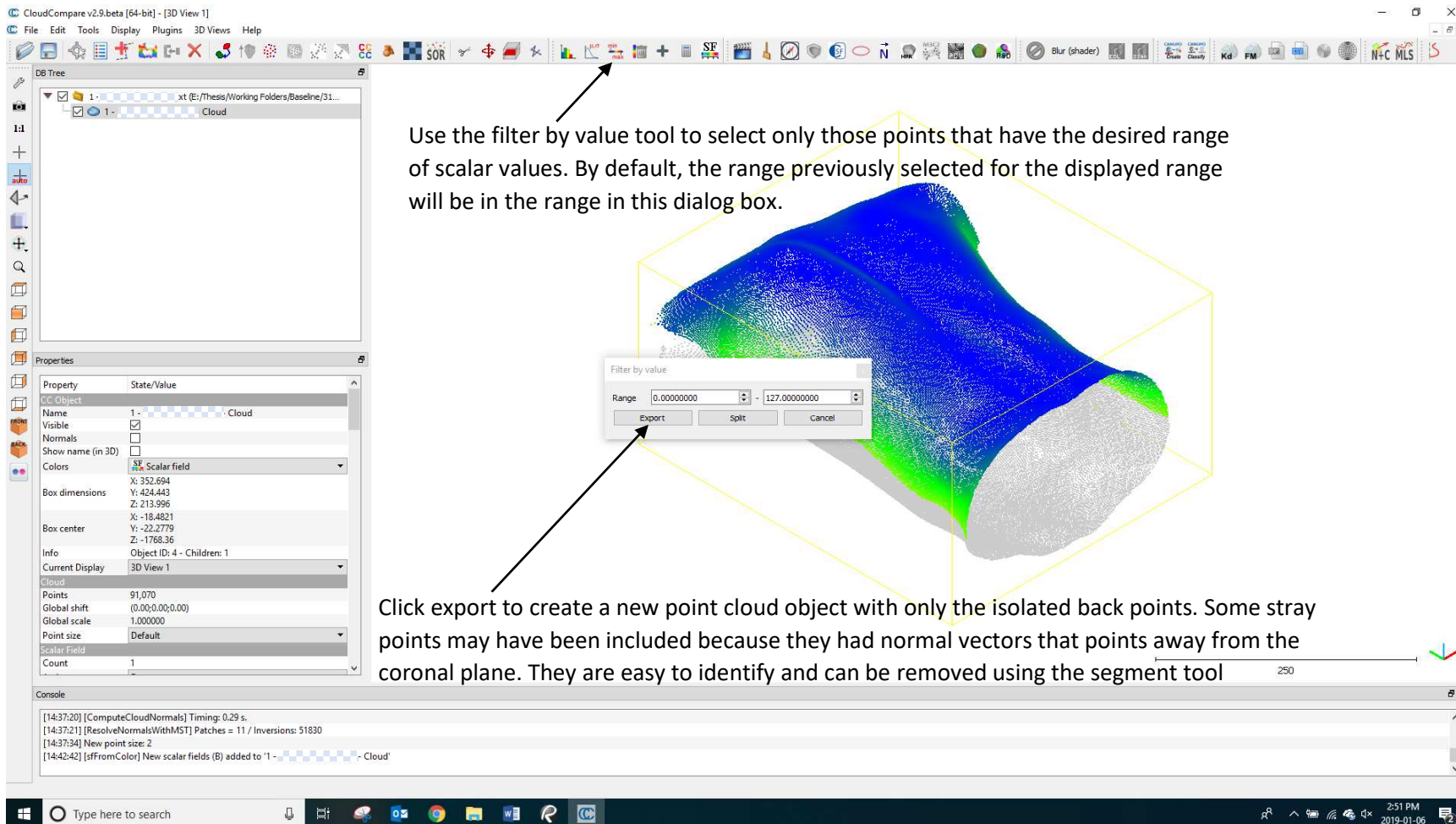
By default, the new Scalar Field created from the 'B' color channel becomes the active scalar field. Under the 'SF Display Properties' dialogue in the Properties panel the values can be visually filtered. Normal vector z values between -90 and 0 degrees became blue channel values from 0 to 127, and z values between 0 to +90 degrees became blue channel values between 127. Use the display parameters to hide 0 to 127, or 127 to 254 by inputting 127 into the one of the left text box for the upper range, or the right text box for the lower range. If the back is showing as the lower values (0 to 127) then the normal vectors were inverted. This does not affect the results, it just means that the points to be filtered out will need to be the lower range.

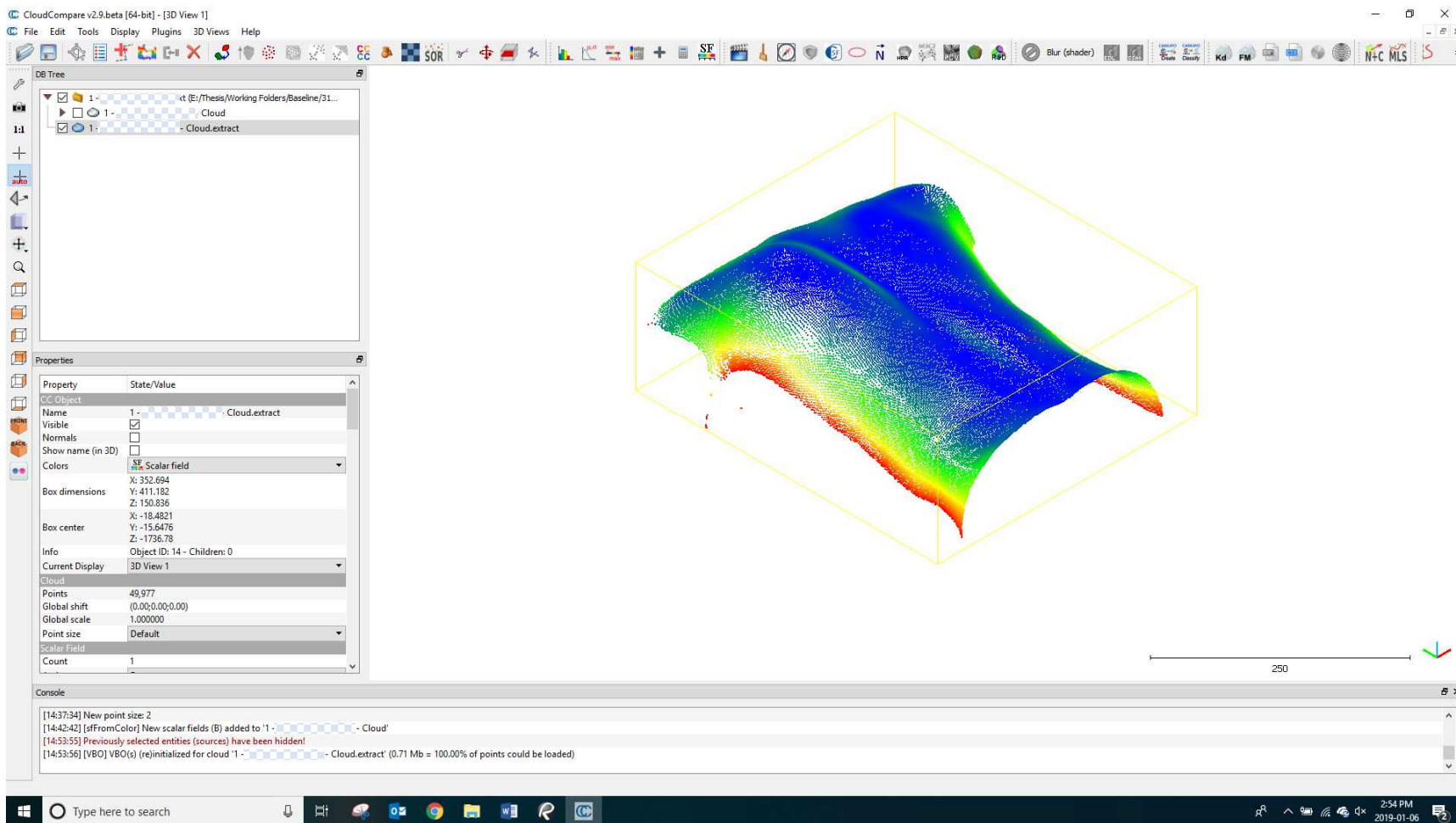


In this case the normal vectors were inverted, so the lower range of 0 to 127 will be used to show the back only points. This step provides visual verification of the back only points. The next step deletes all points that are not part of the back only.

The screenshot shows the CloudCompare v2.9.0 beta [64-bit] interface. The main 3D view displays a point cloud of a bone, colored with a gradient from blue to green. The software interface includes a DB Tree on the left, a Properties panel in the middle, and a Console at the bottom. The Properties panel shows the 'SF display params' section with 'displayed' set to 127.00000000. The Console shows the following log entries:

```
[14:37:20] [ComputeCloudNormals] Timing: 0.29 s.  
[14:37:21] [ResolveNormalsWithMST] Patches = 11 / Inversions: 51830  
[14:37:34] New point size: 2  
[14:42:42] [sfFromColor] New scalar fields (B) added to '1 - Cloud'
```

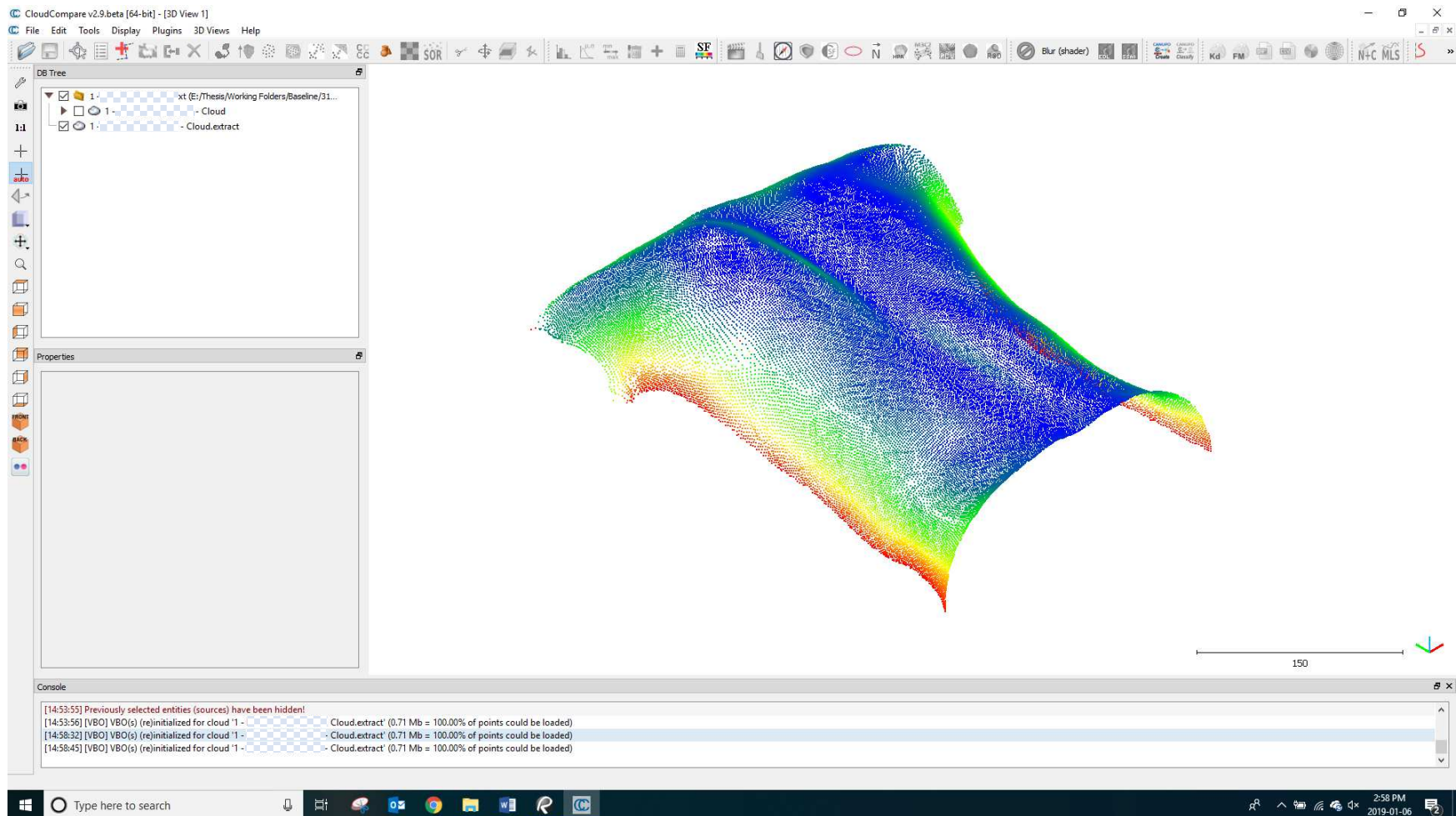





This is the view of the isolated back points.

The screenshot displays the CloudCompare v2.9.0 beta [64-bit] - [3D View 1] interface. The main 3D view shows a point cloud with a color gradient from blue to green. A yellow polygonal selection is visible, and a black arrow points to it. The top toolbar contains various tools, with two arrows pointing to the 'Segmentation [ON] (polygonal selection)' button and the 'confirm and delete hidden points' button. The left sidebar includes the 'Db Tree' and 'Properties' panels. The 'Properties' panel shows details for the selected object, including 'Name', 'Visible', 'Normals', 'Show name (in 3D)', 'Colors', 'Box dimensions', 'Box center', 'Info', 'Current Display', 'Cloud', 'Points', 'Global shift', 'Global scale', 'Point size', 'Point size', 'Scalar Field', and 'Count'. The 'Console' window at the bottom shows log messages: [14:37:34] New point size: 2; [14:42:42] [sfFromColor] New scalar fields (8) added to '1 - Cloud'; [14:53:53] Previously selected entities (sources) have been hidden!; [14:53:56] [VBO] VBO(s) (re)initialized for cloud '1 - Cloud.extract' (0.71 Mb = 100.00% of points could be loaded). The Windows taskbar at the bottom shows the system tray with the time 2:56 PM and date 2019-01-06.

Use the segment tool to choose stray points, then use the 'segment out' button, followed by the 'confirm and delete hidden points button'



The back points are now in a single point cloud object. This can be saved as a text file that will contain only the isolated back points. This point cloud object can now be analyzed using the same procedure as the asymmetry analysis process used on the full torso point cloud in appendix A.